Beata Szymczycha
Janusz Pempkowiak

The Role of Submarine Groundwater Discharge as Material Source to the Baltic Sea

Springer

GeoPlanet: Earth and Planetary Sciences

Editor-in-chief

Paweł Rowiński

Series editors

Marek Banaszkiewicz, Warsaw, Poland
Janusz Pempkowiak, Sopot, Poland
Marek Lewandowski, Warsaw, Poland
Marek Sarna, Warsaw, Poland

More information about this series at http://www.springer.com/series/8821

Beata Szymczycha · Janusz Pempkowiak

The Role of Submarine Groundwater Discharge as Material Source to the Baltic Sea

Beata Szymczycha
Institute of Oceanology
Polish Academy of Sciences
Sopot
Poland

Janusz Pempkowiak
Institute of Oceanology
Polish Academy of Sciences
Sopot
Poland

Series Editors

Managing Editor

Anna Dziembowska
Institute of Geophysics, Polish Academy of Sciences

Advisory Board

Kon-Kee Liu
Institute of Hydrological and Oceanic
Sciences
National Central University Jhongli
Jhongli, Taiwan

Teresa Madeyska
Research Centre in Warsaw
Institute of Geological Sciences
Warszawa, Poland

Stanisław Massel
Institute of Oceanology
Polish Academy of Sciences
Sopot, Poland

Antonio Meloni
Instituto Nazionale di Geofisica
Rome, Italy

Evangelos Papathanassiou
Hellenic Centre for Marine Research
Anavissos, Greece

Kaja Pietsch
AGH University of Science and
Technology
Kraków, Poland

Dušan Plašienka
Prírodovedecká fakulta, UK
Univerzita Komenského
Bratislava, Slovakia

Barbara Popielawska
Space Research Centre
Polish Academy of Sciences
Warszawa, Poland

Tilman Spohn
Deutsches Zentrum für Luftund
Raumfahrt in der Helmholtz
Gemeinschaft
Institut für Planetenforschung
Berlin, Germany

Krzysztof Stasiewicz
Swedish Institute of Space Physics
Uppsala, Sweden

Ewa Szuszkiewicz
Department of Astronomy and
Astrophysics
University of Szczecin
Szczecin, Poland

Roman Teisseyre
Department of Theoretical Geophysics
Institute of Geophysics
Polish Academy of Sciences
Warszawa, Poland

Jacek Tronczynski
Laboratory of Biogeochemistry of
Organic Contaminants
IFREMER DCN_BE
Nantes, France

Steve Wallis
School of the Built Environment
Heriot-Watt University
Riccarton, Edinburgh
Scotland, UK

Wacław M. Zuberek
Department of Applied Geology
University of Silesia
Sosnowiec, Poland

Piotr Życki
Nicolaus Copernicus Astronomical
Centre
Polish Academy of Sciences
Warszawa, Poland

Preface

Global environment consists of a variety of ecosystems of different sizes and compositions. Within each of them, and between them, of particular interest are zones characterized by gradients of properties. This concerns both transfers between phases (solid–gaseous, solid–liquid, and liquid–gaseous) and gradients of properties within a phase (redox, density, temperature, chemical composition). Many of the features are characteristic of areas where land meets ocean. Seawater properties and processes are largely different from those appearing in freshwater. Thus, the land–sea interface is interesting by itself. Moreover, land and coastal zones are areas of intensive anthropogenic activity. The unwanted results of the activity are contamination of freshwater and degradation of coastal areas. Therefore, zones where freshwater meets seawater are of particular interest due to both natural phenomena and transfer of contaminants to the marine environment.

Discharges of freshwater to the sea are well characterized as long as river runoff is considered. This, without doubt, is in relation to the importance of the discharges and relative ease of collecting representative samples of river runoff. Another way of discharge from land to the sea is direct discharge of groundwater. Groundwater flows under the seafloor and seeps through porous sediments to the overlaying seawater. The phenomenon is called submarine groundwater discharge (SGD). Numerous problems occur regarding identifying SGD sites, quantification of SGD fluxes, and collecting the SGD representative samples. Thus, studies on SGD are difficult and require specific methods.

Appreciation of SGD has a long history. For example, both Romans and middle-aged Europeans used SGD as a source of freshwater. However, it was only recently that the importance of SGD for coastal ecosystems was recognized. The appreciation has come with the discovery of the SGD role as a source of nutrients and other chemical substances in the coastal zone. This was followed by studies on the role of SGD as a factor influencing benthic biota in the discharge zone. Recently, the importance of carbon species loads, both organic and inorganic, delivered to the marine environment with seeping groundwater was documented. Interest in the SGD-derived carbon species is due to the common appreciation that

carbon dioxide concentration in the atmosphere is a primary driving force of climate warming.

Decades of research on the qualitative and quantitative composition of groundwater seeping to the coastal zone led to the conclusion that SGD plays important role in developing equilibria in the coastal zone environment. Both enrichment of seawater with inorganic ions and dilution of ions occurring in seawater have been documented. The range of seawater–groundwater interactions depends on many factors such as individual characteristics of aquifers, including rock type, groundwater flow velocity, and anthropogenic contribution. New studies are undertaken in order to increase the amount of data characterizing SGD so that appropriate generalization and scaling up could be carried out.

This volume summarizes recent achievements in the field of SGD studies performed in the Baltic Sea, a European landlocked brackish water body in the temperate climate. For a number of years, SGDs in the area had been investigated with respect to the groundwater flow rate. Within the last 5 years, new findings regarding chemical composition of seeping groundwater have been presented. In the book, concentrations, in groundwater seeping through sandy bottom sediments to the coastal zone along the southern coast of the sea, are presented and discussed. Research on speciation changes of chemical constituents on mixing of groundwater and seawater has also been carried out, and the results are presented in the book. Studies on chemical composition were accompanied with detailed studies of the discharge rates. These have made possible estimation of the chemical loads delivered to the study area and scaling up the loads to the entire Baltic Sea using the literature-derived discharge rates. Some of the loads have been scaled up to the World Ocean. Although both the former and the latter results should be regarded as indicative, they underline the worldwide importance of SGD.

The authors hope that the readers will find the data themselves, the discussion, and conclusions of interest, and that the book will strengthen the appreciation of the SGD's importance to the coastal marine environment.

Beata Szymczycha
Janusz Pempkowiak

Contents

List of Figures

List of Tables

Chapter 1
Introduction

A significant part of the flux of dissolved substances from land to the sea occurs through river transport via the drainage basins network (Turner et al. 1999). The input from major rivers is gauged and well analyzed with relatively precise estimates of the quantities of freshwater and chemical constituents entering the marine environment. Recently, submarine groundwater discharge (SGD) has been recognized as an important factor influencing coastal zones (Burnett et al. 2006; McCoy and Corbett 2009; Moore 2010). It has been indicated that subterranean non-point pathways of material transport may be of considerable importance in some coastal areas (Beck et al. 2010; Lee et al. 2011; Kim and Kim 2014). SGD is an essential component of the water cycle and can be, in selected areas, comparable in volume to the riverine flux (e.g. Atlantic Ocean, Moore 2010). Coastal groundwater, in many areas, becomes enriched with chemical constituents and, therefore, is a source of nutrients, metals and organic compounds. As SGD often contains higher concentrations of dissolved substances (nutrients, dissolved carbon, metals) than rivers, the calculated loads suggest that SGD can be a more important source of dissolved substances than rivers in oceanic budgets (Moore 2010). Hence SGD is a significant factor influencing the marine geochemical cycles of chemical substances and may cause environmental deterioration of coastal ecosystems. Numerous studies show the ecological impact of the groundwater flow into coastal areas. The knowledge of SGD nutrient loads is of major importance to coastal eutrophication (Valiela et al. 1992). SGD has been also identified as a critical threat to biodiversity around the world (Eemus et al. 2006). Kotwicki et al. (2014) suggest that submarine groundwater discharge has an effect on the spatial distribution, abundance and taxonomic composition of benthic communities resulting in a significant reduction of meiofauna density in groundwater impacted sediments. Understanding the significance of groundwater pathways for material transport at the land–sea interface will, most likely, advance knowledge of the dynamics of the coastal systems. Recent international studies indicate that groundwater-seawater interactions in "subterranean estuary" (groundwater–seawater mixing zone; Moore 1999) may be important sources of dissolved constituents from groundwater to seawater (Charette and Sholkovitz 2006; Beck et al. 2006, 2007). The Baltic Sea is an example of a region highly influenced by a variety of human activities that affect the ecosystem. SGD remains one of a number of sources introducing dissolved substances into the

Baltic Sea that has not been quantified so far. Little is known regarding the concentrations and fluxes of chemical substances in groundwater discharged directly to the Baltic Sea and chemical reactions that control their flux into the coastal ecosystem. Studies concerning the importance of geochemical transformations in determining SGD-derived metals, nutrients, dissolved organic carbon and dissolved inorganic carbon fluxes to the Baltic Sea are scarce.

References

Beck AJ, Tsukamato Y, Tovar-Sanchez A, Huerta-Diaz M, Bokuniewicz HJ, Sañudo-Wilhelmy SA (2006) Importance of geochemical transformations in determining submarine groundwater discharge-derived trace metal and nutrient fluxes. Appl Geochem 22:477–490

Beck AJ, Rapaglia JP, Cochran JK, Bokuniewicz HJ (2007) Radium mass-balance in Jamaica Bay, NY: Evidence for substantial flux of submarine groundwater. Mar Chem 106:419–441

Beck AJ, Cochran JK, Sañudo-Wilhelmy SA (2010) The distribution and speciation of dissolved trace metals in a shallow subterranean estuary. Mar Chem 121:145–156

Burnett WC, Aggarwal PK, Aureli A, Bokuniewicz HJ, Cable JE, Charette MA, Kontar E, Krupa S, Kulkarni KM, Loveless A, Moore WS, Oberdorfer JA, Oliveira J, Ozyurt N, Povinec P, Privitera AMG, Rajar R, Ramessur RT, Scholten J, Stieglitz T, Taniguchi M, Turner JV (2006) Quantifying submarine groundwater discharge in the coastal zone via multiple methods. Sci Total Environ 367:498–543

Charette MA, Sholkovitz ER (2006) Trace element cycling in a subterranean estuary: Part 2. Geochemistry of the pore water. Geochemica et Cosmochimica Acta 70:811–826

Eemus D, Froend G, Lommes R, Hose G, Murray B (2006) A functional methodology for determining the groundwater regime needed to maintain health of groundwater-dependent vegetation. Austr J Botan 54:97–114

Kim G, Kim JS (2014) Submarine groundwater discharge as a main source of rare earth elements in coastal waters. Mar Chem 160:11–17

Kotwicki L, Grzelak K, Czub M, Dellwig O, Gentz T, Szymczycha B, Böttcher M (2014) Submarine groundwater discharge to the Baltic coastal zone—Impact on meiofaunal community. J Mar Syst 129:118–126

Lee YW, Rahman MDM, Kim G, Han S (2011) Mass balance of total mercury and monomethylmercury in coastal embayments of a volcanic islands: significance of submarine groundwater discharge. Environ Sci Technol 45:9891–9900

McCoy CA, Corbett DR (2009) Review of submarine groundwater discharge (SGD) in coastal zones of the Southeast and Gulf Coast regions of the United States with management implications. J Environ Manag 90:644–651

Moore WS (1999) The subterranean estuary: a reaction zone of ground water and sea water. Mar Chem 65:111–125

Moore WS (2010) The effect of submarine groundwater discharge on the ocean. Ann Rev Mar Sci 2:59–88

Valiela I, Foreman K, LaMontagne M, Hersh D, Costa J, Peckol P, DeMeo-Anderson B, D'Avanzo D, Babione M, Sham CH, Brawlej J, Lajtha K (1992) Coupling of watersheds and coastal waters: sources and consequences of nutrient enrichment in Waquoit Bay, Massachusetts. Estuaries 15:443–457

Turner RK, Georgiou S, Gren I-M, Wulff F, Barret S, Söderqvist T, Bateman IJ, Folke C, Langaas S, Żylicz T, Mäler K-G, Markowska A (1999) Managing nutrient fluxes and pollution in the Baltic: an interdisciplinary simulation study. Ecolog Econ 30:333–352

Chapter 2
State of Art and Theory of Submarine Groundwater Discharge (SGD)

2.1 Definition and Drivers of SGD

The water discharge is the most important pathway connecting land and ocean. Surface water inputs (e.g., rivers and streams) are usually easily visible and are typically large point material sources to the coastal ocean (Mulligan and Charette 2009). Hence, the contribution of surface water discharge to the ocean geochemical budgets has been well studied. The hydrodynamics and impact of terrestrial water on geochemical cycles of elements and its influence on the ocean ecosystem has been well recognised.

Another pathway connecting land and ocean is a direct groundwater flow. Groundwater discharge typically has a smaller water flow rate compared to river flow rate although locally it can be an important point source. However, chemical fluxes associated with groundwater discharge can be comparable to river chemical fluxes (Moore 2010). Thus, groundwater flow through coastal sediments to the marine ecosystem can have a significant impact on many processes taking place in the coastal areas and therefore there is a need for the process to be better understood.

Coastal aquifers usually consist of complicated systems described as confined, semi-confined and unconfined (Fig. 2.1). Freshwater can flow through an aquifer forced by hydraulic head and entrain seawater that is diffusing and dispersing up from the salty aquifer that lies underneath. On the other hand, seawater can percolate the seabed driven by a variety of forces. The zone of intermediate salinity extended between fresh water and seawater is called subterranean estuary (Moore 1999).

There are several forces that drive groundwater flow to the coastal ecosystem. The primary terrestrial driving force of fluid flow through coastal aquifers is the hydraulic gradient. Groundwater flows from the upland region of a watershed to unconfined or semi-confined aquifers on the coast where it can meet salty pore water that has infiltrated from the ocean (Burnett et al. 2006; Moore 2009; Mulligan
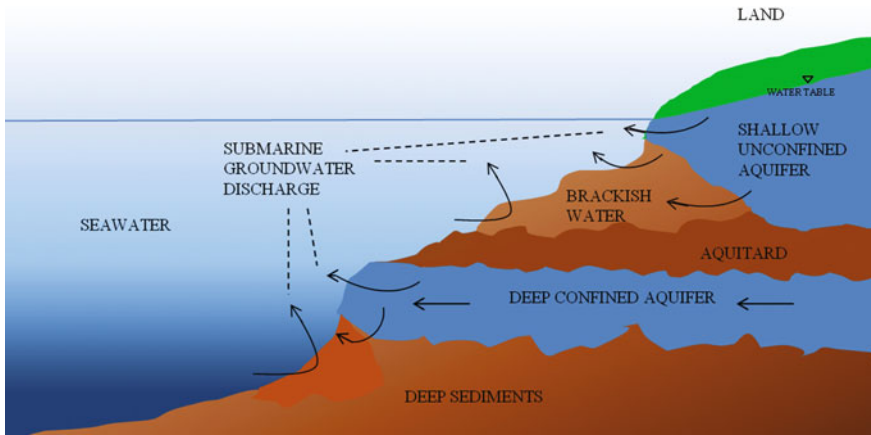
Fig. 2.1 General scheme of SGD. Groundwater located in the shallow, unconfined aquifer can discharge directly to the coastal ocean or can mix with seawater already in the sediment and be discharged as brackish water (seepage water). SGD is determined by both terrestrial and marine forces. Based on Burnett et al. (2006)

and Charette 2009). Usually, there is not one driving force behind SGD but a number of them including terrestrial and marine forces (Moore 2010). The main forces that influence submarine groundwater discharge are: water level differences across a permeable barrier; tidal pumping, wave setup (Taniguchi et al. 2002; Burnett et al. 2003; Massel et al. 2005), storms, current-induced pressure gradients in the coastal zone; upland recharge causing seasonal inflow and outflow of seawater into the aquifer (Michael et al. 2005) and geothermal heating (Kohout 1965).

As there are a number of different forces causing SGD, there are also many modes of SGD. The most modern and cited definition of groundwater is "water that resides within the saturated zone of geologic material" (Burnett et al. 2006; Moore 2010). Hence, pore water that fills space among sediments grains and thus makes sediments saturated like submerged, porous materials, is synonymous with groundwater (Moore 2010). There is considerable confusion regarding groundwater discharge definition, because it occurs as a slow diffuse flow or seepage through sediment and is characterized by substantial temporal and spatial variability (Burnett et al. 2006). Therefore, other definitions are in use. The first one considers only the discharge of terrestrial groundwater and often identify groundwater as rainwater that has infiltrated and percolated to the water table, or put on some similar qualifications, consistent with the applications to freshwater in terrestrial systems (Burnett et al. 2006). The second one characterizes submarine groundwater discharge as "any flow of water from seabed to the coastal ocean, regardless of fluid composition or driving force" (Burnett et al. 2003) and include fresh SGD, saline SGD and brackish SGD. The latter being a mixture of end-members (groundwater end-member and seawater end-member).

There are also definitions characterizing SGD that occurs farther from the shoreline (Fig. 2.1) forced by the advection of water through permeable shelf sediments and rocks. As SGD occurrence on the continental shelf (coming from deeper aquifers) is driven by buoyancy and pressure gradients, it can also be called deep pore water upwelling (DPU) (Piekarek-Jankowska 1996; Moore 2010) . When the flow of water is driven by an inland hydraulic head through highly permeable aquifers or by large-scale cyclic movement of water caused by thermal heating, the process is called offshore submarine springs (Moore 2010).

In sandy, coastal areas seafloor currents are strong enough to create ripples (Fig. 2.2). Waves generate pressure gradients that can drive pore water exchange. This is also a type of SGD (Moore 2009). In the ripple troughs water percolates through the sediments and flows on a curved path toward the ripple crests, where pore water is released.

There are pros and cons of each of the groundwater discharge definitions. The advantage of defining groundwater discharge as a flow of water from the seabed to the marine environment (including fresh, saline and brackish SGD) is that it takes into account discharges of both: terrestrial groundwater and recirculated seawater. It is obvious that in the coastal ecosystem the seawater intrusion into the sediment is a common process (Massel et al. 2005). However, the recirculated seawater is not a new source of water and associated material fluxes for the marine environment. Moreover, SGD has been identified as a material pathway from land to the sea and consequently the above mentioned definition does not fulfil the criterion. Hence, for the purpose of this study, SGD is defined as groundwater (terrestrial water) discharge, while groundwater is identified as water which has salinity below 0.5. As a result groundwater is discharged to the coastal ecosystem as sediment porewater. The mixture of groundwater and seawater is referred to seepage water. The main aim of defining SGD as terrestrial groundwater flow is to characterize a new source of chemical substances loads to the study area and the Baltic Sea.
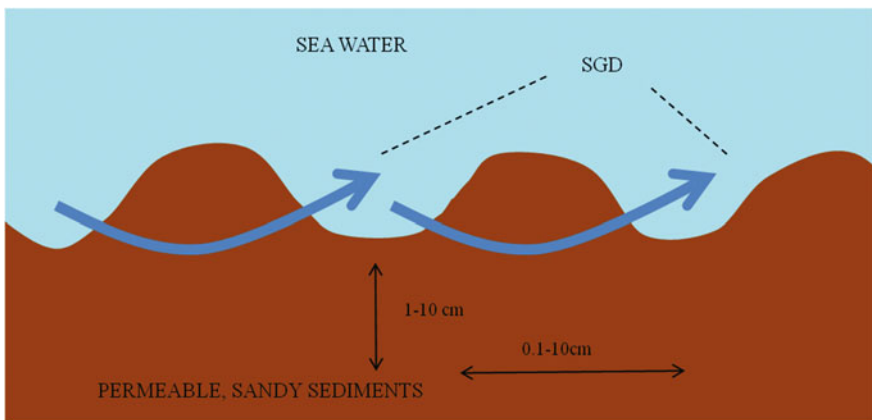
Fig. 2.2 Pore water exchange forced by differential pressure gradients. Based on Moore (2009)

2.2 The Worldwide Studies of SGD

Generally, submarine groundwater discharge into oceans and seas occurs constantly all over the world along coast lines (Peltonen 2002; Moore 2010). Groundwater discharge to the sea has been a topic of interest for many centuries (Burnett et al. 2006). A Roman geographer, Starbo (63BC-21AD) mentioned a submarine spring 4 km offshore from Latakia, Syria in the Mediterranean Sea (Kohout 1966). The spring was used as a source of fresh water which was transported to the town. Pliny the Elder (23–79 AD) described submarine springs in the Black Sea and in the Mediterranean Sea (Kohout 1966).

Later, groundwater hydrologists made efforts to identify drinking groundwater reserves and evaluate the behaviour of freshwater arriving in seawaters. Their studies were also focused on the identification of the groundwater-seawater (freshwater-saltwater) interface in the coastal zone. The first physical formulations of seawater intrusion were made by Badon-Ghyben and Herzberg (Badon-Ghyben 1888–1889; Herzberg 1901 both as cited in Bear et al. 1999), and thus called the Ghyben-Herzberg relationship. The relationship was based on a number of assumptions describing the elevation of the water table and the density difference of fresh water and seawater. The assumptions defined an unrealistic, hydrostatic situation because the idea of freshwater and seawater mixing was not allowed. This hydrostatic process would find saline groundwater everywhere below the sea level (Burnett et al. 2003; Moore 2010). In time scientists recognised that a more sophisticated equation is required to describe freshwater flow. Dupuit (1863 as cited in Freeze and Cherry 1979) identified hydrostatic distribution of fresh groundwater and seawater by making several assumptions: flow of groundwater was entirely horizontal; the seawater-groundwater interface was a no-flow boundary; and that salty groundwater was stationary. The Dupuit-Ghyben-Herzberg relationship leads to the awkward idea that all the groundwater had to escape at the shoreline (Burnett et al. 2003; Moore 2010). This was later improved by Hubbert (1940) who implemented the concept of an outflow interval. As a result seawater-groundwater interface intersected at the sea floor at some distance from the shore, producing a discharge area of intermediate salinity (Moore 2010). This concept was modified by Glover (1964) and Henry (1964). Both of them calculated the size of the interval and the position of the seawater-groundwater interface. Later Vacher (1988) used Herzberg's methodology as a boundary condition in order to calculate the width of the outflow interval.

The development of numerical models allowed for the calculation of more realistic SGD hydrodynamics. The first use of the notion of exponential decrease to estimate the distribution of seepage rates offshore was made by McBride and Pfannkuch (1975). They calculated groundwater discharge rate into lakes. Others scientists used similar models in coastal ecosystems. Models allowed for saline groundwater to circulate in reaction to hydraulic gradient, however flow across the seawater-groundwater interface was forbidden. The improvement in relation to the earlier models was that seawater-groundwater interface itself might change

locations. Currently models allow water to cross seawater-groundwater interface. The density driven circulation on a wide range of time and space is also possible. However, there are still some limitations to the method application (Burnett et al. 2006).

Studies concerning SGD have been neglected for many years because of the difficulty in the valuation of the importance of SGD. However, this perception has changed and scientists have recognized SGD as an important factor influencing coastal zones, thus meriting further study. As a result the Scientific Committee on Oceanic Research (SCOR) created two groups (working groups- WPs) to examine SGD. In 1997 SCOR WG-112 was formed to study more accurately and completely how submarine groundwater discharge impacts chemical and biological processes in the coastal ocean (Burnett 1999). SCOR WG-114 was established in 1999 to determine the fluid flow through permeable sediments and rocks to local and global ocean and SGD contribution to biogeochemical cycling and its impact on the environment (Boudreau et al. 2001). The growing number of publications demonstrates how interest in SGD studies increased over time. According to Web of Science (Thompson Reuters, https://apps.webofknowledge.com) in 1980s and 1990s number of published manuscripts per year oscillated from 0 to 4, in 2008 the number of published manuscripts increased to 79 and in 2014 to 123 (Thompson Reuters, https://apps.webofknowledge.com). These articles cover many aspects of SGD. The main focus has been on SGD measurements and SGD modelling leading to the development of methods of identifying and quantifying SGD. Recently scientists have started determining SGD influence on the environment and chemical substances fluxes via SGD, however there are still issues that need to be solved as well as a number of unrecognized geographical areas impacted by groundwater discharge. One of the most challenging issues is identifying the effect of chemical substances fluxes via SGD on their concentrations and the reactions taking place in subterranean estuaries. Another outstanding issue would be the recognition of the local and global importance of SGD and its influence on chemical substances budgets (Moore 2010).

2.3 Significance of SGD

Submarine groundwater discharges to the coastal ecosystems have been recognised as a sources of dissolved chemical substances that cause chemical and ecological effects in receiving waters. Groundwater, in many coastal areas, becomes contaminated or at least enriched with a variety of chemical substances (e.g. nutrients, metals, organic compounds) and can have higher concentrations of dissolved solids than river water. As a result SGD makes a larger contribution to the flux of dissolved chemical compounds than river run-off. Additionally, groundwater seeping through the sediments interacts with recirculated seawater and impacts the marine environment.

2.3.1 SGD as a Source of Nutrients and Biological Effects on the Coastal Ocean

Pioneering investigations concerning the biological importance of groundwater seepage into the sea were conducted by Kohout and Kolpinski (1967). They documented an explicit connection between groundwater discharge into the Biscayne Bay, Florida and biological zonation. Marsh (1977) presented SGD as a source of nutrients for coral reefs along the coast of Guam island. Similar phenomena were documented by D'Elia et al. (1981). Valiela et al. (1978, 1992, 2002) suggested that nitrogen fluxes via SGD can be critical to the nutrient economy of salt marshes. The harmful algal blooms in some areas were also related to nutrient supply via SGD (Lapointe and O'Connell 1989; LaRoche et al. 1997; Hwang et al. 2005; Hu et al. 2006; Lee and Kim 2007). A study in Masan Bay, Korea showed that large nutrient fluxes via SGD could lead not only to eutrophication but also to the occurrence of red tides (Lee et al. 2009). McCoy and Corbett (2009) suggested that eutrophication of coastal ecosystems as well as the continental shelf can be related to nutrient loads supplied via SGD.

Numerous studies have proven that the flux of nutrients via SGD is equal or greater than that from surface runoff: along the western Australian coast, North Perth (Johannes 1980); on eastern coast of Florida Bay (Corbett et al. 1999, 2000), in Florida Keys (Lapointe et al. 1990), in the Upper Floridan aquifers (Crotwell and Moore 2003); in Tampa Bay, Florida (Kroeger et al. 2007), in the Tomales Bay, California (Oberdorfer et al. 1990); along the South Carolina coast (Krest et al. 2000); in the Great South Bay, New York (Bokuniewicz 1980; Capone and Bautista 1985; Bokuniewicz and Pavlik 1990; Capone and Slater 1990); on the Georgia Shelf (Simmons 1992); in the Ria Formosa lagoon, Portugal (Leote et al. 2008) and in Hwasung and Bangdu Bay, off the volcanic island of Jeju, Korea (Kim et al. 2011).

Scientists not only tried to estimate nutrient fluxes via SGD but also investigated the sources of groundwater nutrients and processes taking place in the coastal ecosystems. Slomp and Van Cappellen (2004) first addressed the main sources of nutrients in groundwater as both natural loads from organic matter decomposition, mineral dissolution (phosphorous) and anthropogenic input from fertilizers, manure and wastewater. They suggested that the residence time of groundwater and redox conditions strongly determine the transformation, removal and transport of groundwater nitrogen and phosphorous into the coastal marine environment. Waska and Kim (2011) indicated that the nutrient biogeochemistry of SGD was impacted by tidal oscillations, seasonal precipitation changes and switched nutrient regimes. Moreover, they suggested that nutrient fluxes via SGD can be related to primary production dynamics in Hampyeong Bay, Yellow Sea. Ibánhez et al. (2012) reported that a high rate of groundwater seepage can promote the mitigation of nitrate ions whereas a low rate of groundwater seepage can promote net amplification of nitrate ions into the Ria Formosa lagoon throughout the year.

Submarine groundwater discharge and derived nutrient (NO_2^-, NO_3^-, NH_4^+, PO_4^{3-}, and SiO_2) loadings to the coastal sea were systematically assessed along the coast of Majorca Island (Spain) in a general survey around the island and in three representative coves during 2010. Substantial loads of the investigated nutrients were estimated, first of all DIN and SiO_2. Seasonal and yearly variations were documented. The study provides evidence that SGD is a major contributor to the dissolved pool of nutrients in the nearshore waters of Majorca (Travor-Sánchez et al. 2014). The conclusion of the study was confirmed by results of investigations carried out in coastal waters of Balearic Islands (Spain) that showed that SGD is a major pathway for delivering DIN (1900 mmol m^{-1} d^{-1}), dissolved Fe (4.1 mmol m^{-1} d^{-1}) and, to a lesser extent, DIP (16 mmol m^{-1} d^{-1}) into the nearshore waters. This allochthonous input may sustain a substantial phytoplankton biomass resulting in an onshore–offshore gradient (4.7–7.1 mg m^{-3} in nearshore seawater as compared with <1 mg m^{-3} in offshore stations). Both studies emphasize the relevance of SGD-driven nutrient inputs in the regulation of nearshore phytoplankton communities of oligotrophic areas.

Several recent studies have indicated that loads of nutrients delivered to the coastal zone via SGD exceed these delivered via local river run-off (Wong et al. 2014; Wang et al. 2015; Makings et al. 2014; McAllister et al. 2014). The various nutrients may be delivered to the estuary by different mechanisms (Ji et al. 2013). The intensity of nutrients discharge greatly depends on hydrologic conditions, as established in one subterranean system (Waquoit Bay, MA, USA). More than a doubling of the groundwater-associated nitrogen flux to surface water during the summer as compare to winter was due, primarily, to a reduction in nitrogen attenuation within the subterranean estuary. Because marine groundwater intrusion has been shown to increase during the summer, a greater contribution of recycled nutrients from the coastal ocean to the subterranean estuary was calculated. Also the longer residence times within the subterranean estuary during the winter, which would result from reduced marine groundwater circulation, allow oxygen depletion of the groundwater, creating a favorable environment for important nutrient transformations such as nitrification, denitrification, and anammox (Gonneea et al. 2014). This is supported by results presented by Santos et al. (2013) who, as a result of a four months of daily nutrient and radon (a natural groundwater tracer) observations at the outlet of a heavily drained coastal wetland, illustrated how episodic floods and diffuse groundwater seepage influence the biogeochemistry of a sub-tropical estuary (Richmond River, New South Wales). The authors report significant correlations between radon and ammonium and N/P ratios and between radon and dissolved organic nitrogen (DON) during the post-flood stage. While in this specific event the flood lasted for 14 % of the time of the surface water time series, it accounted for 18 % of NH_4, 32 % of NO_x, 66 % of DON, 58 % of PO_4 and 55 % of dissolved organic phosphorus (DOP) catchment exports. The groundwater contribution to the total surface water catchment exports was nearly 100 % for ammonium, and <20 % for the other nutrients. Post-flood groundwater seepage shifted the system from a DON to a dissolved inorganic N-dominated one and

doubled N/P ratios in surface waters. It is hypothesized that the Richmond River Estuary N/P ratios may reflect a widespread trend of tidal rivers and estuaries becoming more groundwater-dominated and phosphorus-limited as coastal wetlands are drained for agriculture, grazing and development (Santos et al. 2013). The delivered loads of nutrients can enhance local primary productivity by as much as 50 % (Luo et al. 2014; Makings et al. 2014), however the percentage greatly depends on the nutrient in question (Makings et al. 2014).

The role of submarine groundwater discharge (SGD), the leakage of groundwater from aquifers into coastal waters, in coastal eutrophication has been demonstrated mostly for the North American and European coastlines, but poorly quantified in other regions. Global estimates of N inputs via SGD to coastal waters show that it has increased from about 1.0 to 1.4 Tg of nitrate (NO_3–N) per year over the second half of the 20th century. Since this increase is not accompanied by an equivalent increase of groundwater phosphorus (P) and silicon (Si), SGD transport of nitrate is an important factor for the development of harmful algal blooms in coastal waters (Beusen et al. 2013).

2.3.2 SGD as a Source of Metals to the Marine Coastal Ecosystems

Submarine groundwater discharge (SGD) and fluxes of several chemical compounds via SGD have received particular attention recently. However, studies of SGD impact on metal fluxes in the coastal ocean are scarce.

Studies on the flux of metals via SGD generally indicate that SGD is a significant source of metals for the marine environment. Barium and strontium, similarly to radium, have higher concentrations in groundwater than seawater. Barium fluxes via SGD were equal or higher than river barium fluxes (Moore 1997; Shaw et al. 1998; Santos et al. 2009) while Strontium fluxes via SGD were estimated to be comparable to its river flux (Basu et al. 2001). A comparison of both barium and strontium distribution in the subterranean estuary showed that concentrations of these elements differ relatively to salinity. Both are released to the estuary, however the extent of release is greater for barium than strontium (Charette and Sholkovitz 2006). Jeong et al. (2012) determined concentrations of selected trace elements (aluminium, manganese, iron, cobalt, nickel and copper) in groundwater and calculated their fluxes via SGD. The budget calculation showed that SGD was responsible for unusually enhanced concentrations of some trace elements in the summer in coastal seawater of the volcanic island Jeju. Charette et al. (2005) found elevated concentrations of dissolved iron and reduced manganese in groundwater in comparison to seawater. On mixing anoxic groundwater with oxic seawater large fractions of dissolved iron and manganese were oxidized and precipitated within the sediments. Thus, it was made clear that subterranean estuaries represent zones of substantial changes in the anoxic and oxic conditions impacting iron and

manganese distribution and co-precipitation with other metals (Charette and Sholkovitz 2002).

Results of some studies suggested that selected metal concentrations in groundwater exhibit nonconservative behaviours upon mixing with seawater (Charette and Sholkovitz 2002; Windom et al. 2006; Beck et al. 2007, 2009). For example dissolved cobalt and nickel showed nonconservative behaviour as oppose to the conservative behaviour of salinity upon the mixing of groundwater and seawater end-members (Beck et al. 2007). The processes that could influence behaviour of selected metals were mineralization of organic matter, manganese oxidation-reduction cycle, forming or dissolution of colloids and organo-metallic complexes (Sañudo-Wilhelmy et al. 2002; Baumann et al. 2006; Beck et al. 2010). On the other hand, there are elements like dissolved copper, lead, silver, aluminium, and manganese that did not show clear dependences in relation to salinity changes.

Submarine groundwater discharge and derived trace element (Cd, Co, Cu, Fe, Mo, Ni, Pb, V and Zn) loadings to the coastal sea were investigated along the coast of Majorca Island, Spain during 2010. It was established that brackish water discharges through the shoreline are important contributors to Fe, and Zn budgets of the near-shore waters. Furthermore the results of the study showed that SGD-derived elements are conditioned by the hydrogeological formations of the aquifer and discharge type. Thus, while rapid discharges through karstic conduits are enriched in SiO_2 and Zn, the large detrital aquifers of the island typically present enhanced concentrations of Fe. The study provides evidence that SGD is a major contributor to the dissolved pool of trace metals in the nearshore waters of Majorca (Travor-Sánchez et al. 2014). Similar study was carried out in the coastal area of Balearic Islands. The results show that SGD is a major pathway for delivering dissolved Fe (4.1 mmol m^{-1} d^{-1}) and nutrients into the nearshore waters. This work emphasizes the relevance of SGD-driven trace metal inputs in the regulation of near-shore phytoplankton communities of oligotrophic areas (Rodellas et al. 2014). The discharge can be modified by red-ox phenomena as concluded by McAllister et al. (2014). However, geochemical cycles occurring at the interface between terrestrial and marine groundwater are not well understood for most elements. This is particularly true of the transition metals, many of which have particular ecological relevance as micronutrients or toxicants. The distribution of nine dissolved metals (Fe, Mn, Mo, V, Co, Ni, Cu, Pb, and Al) was investigated in the Great South Bay, New York, USA accompanied by a simple kinetic and chemical separation of labile and organic-complexed metal species. Dissolved Mn showed marked subsurface enrichment- suggestive of diagenetic remobilization. Dissolved Fe, however, was higher by more than three orders-of-magnitude in fresh groundwater (90 μM) as compared to marine groundwater (0.02 μM), and pH-mediated removal was evident as slightly acidic fresh groundwater (pH 6.8) mixed with marine groundwater (pH ~ 8.0). Dissolved Mo, Co, and Ni were primarily cycled with Mn, and highly elevated concentrations relative to bay surface waters were observed. High levels of dissolved Pb (up to 4250 pM) observed in the fresh groundwater were nearly quantitatively removed within the groundwater-seawater mixing zone. Dissolved Cu exhibited nonconservative removal, and was correlated with the

redox potential of the pore-waters. Substantial percentages (>15 %) of organic-metal species were only observed for Cu and Ni, suggesting that these complexes were not generally very important for the investigated metal cycling in the subterranean estuary. Kinetically labile species were observed for all metals examined except Cu and Pb, and represented an approximately constant proportion (between 10 and 70 %) of the total dissolved pool for each metal, indicating equilibrium between labile and non-labile species throughout the mixing zone. The nonconservative behavior observed for all metals examined in this study suggests that occuring reactions are vastly important to the source/sink function of permeable sediments. Thus studies seeking to quantify SGD-derived trace metal fluxes must take into account biogeochemical processes occurring in the subterranean estuary (Beck et al. 2010). In order to evaluate the role of SGD as a source of rare earth elements (REEs) in the coastal ocean, the SGD associated discharge of REEs were estimated into two semi-enclosed coastal bays in the southern coast of Korean peninsula. The mass balances of REEs proved that the REE fluxes were two to three orders of magnitude higher than those through other sources, such as diffusion from bottom sediments and atmospheric dust fallout. The neodymium (Nd) inputs from the two small coastal bays, Gamak Bay (148 km^2) and Hampyeong Bay (85 km^2), were estimated to be from 0.7×10^4 to 1.3×10^4 mol y^{-1}, which is 0.06–0.3 % of the total Nd flux from global rivers. In the study area coastal seawater was observed to have a substantially higher middle REE (MREE) due to a large discharge of highly enriched with MREE groundwater. The results suggest that the SGD-driven REE fluxes may contribute considerably to the global budget of REEs in the ocean (Kim and Kim 2014).

2.3.3   SGD as a Source of Mercury to the Marine Coastal Ecosystems

The mercury concentrations in groundwater and mercury flux associated with SGD have been a topic of several studies (Laurier et al. 2007; Bone et al. 2007; Black et al. 2009; Lee et al. 2011; Ganguli et al. 2012; Rahman et al. 2014). Laurier et al. (2007) measured the mercury concentrations not only in groundwater and seawater but also in blue mussels (Mytilus edulis) and concluded that high mercury concentrations were associated with strong seepage or long groundwater pathways. They also recognized SGD as a significant source of bioavailable mercury for mussels in the eastern part of the Seine Bay. Bone et al. (2007) observed high mercury release within the subterranean estuary, in the Waquoit Bay. They calculated that mercury flux via SGD is one order of magnitude greater than its atmospheric flux in the area. Black et al. (2009) calculated not only mercury concentrations and fluxes but also monomethylmercury concentrations and fluxes related to SGD on the California coast. They also proved that SGD could be

important source of both mercury and monomethylmercury to the coastal ecosystem similarly to Lee et al. (2011) and Ganguli et al. (2012).

Kwokal et al. (2014) assessed mercury speciation and distribution, for the first time, from the water, sediment, rock, soil and air of anchialine caves. They evaluated the origin and distribution of four mercury species—total (THg), reactive (RHg), dissolved gaseous mercury (DGHg) and monomethylmercury (MeHg) in water from Bjejajka cave and Lenga Pit in the Croatian Adriatic Sea from 2006 to 2011. Concentrations of all mercury species were elevated at both sites compared to adjacent seawater. The vertical distribution of MeHg concentrations followed that of THg, however the ratio of MeHg/THg above the Bjejajka halocline was drastically higher (up to 57 %) compared to MeHg proportion (1–2 %) below the halocline, which was similar to that of surface seawater. In sediment of Bjejajka, THg concentrations were considerably above concentrations in unpolluted Adriatic marine. The highest THg amounts found in soil and air were inside and in close proximity to Bjejajka, while THg in rock (≤ 0.01 mg kg^{-1}) were below reported values for unaltered carbonates.

Ganguli et al. (2012) evaluated the influence of groundwater-seawater interaction on mercury dynamics in Maunalua Bay, a coral reef ecosystem located on the south shore of 0'ahu, (Hawaii), by combining geochemical data with submarine groundwater discharge rates. During a rising tide, unfiltered total mercury (U–HgT) concentrations in seawater increase. It was attributed to an increase in suspended particulate matter at high tide. Approximately 90 % of mercury in groundwater was in the filtered (<0.45 μm) fraction. Groundwater discharge during a period of amplified SGD appeared to contribute to an increase in total mercury concentrations in filtered seawater and in unfiltered seawater. The larger magnitude of change in F–Hg$_T$ relative to U–Hg$_T$ suggests mercury complexation and/or solubility dynamics in seawater were altered by the addition of groundwater. The site specific Rn-222 derived SGD flux estimates and groundwater F–Hg$_T$ concentrations were used to calculate mercury loadings. A reported weighted average Maunalua Bay groundwater mercury flux of 0.68 ± 0.67 mol Year^{-1} was obtained by combining the proportional flux of F–HgT from three distinct SGD zones, and place these results into a broader context by comparing and contrasting flux estimates from locations around the world. It was concluded that results from existing SGD studies should be evaluated to develop future sampling strategies. Szymczycha et al. (2013) investigated both groundwater flow and mercury concentrations in pore water and seawater at a seeping site of the Bay of Puck, southern Baltic Sea. Seawater samples were characterized by elevated HgT$_D$ (total dissolved mercury) concentrations, as compared to concentrations in groundwater. High HgT$_D$ concentrations in pore water of the uppermost sediment layers were attributed to seawater intrusion into the sediment. The relationship between HgT$_D$ concentrations and salinity of pore water was nonconservative, indicating removal of dissolved mercury upon mixing seawater with groundwater. The mechanism of dissolved mercury removal was further elucidated by examining its relationships with both dissolved organic

matter, dissolved manganese (Mn II), and redox potential. It was concluded that groundwater is a factor that dilutes the mercury concentrations in pore water.

Rahman et al. (2014) investigated submarine groundwater discharge (SGD) and various solutes released with SGD, including Hg, in the Hampyeong Bay, a coastal embayment in the Yellow Sea, recently. It was established that SGD was the prime input source of Hg in the bay (12–18 mol Year^{-1}), contributing 65 % of the total input. Atmospheric deposition was the second dominant source of Hg (8.5 ± 2.7 mol Year^{-1}), contributing 31 % to the total input. The results of the current study suggest that SGD can be a significant source of Hg in estuarine/coastal systems; therefore, estimating the coastal mass budgets of Hg must include SGD as a prime source of Hg (Rahman et al. 2014).

2.3.4   SGD as a Source of Dissolved Carbon Species to the Coastal Marine Ecosystems

There are studies documenting that SGD is an important source of both dissolved organic carbon (DOC) and dissolved inorganic carbon (DIC) to the marine environment (Cai et al. 2003; Goñi and Gardner 2003; Moore 2003; Santos et al. 2009; Kim et al. 2011; Liu et al. 2012; Smith and Cave 2012; Brodecka et al. 2013). Cai et al. (2003) indicated that DIC concentration in groundwater is few orders of magnitude greater than in local rivers on the South Carolina coast. Goñi and Gardner (2003) estimated DOC fluxes via SGD in the same study area, however these fluxes were smaller in comparison with DIC fluxes. DIC and DOC fluxes via SGD into the Okatee, South Carolina exceeded river inputs to the marsh (Moore 2003). Both Santos et al. (2009) and Smith and Cave (2012) indicated that DOC fluxes via SGD were a source of dissolved organic carbon to the study areas, which were the west coast of Florida, Kinvara and Aughinish Bays, West Ireland respectively. Liu et al. (2012) proved that in spite of small SGD rates and the associated DIC fluxes were high compared to rivers. The DIC flux ranged from 23 to 53 % of the river DIC flux.

Substantial influence of SGD on CO_2 and methane distribution in coastal waters off Australia was reported by Maher et al. (2014), while large CO_2 loads delivered to the coastal sea-water via SGD—by Macklin et al. (2014). The later study proved that melioration of the near-shore swamps for developing housing districts greatly enhanced the loads. In the former study, however the question was not answered whether methane is delivered with SGD or diffuses from subsurface sediments layers, as documented in studies carried out in the southern Baltic Sea (Reindl and Bolalek 2012).

Liu et al. (2014) measured the average SGD flux (marine plus terrestrial groundwater) into the southwest Florida Shelf (SWFS). The terrestrial groundwater flux was of the same order of magnitude as the local river discharge. Shelf-water total alkalinity (TAlk) and dissolved inorganic carbon (DIC) concentrations could

not be explained by river inputs alone, suggesting a groundwater source. These T_{Alk} and DIC fluxes exceeded by a factor of 11–71 the combined input of local rivers, suggesting that SGD was the dominant source of TAlk and DIC to the SWFS during 2009. SGD is an important component of the inorganic carbon budget for the coastal ocean.

Porubsky et al. (2014) used multiple techniques, including thermal infrared aerial remote sensing, geophysical and geological data, geochemical characterization and radium isotopes, to evaluate the role of groundwater as a source of dissolved nutrients, carbon, and trace gases to the Okatee River estuary, South Carolina. Thermal infrared aerial remote sensing surveys illustrated the presence of multiple submarine groundwater discharge sites in Okatee headwaters. Significant relationships were observed between groundwater geochemical constituents and [226]Ra activity in groundwater with higher [226]Ra activity correlated to higher concentrations of organics, dissolved inorganic carbon, nutrients, and trace gases to the Okatee system. A system-level radium mass balance confirmed a substantial submarine groundwater discharge contribution of these constituents to the Okatee River. Diffusive benthic flux measurements and potential denitrification rate assays tracked the fate of constituents in creek bank sediments. Groundwater geochemical data indicated significant differences in groundwater chemical composition and radium activity ratios between the eastern and western sides of the river; these likely arose from the distinct hydrological regimes observed in each area. Groundwater from the western side of the Okatee headwaters was characterized by higher concentrations of dissolved organic and inorganic carbon, dissolved organic nitrogen, inorganic nutrients and reduced metabolites and trace gases, i.e. methane and nitrous oxide, than groundwater from the eastern side. Differences in organic matter supply, and/or groundwater residence time likely contributed to this pattern. The contrasting features of the east and west sub-marsh zones highlight the need for multiple techniques for characterization of submarine groundwater discharge sources and the impact of biogeochemical processes on the delivery of carbon to coastal areas via submarine groundwater discharge.

Intensity of carbon export from some areas seem to be especially intensive. These include mangrove areas. A majority of the global net primary production of mangroves is unaccounted for by current carbon budgets. It has been hypothesized that this "missing carbon" is exported as dissolved inorganic carbon (DIC) from subsurface respiration and groundwater (or pore-water) exchange driven by tidal pumping. Concentrations and $\delta^{13}C$ values of DIC, dissolved organic carbon (DOC), and particulate organic carbon (POC), along with radon (Rn-222, a natural submarine groundwater discharge tracer), were measured in a tidal creek in Moreton Bay, Australia. Concentrations and $\delta^{13}C$ values displayed consistent tidal variations, and mirrored the trend in Rn-222 in summer and winter. DIC and DOC were exported from, and POC was imported to, the mangroves during all tidal cycles. The exported DOC had a similar $\delta^{13}C$ value in summer and winter (about −30 parts per thousand). The exported $\delta^{13}C$ -DIC showed no difference between summer and

winter and had a δ^{13}C value slightly more enriched (similar to -22.5 parts per thousand) than the exported DOC. The imported POC had differing values in summer (similar to -16 parts per thousand) and winter (about -22 parts per thousand), reflecting a combination of seagrass and estuarine particulate organic matter (POM) in summer and most likely a dominance of estuarine POM in winter. A coupled Rn-222 and carbon model showed that 93–99 % of the DIC and 89–92 % of the DOC exports were driven by groundwater advection. DIC export averaged 3 g C m^{-2} d^{-1} and was an order of magnitude higher than DOC export, and similar to global estimates of the mangrove missing carbon (Maher et al. 2013). Carbon dioxide entering the coastal ecosystem with SGD is likely to influence pH of sea water there.

To better predict how ocean acidification will affect coral reefs, it is important to understand how biogeochemical cycles on reefs alter carbonate chemistry over various temporal and spatial scales. The study that quantifies the contribution of shallow pore-water exchange (as quantified from advective chamber incubations) and fresh groundwater discharge (as traced by Rn-222) to total alkalinity (TA) dynamics was carried out on a fringing coral reef lagoon along the southern Pacific island of Rarotonga over a tidal and diel cycle. Benthic alkalinity fluxes were affected by the advective circulation of water through permeable sediments, depending on the advection rate. Submarine groundwater discharge was a source of total alkalinity (TA) to the lagoon, with the highest flux rates measured at low tide, and an average daily TA flux of 1080 mmol m^{-2} d^{-1} at the sampling site. Both sources of TA were important on a reef-wide basis, although SGD acted solely as a delivery mechanism of TA to the lagoon, while pore water advection was either a sink or source of TA dependent on the time of day. This study describes overlooked sources of TA to coral reef ecosystems that can potentially alter water column carbonate chemistry. The authors suggest that pore-water and groundwater fluxes of TA should be taken into account in ocean acidification models in order to properly address changing carbonate chemistry within coral reef ecosystems (Cyronak et al. 2013). Szymczycha et al. (2014) ascent to the understanding that submarine groundwater discharge is an important yet poorly recognised pathway of material transport to the marine environment. They report on the results of dissolved inorganic carbon (DIC) and dissolved organic carbon (DOC) concentrations and loads in the groundwater seeping into the southern Baltic Sea. Most of the research was carried out in the Bay of Puck (2009–2010), while in 2013 the study was extended to include several other groundwater seepage impacted areas situated along the Polish coastline. The annual average concentrations of DIC and DOC measured in the groundwater were equal to 64.5 ± 10.0 mg C L^{-1} and 5.8 ± 0.9 mg C L^{-1} respectively. The carbon specific flux into the Bay of Puck was estimated at 850 mg m^{-2} year^{-1}. The loads of carbon via SGD were significant locally yet of limited importance for the entire Baltic Sea. It is concluded that the SGD derived carbon load to the Baltic Sea is an important component of the carbon budget, which gives the sea a firmly heterotrophic status.

Seidel et al. (2014) believes that seawater circulation in permeable coastal sediments is driven by tidal changes in hydraulic gradients. The resulting submarine groundwater discharge is a source of nutrients and dissolved organic matter (DOM) to the water column. Yet, little is known about the cycling of DOM within tidal sediments, because the molecular DOM characterization remains analytically challenging. One technique that can dissect the multitude of molecules in DOM is ultrahigh-resolution Fourier transform ion cyclotron resonance mass spectrometry (FT-ICR-MS). To aim at a high resolution DOM analysis the authors studied the seasonal turnover and marine and terrestrial sources of DOM in an intertidal creek bank of the southern North Sea down to 3 m depth and link the biogeochemical processes to FT-ICR-MS data and the analyses of inorganic pore water chemistry, $\delta^{13}C$ of solid-phase extracted dissolved organic carbon (SPE-DOC), dissolved black carbon (DBC) and dissolved carbohydrates (DCHO). Increasing concentrations of dissolved Fe, Mn, P, total alkalinity, dissolved nitrogen, DOC and a concomitant decrease of sulfate along the seawater circulation path from the upper tidal flat to the tidal flat margin indicate continuous microbial activity. The relative increase of Si concentrations, unsaturated aliphatics, peptide molecular formulae and isotopically more ^{13}C-enriched SPE-DOC towards the tidal flat margin suggests that remineralization processes mobilize DOM from buried algal (diatoms) and microbial biomass. Pore water in sediments <100 cm depth contains ^{13}C-depleted SPE-DOC and highly unsaturated compounds which are probably derived from eroded peats, suggesting rapid removal of bioavailable marine DOM such as DCHO from the water column and selective enrichment of terrestrial DOM. DBC concentrations are highest in the discharging pore water close to the tidal creek suggesting that the intertidal flat is an important DBC source to the coastal ocean. Pore water DOM accumulating at the low water line is enriched in N and S. Seidel et al. (2014) hypothesize that this is partly due to DOM reacting with dissolved sulfide and ammonium which may increase the refractory character of the DOM, hence making it less bioavailable for in situ active microbes. Maher et al. (2015) indicated that a majority of the global net primary production of mangroves is unaccounted for by current carbon budgets. The author hypothesized that this "missing carbon" is exported as dissolved inorganic carbon (DIC) from subsurface respiration and groundwater (or pore-water) exchange driven by tidal pumping. They measured $\delta^{13}C$ of dissolved organic carbon (DOC), and particulate organic carbon (POC), along with radon (Rn-222, a natural submarine groundwater discharge tracer), in a tidal creek in Moreton Bay, Australia. Concentrations and $\delta^{13}C$ values displayed consistent tidal variations, and mirrored the trend in Rn-222 in summer and winter. DOC was exported from, and POC was imported to, the mangroves during all tidal cycles. The exported DOC had a similar $\delta^{13}C$ value in summer and winter (equal to −30 parts per thousand). The imported POC had differing values in summer (equal to −16 parts per thousand) and winter (similar to −22 parts per thousand), reflecting a combination of seagrass and estuarine particulate organic matter (POM) in summer and most likely a dominance of estuarine POM in winter. A coupled Rn-222 and carbon model showed that 89–92 % of the DOC exports were driven by groundwater advection. Szymczycha et al. (2014)

measured dissolved organic carbon (DOC) concentrations and loads in the groundwater seeping into the southern Baltic Sea. Most of the research was carried out in the period 2010–2013. The annual average concentrations of DOC in the groundwater (5.8 ± 0.9 mg C L^{-1}) were an order of magnitude smaller than DIC.

2.3.5   SGD Impact on Coastal Ecology

The "Olhos de Agua" beach is the only area on the South coast of Portugal where submarine freshwater seepages have been identified. Encarnação et al. (2014) investigated the influence of SGD on benthic community there. According to the authors submarine groundwater discharges have been documented as contributing to the biological productivity of coastal areas, through a bottom-up support to higher trophic levels. Nevertheless, the effects on the bottom levels of the coastal food web, namely the meiofauna, are still very poorly known. In their study, meiofauna assemblages in the area impacted by SGD were compared with the meiofauna from a similar area, but without SGD. Samples were taken in Spring and Summer 2011, under different hydrological regimes, aquifer recharge (after Winter) and dryness (after Spring), respectively. The major changes in the community were recorded at a seasonal level, with higher abundances and number of taxa in Spring, when compared to Summer. This may be explained by better sediment aeration during spring along with higher food availability from the sedimentation of spring phytoplankton blooms. Although no significant differences were detected by multivariate analysis on the meiofauna abundances between Control and Impact areas, pair-wise tests on the interactions between factors in number of taxa (S) and species richness (Margalefs d) suggested that the discharge of groundwater stimulated an increase in meiofauna diversity. Such effect can be observed between the meiofauna assemblages from impacted and control areas and also between periods with different discharge regimes (Spring and Summer) in the impacted area. These findings highlight the role that freshwater discharges from coastal aquifers have on meiofauna assemblages and suggest that SGD contribute to enhance the transfer of energy from the lower levels of the trophic web to upper levels.

Results obtained by Kotwicki et al. (2014) support the findings. The discharge of groundwater into the sea affects surrounding environments by changing the salinity, temperature and nutrient regimes. This should lead to the spatial effects of a submarine groundwater discharge (SGD) on the abundance and structure of the meiofaunal community. The effect was investigated by Kotwicki et al. (2014) in the shallow area of Puck Bay (Baltic Sea). Result of several field expeditions in the years 2009 and 2010 indicated that low-saline groundwater escapes into the bay from permeable, sandy, near-shore sediments. The results provided evidence that the discharge of groundwater has a clear effect on meiofaunal assemblages in the research area. This effect was reflected in a significant decline of certain meiofaunal taxa, mainly Nematodes and Harpacticoids, as well as in altered patterns of temporal distribution and small-scale (vertical) zonation of meiofaunal assemblages.

2.4   Methods Used to Measure SGD

Quantifying groundwater discharge to the seas is a challenging task since groundwater flow is temporally and spatially variable. Submarine groundwater discharge is a part of a complex hydrological and hydrogeological problem of water exchange between land and sea (Zekster and Dzyuba 2014). Subsurface water exchange between land and ocean involves two inter-related processes: submarine discharge into seas and oceans and seawater intrusion into the shore. Quantification of groundwater discharge is a very difficult tusk as it depends on many factors such as hydrogeological conditions, weather parameters shifts and human management of the coastal ecosystem (McCoy and Corbett 2009). Groundwater discharge to the coastal ecosystem can be estimated by a number of methods. However, each technique has certain limitations because of generalized assumptions and natural variability. Typically researchers address limitations of the implemented method at particular study area or use several techniques to detect and measure SGD. The most popular methods used to quantyfy SGD are: hydrodynamic method for calculating lateral groundwater flow (Zekster and Dzyuba 2014); methods based on investigation of the coastal drainage area (Pierkarek-Jankowska 1994; Peltonen 2002); methods based on investigation of the sea (Peltonen 2002); modelling (Burnett et al. 2006; Moore 2010), direct measurements (Burnett et al. 2006; Moore 2010) and tracer techniques (Burnett et al. 2001, 2006; Moore 2010).

2.4.1   Seepage Meter

The direct measurement of groundwater seepage rates can be made using manual "seepage meter". First seepage meter was developed to measure water loss from irrigation canals by Israelsen and Reeve (1944). In 1977 Lee designed a seepage meter consisting of a 55-gallon (208 L) steel drum, fitted with a sample port and plastic collection bag (Fig. 2.3). The drum, in a shape of a chamber, is "open end down" inserted into the sediment. Groundwater seeping through the sediment displace water trapped in the chamber and forces it up through the port into the plastic bag. The actual volume of groundwater can be calculated using the end-member approach (Burnett et al. 2006; Szymczycha et al. 2012). The change in volume of water in the plastic bag over a measured time interval provides submarine groundwater discharge rate (Burnett et al. 2006; Taniguchi et al. 2006). There are several recommendation while using the seepage meter method. Typically, installation of few seepage meters is essential in order to average groundwater seepage rate because of temporal and spatial variability (Shaw and Prepas 1990a, b). The resistance of the tube and bag have to be minimized to prevent artefacts (Fellows and Brezonik 1980; Shaw and Prepas 1989; Belanger and Montgomery 1992). Covering the plastic bag may decrease the effects of surface water movements due to waves, currents or other activities (Libelo and MacIntyre 1994). Corbett and Cable (2000) suggested that
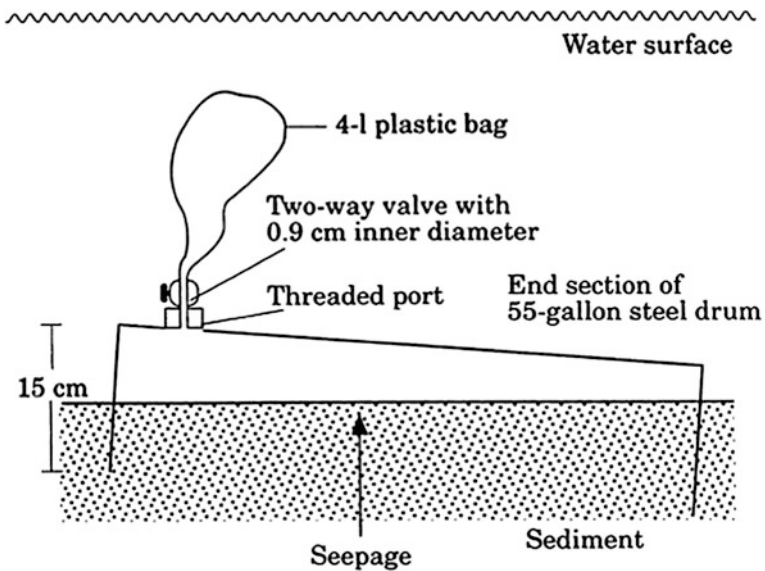
Fig. 2.3 Lee-type, manual seepage meter (Lee 1977). Water seeps through the sediment into the chamber and is forced into a plastic bag attached to a tube in the top of the drum. The change in volume over a measured time interval provides the groundwater seepage rate

seepage meter is a practical device for measuring groundwater rates, however it proves very labor intensive and time consuming.

This was a reason for developing automated seepage meters. Many types of automated seepage meters using different methods of water sensing were constructed (Burnett et al. 2006). Fukuo (1986), Cherkauer and McBride (1998), Boyle (1994) installed remote device from the surface of various water bodies. Others used: hydrothermal vents (Sayles and Dickinson 1990), ultrasonic measurements (Paulsen et al. 2001), heat-pulse devices (Krupa et al. 1998; Taniguchi and Fukuo 1993), continuous heat type automated seepage meters based on Granier method (Taniguchi and Iwakawa 2001) or dye-dilution seepage meters (Sholkovitz et al. 2003). The following conclusions and recommendations were suggested for using the seepage meter method: seepage meters (manual or automated) can give good results of groundwater discharge rates when used in a relatively calm environment (Burnett et al. 2006; Swarzenski and Izbicki 2009). In calm conditions seepage meters provide a direct measure of SGD, however the results are required to evaluate the pattern of SGD. These patterns most often relay on higher seepage at low tide and often, but not always, a decrease in seepage with increasing distance from the shore.

Seepage meters most often collect samples composed of both seeping groundwater and recirculated seawater. Contribution of both fractions can be separated applying the so called 'end members approach'.

The end-member method is one of the hydrograph separation methods based on the use of geochemical end-member concentrations (Burnett et al. 2006). The end-member approach is based on the mass balance:

$$D_S = D_G + D_{SW}$$
$$C_S D_S = C_G D_G + C_{SW} D_{SW}$$

where: C and D are the geochemical concentrations (C) and discharge rate (D). Subscripts S, G, SW represent respectively: collected sample, groundwater and seawater. Using the above two equations and the measured values of C_S, C_G, C_{SW}, D_S, the two unknowns, namely D_G and D_{SW} can be calculated. When salinity is used as a geochemical tracer, the separation of SGD into the seepage water components, fresh groundwater and recirculated seawater, is possible (Burnett et al. 2006; Szymczycha et al. 2012). Usually the end-member approach is used together with other methods. Good example of the end-member approach usage is described by Luek and Beck (2014). They indicated that the SGD ^{224}Ra end-member activity varied with seasonal pore water salinity fluctuations, representing end-member control on seasonal ^{224}Ra flux. Each Ra isotope suggested a different SGD volume flux, indicating that different nuclide regeneration rates can respond to and reflect different flow mechanisms in the subterranean estuary. The study designates that volume fluxes estimated using geochemical tracers are sensitive to SGD end-member variations and the end-member variability must be well-characterized for reliable SGD flux estimates.

2.4.2   Piezometers

In general, measurements of hydraulic conductivity and gradient of pore water combined with the Darcy Law characterise the principles of the method. Piezometer (usually multi-level piezometer nest) is inserted into the sediment in the groundwater impacted area. The groundwater potential can be measured at few depths (Freeze and Cherry 1979; Povinec et al. 2008) and the Darcian flux (q-groundwater discharge volume per unit area per unit time) can be calculated:

$$q = -K dh/dL$$

where K is hydraulic conductivity and dh/dL is the hydraulic gradient in which h is the hydraulic head and L is distance.

The serious limitation of the method is the natural variability in seepage fluxes. Because of that obtaining the representative hydraulic conductivity is difficult. However, the problem can be solved by combing the method with seepage meter method in order to estimate hydraulic conductivity from obtained seepage fluxes and the hydraulic gradient (Taniguchi 1995).

Piezometers referred to as groundwater lances (Szymczycha et al. 2012) can be applicative devices for pore water samples collecting, in order to obtain a two dimensional distribution of SGD composition (Charette et al. 2005; Beck et al. 2007). This method allows collecting pore water samples with high resolution and consequently the biogeochemistry of groundwater impacted coastal aquifer can be better characterized (Charette et al. 2005; Charette and Sholkovitz 2006; Beck et al. 2007, 2010; Pempkowiak et al. 2010; Szymczycha et al. 2012).

2.4.3 Natural Tracers

The natural tracers approach has been used over a wide range of scales from estuaries to continental shelves to estimate SGD. Natural tracers present an integrated signal when they enter seawater via different pathways. The selected natural geochemical tracers should be highly enriched or decreased within groundwater of the studied aquifer, compared to other sources of water e.g. rivers or rain (Burnett et al. 2006). To assess SGD by applying the natural tracer approach several others conditions also need to be defined, including concentrations of the tracer, water and tracer sources and sinks, boundary conditions (e.g. the study area, volume) and resistance time of the surface water body. After determining the conditions, simple mass balances or box models for the system can be constructed and SGD can be assessed.

Radium isotopes (^{223}Ra, ^{224}Ra, ^{226}Ra, ^{228}Ra) are highly concentrated in coastal groundwater and show conservative mixing (after radiation decay is considered) in the course of hydrogeological processes. This makes them ideal chemical tracers to quantify SGD and water mass ages in coastal zones (Moore 2010; Luo et al. 2014). Thus, radium isotopes (^{223}Ra, ^{224}Ra, ^{226}Ra) and radon (^{222}Rn) have been fairly frequently exploited for groundwater discharge quantification (Burnett et al. 2006). ^{224}Ra and ^{223}Ra were adopted as tracers to qualify submarine groundwater discharge (SGD) in Tolo Harbor, a highly urbanized embayment in Hong Kong (Luo et al. 2014). SGD was estimated to be 1.2–3.0 cm d^{-1}, lateral SGD was 5.7–7.9 cm d^{-1} and bottom SGD was 0.3–2.0 cm d^{-1}. Fresh SGD was estimated to be $(2.1$–$5.5) \times 10^5$ m^3 d^{-1} from the study area. The results expose that total SGD in this area represents about 1–2.4 % of the total sea water in the harbor and that fresh groundwater discharge is about 1.5–4 times larger than the total river discharge in the area. There is a good reason for radium isotopes and radon to be used to determine SGD. Relatively to the sea, they are highly enriched in salty and fresh coastal groundwater, thus even small fluxes of SGD can be identified through their strong signal.

Methane (CH$_4$), several natural radioactive isotopes (^{3}H,^{14}C, U) and stable isotopes (^{2}H, ^{3}He,^{4}He,^{13}C,^{15}N,) have also been used as geochemical tracers in SGD studies (Moore 2010). It has been proven that SGD can be an important source of CH$_4$ to coastal waters (Bugna et al. 1996). Other studies (Cable et al. 1996) presented that ^{222}Rn and CH$_4$ concentrations not only show positive relationships with seepage meters measurements but are also closely related to salinity.

Some isotopes, like uranium can be removed from anoxic sediments via saline SGD (Burnett et al. 2006) and therefore can be used as SGD tracers. Basu et al. (2001) recognized SGD as an important supplier of strontium to global oceans based on their studies on Sr and ^{87}Sr/^{86}Sr in the Bengal basin. Rahaman and Singh (2012) used strontium, ^{87}Sr/^{86}Sr and an inverse model to characterise SGD (combined freshwater and recycled seawater) with knowledge of seawater and river water end-member composition.

The natural tracer approach renders fine results in cases of big scale studies compared to the seepage meters or piezometers approach, however the challenging objective is identifying not only groundwater tracers but also all the other tracer sources and sinks in the system.

2.4.4 Infrared Imaging

Infrared thermography has been used to detect the location and spatial variability of SGD. The method exploits the temperature difference between surface water and groundwater during certain seasons and the fact that coastal and submarine springs can modify the colour and transparency of seawater (Mejías et al. 2012). The temperature of surface seawater (sea surface temperature-SST) can be detected by several methods like: NOAA-AVHRR, TERRA-MODIS and ARS/ENVISAT-AATSR satellite images (McClain et al. 1985; Reynolds and Smith 1994; Zavody et al. 1995; Mejías et al. 2012) which gives a suitable spatial and temporal resolution for detecting SGD. Infrared imaging is commonly used for SGD identification, but has not been applied to estimating the flux of SGD. Usually single images are not useful for quantifying SGD, they are quite appreciated in guiding field-work such as hydrogeologic and geochemical tracer based studies. The infrared image of the field site helped in planning field-work and in interpreting the hydraulic head data and seepage measurements (Mulligan and Charette 2006).

2.4.5 GIS Topology

Although many researchers agree on the importance of submarine groundwater discharge (SGD), it remains difficult to locate and quantify this process. A groundwater typology was developed based on local digital elevation models and compared to concurrent radon mapping indicative of SGD in the Niantic River, CT, USA (Rapaglia et al. 2015). Areas of high radon activity were located near areas of high flow accumulation lending evidence to the utility of this approach to locate SGD. The benefits of this approach are three-fold: fresh terrestrial SGD may be quickly located through widely-available digital elevation models at little or no cost to the investigator; fresh SGD may also be quantified through the GIS approach by multiplying pixelated flow accumulation with the expected annual recharge; and, as

these data necessarily quantify only fresh SGD, a comparison of these data with SGD, as calculated by Rn activity, may allow for the separation of the fresh and recirculated fractions of SGD. This exercise was completed for the Niantic River where SGD, as calculated by the GIS model, is 1.2 m^3/s, SGD as calculated by Rn activity is 0.73–5.5 m^3/s while SGD as calculated via a theoretical approach is 1.8–4.3 m^3/s. The fresh, terrestrial SGD accounts for 22–100 % of total SGD in the Niantic River.

2.4.6 Hydrologic Approach

The hydrologic approach for determining SGD can be separated into two main methods The first one is the mass balance method (Piekarek-Jankowska 1994; Peltonen 2002; Burnett et al. 2006) while the second is the Darcy's law calculation.

Simple water balance equation has been proven to be useful in some basins as an estimate of fresh SGD and can be described as:

$$P = E_T + D_S + D_G + dS$$

where P is precipitation, is E_T evapotranspiration, D_S is surface discharge, D_G is groundwater discharge and dS is the change in water storage (Burnett et al. 2006). The method is quite simple, but it has some limitations. First, precipitation, evapotranspiration, surface discharge, and the change in water storage need to be precisely determined. Secondly, the aquifer should be isolated by impermeable layers and discharging directly to the sea (Peltonen 2002). Thirdly, the limitation of the method is its implementation, only to formations, where the value of deep infiltration exceeds the accuracy of other components of the water balance equation (Zekster et al. 1973). It is said that water balance method is suitable to estimate the fresh groundwater discharge (Moore 2010).

The Darcy law is usually used together with other methods like piezometers, though the measurement of soil permeability and hydraulic head at few locations are essential. First, the field data are collected and then, SGD rate can be calculated with Darcy law.

2.4.7 Mathematical Models

Different kinds of models have been developed over the past 50 years and have become an invaluable tool for understanding subsurface flow in coastal aquifers (Li et al. 1999; McCOy and Corbett 2009). The mathematical and numerical simulations represent a form of differential equations for both: the flux and the transport phenomena. Analytical solutions to differential equations can be implemented in a limited number of cases, in which the aquifers are both homogenous and isotropic

and boundary conditions are simple whereas numerical models can be used in heterogeneous, anisotropic aquifers (Peltonen 2002). The benefits of numerical hydrogeologic models are that they provide the opportunity to simplify key features in aquifer systems and enable analysis of groundwater and saltwater movement under varying conditions (pre-pumping, pumping, future) that are not possible to estimate by other methods. Once the hydrogeologic framework has been described and effectively simulated, current and future SGD estimates can be evaluated by simply entering and changing model input parameters as they change with time. In general, hydrogeologic models are limited by the availability of data (e.g. groundwater pumping, hydraulic head, hydrostratigraphic, transmissivity) and must be validated periodically by other independent methods such as direct measurement and/or geochemical tracers.

There are several different model approaches, each characteristic to a certain study area or interactions between surface water, groundwater and seawater (Sadurski 2000; Massel et al. 2005).

The general suggestion for using numerical models to simulate groundwater flow is to implement the complementary numerical approach, in which the salinity distribution in the surface water is simulated by a three dimensional (3D) numerical model in order to determine the location and strength of SGD (Burnett et al. 2006). A good example of such model is PCFLOW3D, a 3D, non-linear baroclinic numerical model which was used in the groundwater impacted area of Donnalucata, Sicily (Burnett et al. 2006). The simulation results were in line with the observations of SGD-rates.

In the Baltic Sea region estimation of groundwater discharge from the territory of Poland was also calculated using analytical and numerical models (Kryza and Kryza 2006). The geological construction and hydrogeological conditions were characterized on the basis of regional elaboration and numerous publications. Then hydrogeological schema was set for area of water supply of the waterside zone of the sea. Four main aquifers were assigned and their parameters were characterized. Along cross-section above 500 km long analytic counts of direct inflow of groundwater to the Baltic Sea were performed. Numeric models for four representative areas ware constructed indicating zones of groundwater direct inflow to the Baltic Sea. Calculations based on analytical and numerical models were reported comparable.

References

Badon-Ghyben W (1888–1889) Nota in verband met de voorgenomen putboring nabij Amsterdam. Koninklyk Instituut Ingenieurs Tijdschrift. The Hague 8-22 in Bear J, Cheng HD, Sorek S, Ouuzar D, Herrera I, 1999. Seawater intrusion in coastal aquifers—Concepts, methods and practices. Kluwer Academic Publishers, Dordrecht, the Netherlands, 625 pp

Basu AR, Jacobsen SB, Poreda RJ, Dowling CB, Aggarwal PK (2001) Large groundwater strontium flux to the oceans from the Bengal Basin and the marine strontium isotope record. Science 293:1470–1473

Baumann T, Fruhstorfer P, Klein T, Niessner R (2006) Colloid and heavy metal transport at landfill sites in direct contact with groundwater. Water Res 40:2776–2786

Bear J, Cheng HD, Sorek S, Ouuzar D, Herrera I (1999) Seawater intrusion in coastal aquifers - concepts, methods and practices. Kluwer Academic Publishers, Dordrecht, the Netherlands, p 625

Beck AJ, Rapaglia JP, Cochran JK, Bokuniewicz HJ (2007) Radium mass-balance in Jamaica Bay, NY: evidence for substantial flux of submarine groundwater. Mar Chem 106:419–441

Beck AJ, Cochran JK, Sañudo-Wilhelmy SA (2009) Temporal trends of dissolved trace elements in Jamaica Bay, NY: importance of wastewater input and submarine groundwater discharge in an urban estuary. Estuar Coasts 32:535–550

Beck AJ, Cochran JK, Sañudo-Wilhelmy SA (2010) The distribution and speciation of dissolved trace metals in a shallow subterranean estuary. Mar Chem 121:145–156

Belanger TV, Montgomery ME (1992) Seepage meter errors. Limnol Oceanogr 37:1787–1795

Beusen AHW, Slomp CP, Bouwman AF (2013) Global land-ocean linkage: direct inputs of nitrogen to coastal waters via submarine groundwater discharge. Environ Res 8. doi:10.1088/1748-9326/8/3/034035

Black FJ, Payian A, Knee KL, De Sieyes NR, Ganguli PM, Gray E, Flegal R (2009) Submarine groundwater discharge of total mercury and monomethylmercury to central coastal waters. Environ Sci Technol 43:5652–5659

Bokuniewicz H (1980) Groundwater seepage into Great South Bay, New York. Estuarine Coastal and Shelf. Science 10:437–444

Bokuniewicz H, Pavlik B (1990) Groundwater seepage along a barrier island. Biogeochemistry 10:257–276

Bone SE, Charette MA, Lamborg CH, Gonneea ME (2007) Has Submarine groundwater discharge been overlooked as a source of mercury to a coastal waters? Environ Sci Technol 41:3090–3095

Boudreau BP, Huettel M, Froster S, Jahnke RA, McLachlan A, Middelburg JJ, Nielsen PV, Sansone F, Taghon G, Van Raaphorst W, Webster I, Węsławski JM, Wiberg P, Sundby B (2001) Permeable marine sediments: overturning an old paradigm. Trans Am Geophys Union 8:133–136

Boyle DR (1994) Design of a seepage meter for measuring groundwater fluxes in the nonlittoral zones of lakes-evaluation in a boreal forest lake. Limnol Oceanogr 39:670–681

Brodecka A, Majewski P, Bolałek J, Klusek Z (2013) Geochemical and acustic evidence for the occurance of methane in sediments of the Polish sector of the southern Baltic Sea. Oceanologia 55:951–978

Bugna GC, Chanton JP, Young JE, Burnett WC, Cable PH (1996) The importance of groundwater discharge to the methane budget of nearshore and continental shelf waters of the NE Gulf of Mexico. Geochim Cosmochim Acta 60:4735–4746

Burnett WC (1999) Offshore springs and seeps are focus of working group. Trans Am Geophys Union 80:13–15

Burnett WC, Taniguchi M, Oberdorfer J (2001) Measurements and significance of the direct discharge of groundwater into the coastal zone. J Sea Res 46:109–116

Burnett WC, Bokuniewicz HJ, Huettel M, Moore WS, Taniguchi M (2003) Groundwater and pore water inputs to the coastal zone. Biogeochemistry 66:3–33

Burnett WC, Aggarwal PK, Aureli A, Bokuniewicz HJ, Cable JE, Charette MA, Kontar E, Krupa S, Kulkarni KM, Loveless A, Moore WS, Oberdorfer JA, Oliveira J, Ozyurt N, Povinec P, Privitera AMG, Rajar R, Ramessur RT, Scholten J, Stieglitz T, Taniguchi M, Turner JV (2006) Quantifying submarine groundwater discharge in the coastal zone via multiple methods. Sci Total Environ 367:498–543

Cable JE, Bugna G, Burnett W, Chanton J (1996) Application of 222Rn and CH$_4$ for assessment of groundwater discharge to the coastal ocean. Limnol Oceanogr 41:1347–1353

Cai WJ, Wang YC, Krest J, Moore WS (2003) The geochemistry of dissolved inorganic carbon in a surficial groundwater aquifer in North Inlet, South Carolina, and the carbon fluxes to the coastal ocean. Geochim Cosmochim Acta 67:631–639

Capone DG, Bautista MF (1985) A groundwater source of nitrate in nearshore marine sediments. Nature 313:214–216

Capone DG, Slater JM (1990) Interannual patterns of water table height and groundwater derived nitrate in nearshore sediments. Biogeochemistry 10:277–288

Charette MA, Sholkovitz ER (2002) Oxidative precipitation of groundwater-derived ferrous iron in the subterranean estuary of a coastal bay. Geophys Res Lett 29:1444–1452

Charette MA, Sholkovitz ER (2006) Trace element cycling in a subterranean estuary: Part 2. Geochemistry of the pore water. Geochemica et Cosmochimica Acta 70:811–826

Charette MA, Sholkovitz ER, Hansel CM (2005) Trace element cycling in a subterranean estuary Part 1. Geochemistry of the permeable sediments. Geochemica et Cosmochimica Acta 66:2095–2109

Cherkauer BS, McBride JM (1998) A remotely operated seepage meter for use in large lakes and rivers. Ground Water 26:165–171

Corbett DR, Chanton J, Burnett W, Dillon K, Rutkowski C, Fourqurean J (1999) Patterns of groundwater discharge into Florida Bay. Limnol Oceanogr 44:1045–1055

Corbett DR, Dillon K, Burnett W, Chanton J (2000) Estimating the groundwater contribution into Florida Bay via natural tracers 222Rn and CH$_4$. Limnol Oceanogr 45:1546–1557

Crotwell AM, Moore WS (2003) Nutrient and radium fluxes from submarine groundwater discharge to Port Royal Sound, South Carolina. Aquat Geochem 9:191–208

Cyronak T, Santos IR, Erler DV, Eyre BD (2013) Groundwater and pore water as major sources of alkalinity to a fringing coral reef lagoon (Muri Lagoon, Cook Islands). Biogeosciences 10:2467–2480

D'Elia CF, Webb DKL, Porter JW (1981) Nitrate-rich groundwater inputs to Discovery Bay, Jamaica: a significant source of N to local coral reefs? Bull Mar Sci 31:903–910

Encarnação J, Leitão F, Range P, Piló D, Chícharo MA, Chícharo L (2014) Local and temporal variations in near-shore macrobenthic communities associated with submarine groundwater discharges. Marine Ecology, 1-16. doi:10.1111/maec.12186

Fellows CR, Brezonik PL (1980) Seepage flow in Florida lakes. Water Resour Bull 16:635–641

Freeze RA, Cherry JA (1979) Groundwater. Englewood Cliffs, New York, The United States pp. 604

Fukuo Y (1986) Studies on groundwater seepage in the bottom of Lake Biwa. Report for Environmental Sciences by the Ministry of Education. Sci Culture 4:1949–1953

Ganguli PM, Conway CH, Swarzenski Izbicki JA, Flegal AR (2012) Mercury speciation and transport via submarine groundwater discharge at a southern california coastal lagoon system. Environ Sci Technol 46:1480–1488

Glover RE (1964) The patterns of fresh-water flow in a coastal aquifer: sea water in coastal aquifers. In: Cooper HH, Kohout FA, Henry HR, Glover RE (eds) Geological Survey Water Supply Paper, Washington, The United States, pp. 32–35

Gonneea ME, Charette MA, Liu Q, Herrera-Silveira JA, Morales-Ojeda SM (2014) Trace element geochemistry of groundwater in a karst subterranean estuary (Yucatan Peninsula, Mexico). Geochemica et Cosmochimica 132:31–49

Goñi MA, Gardner LR (2003) Seasonal dynamics in dissolved organic carbon concentrations in a coastal water-table aquifer at the forest-marsh interface. Aquat Geochem 9:209–232

Henry HR (1964) Interface between salt water and fresh water in a coastal aquifer: Sea water in coastal aquifers. In: Cooper Jr. HH, Kohout FA, Henry HR, Glover RE (eds) Geological Survey Water Supply Paper, Washington, The United States, pp. 35–70

Herzberg A (1901) Die wasserversorgung einiger Nordseebader. Journal Gasbeleuchtung und Wasseversorgung 44, 815–819, 842–844 in Bear J, Cheng HD, Sorek S, Ouuzar D, Herrera I, 1999. Seawater intrusion in coastal aquifers—concepts, methods and practices. Kluwer Academic Publishers, Dordrecht, the Netherlands, pp. 625

Hu C, Muller-Karger FE, Swarzenski PW (2006) Hurricanes, submarine groundwater discharge, and Florida's red tides. Geophys Res Lett 33:1–5

Hubbert MK (1940) The theory of ground-water motion. J Geol 48:785–944

Hwang DW, Kim GB, Lee YW, Yang HS (2005) Estimating submarine inputs of groundwater and nutrients to a coastal bay by using radium isotopes. Mar Chem 96:61–71

Ibánhez JSP, Leote C, Rocha C (2012) Seasonal enhancement of submarine groundwater discharge (SGD)-derived nitrate loading into Ria Formosa coastal lagoon assessed by 1-D modeling of benthic NO3- profiles. Estuar Coast Shelf Sci 132, 56–63, doi:10.1016/j.ecss.2012.04.015

Israelsen OW, Reeve RC (1944) Canal lining experiments in the delta area. Utah Agric Exp Stat Technol Bull 313, Utah, The United States, pp. 52

Jeong J, Kim G, Han S (2012) Influence of trace elements fluxes from submarine groundwater discharge (SGD) on their inventories in coastal waters off volcanic island, Jeju, Korea. Appl Geochem 27:37–43

Ji T, Du J, Moore WS, Zhang G, Su N, Zhang J (2013) Nutrient inputs to a Lagoon through submarine groundwater discharge: the case of Laoye Lagoon, Hainan, China. J Mar Syst 111:253–262

Johannes RE (1980) The ecological significance of the submarine groundwater discharge of ground water. Mar Ecol Progress Ser 3:365–373

Kim I, Kim G (2014) Submarine groundwater discharge as a main source of rare earth elements in coastal waters. Mar Chem 160:11–17

Kim G, Kim JS, Hwang DW (2011) Submarine groundwater discharge from oceanic islands standing in oligotrophic oceans: implications for global biological production and organic carbon fluxes. Limnol Oceanogr 56:673–682

Kohout FA (1965) A hypothesis concerning cyclic flow of salt water related to geothermal heating in the Floridian aquifer. Trans NY Acad Sci 28:249–271

Kohout FA (1966) Submarine springs: a neglected phenomenon of coastal hydrology. Hydrology 26:391–413

Kohout FA, Kolpinski MC (1967) Biological zonation related to groundwater discharge along the shore of Biscayne Bay, Miami Florida. Estuaries, Jekyll Island, Georgia, The United States, pp 1–3

Kotwicki L, Grzelak K, Czub M, Dellwig O, Gentz T, Szymczycha B, Brottcher M (2014) Submarine groundwater discharge to the Baltic coastal zone—Impact on the meiofaunal community. J Mar Syst 129:118–126

Krest JM, Moore WS, Gardner LR (2000) Marsh nutrient export supplied by groundwater discharge: evidence from radium measurements. Glob Biogeochem Cycles 14:167–176

Kroeger KD, Swarzenski PW, Greenwood JW, Reich C (2007) Submarine groundwater discharge to Tampa Bay: nutrient fluxes and biogeochemistry of the aquifer. Mar Chem 104:85–97

Krupa SL, Belanger TV, Heck HH, Brok JT, Jones BJ (1998) Krupaseep- the next generation seepage meter. J Coast Res 25:391–413

Kryza J, Kryza H (2006) The analytic and model estimation of the direct groundwater flow to Baltic Sea on the territory of Poland. Geologos 10:154–165

Kwokal Z, Cukrov N, Cuculic V (2014) Natural causes of changes in marine environment: Mercury speciation and distribution in anchialine caves. Estuar Coast Shelf Sci 151:10–20

Lapointe BE, O'Connell JD (1989) Nutrient-enhanced growth of Cladophora prolifera in Harrington Sound, Bermuda: eutrophication of a confined, phosphorous-limited marine ecosystem. Estuar Coast Shelf Sci 28:347–360

Lapointe BE, O'Connell JD, Garrett GS (1990) Nutrient coupling between on-site sewage disposal systems, groundwaters, and nearshore surface waters of Florida Keys. Biogeochemistry 10:289–307

LaRoche J, Nuzzi R, Waters R, Wyman K, Falkowski PG, Wallece DWR (1997) Brown tides blooms in Long Island's coastal waters linked to interannual variability in groundwater flow. Glob Change Biol 3:397–410

Laurier FJG, Cossa D, Beucher C, Brévière E (2007) The impact of groundwater discharges on mercury portioning, speciation and bioavailability to mussels in a coastal zone. Mar Chem 106:352–364

Lee DR (1977) A device for measuring seepage flux in lakes and estuaries. Limnol Oceanogr 22:40–147

Lee YW, Kim G (2007) Linking groundwater-borne nutrients and dinoflagellate red-tide outbreaks in the southern sea of Korea using a Ra tracer. Estuar Coast Shelf Sci 71:309–317

Lee YW, Hwang DW, Kim G, Lee WC, Oh HT (2009) Nutrient inputs from submarine groundwater discharge (SGD) in Masan Bay, an embayment surrounded by heavily industrialized cities, Korea. Sci Total Environ 407:3181–3188

Lee YW, Rahman MDM, Kim G, Han S (2011) Mass balance of total mercury and monomethylmercury in coastal embayments of a volcanic islands: significance of submarine groundwater discharge. Environ Sci Technol 45:9891–9900

Leote C, Ibánhez JPS, Rocha C (2008) Submarine groundwater discharge as a nitrogen source to the Ria Formosa studied with seepage meters. Biogeochemistry 88:185–194

Li L, Barry DA, Stagnitti F, Parlange JY (1999) Submarine groundwater discharge and associated chemical input to a coastal sea. Water Resour Res 35:3253–3259

Libelo EL, MacIntyre WG (1994) Effects of surface-water movement on seepage-meter measurements of flow through the sediment-water interface. Hydrogeol J 2:49–54

Liu Q, Dai M, Chen W, Huh CA, Wang G, Li Q, Charette MA (2012) How significant is submarine groundwater discharge and its associated dissolved inorganic carbon in a river-dominated shelf system. Biogeosciences 9:1777–1795

Liu Q, Charette MA, Henderson PB, Mccorkie DC, Martin W, Dai M (2014) Effect of submarine groundwater discharge on the coastal ocean inorganic carbon cycle. Limnol Oceanogr 59:1529–1554

Luek JL, Beck AJ (2014) Radium budget of the York River estuary (VA, USA) dominated by submarine groundwater discharge with a seasonally variable groundwater end-member. Marine Chemistry 165, 55–65

Luo X, Jiao JJ, Moore WS, Lee CM (2014) Submarine groundwater discharge estimation in an urbanized embayment in Hong Kong via short-lived radium isotopes and its implication of nutrient loadings and primary production. Mar Pollut Bull 82:144–154

Macklin PA, Maher DT, Santos IR (2014) Estuarine canal estate waters: Hotspots of CO_2 outgassing driven by enhanced groundwater discharge? Mar Chem 167:82–92

Maher DT, Santos IR, Golsby-Smith L, Gleeson J, Eyre BD (2013) Groundwater-derived dissolved inorganic and organic carbon exports from a mangrove tidal creek: the missing mangrove carbon sink? Limnolol Oceanogr 58:475–479

Maher DT, Cowley K, Santos IR, Macklin P, Eyre DB (2015) Methane and carbon dioxide dynamics in a subtropical estuary over a diel cycle: insights from automated in situ radioactive and stable isotope measurements. Mar Chem 168:69–79

Makings U, Santos IR, Maher DT, Golsby-Smith L, Eyre RB (2014) Importance of budgets for estimating the input of groundwater-derived nutrients to an eutrophic tidal river and estuary. Estuar Coast Shelf Sci 143:65–76

Marsh JA (1977) Terrestrial inputs of nitrogen and phosphates on fringing reefs on Guam. In: Proceedings of third international cora reef symposium, Miami, Florida, The United States, pp. 331–336

Massel S, Przyborska A, Przyborski M (2005) Attenuation of wave-induced groundwater pressure in shallow water. Part 2. Theory. Oceanologia 47:232–291

McAllister SM, Barnett JM, Heiss JW, Findlay AJ, MacDonald DJ, Dow CJ, Luther GW III, Michael HA, Chan CS (2014) Dynamic hydrologic and biogeochemical processes drive microbially enhanced iron and sulfur cycling within the intertidal mixing zone of a beach aquifer. Limnol Oceanogr 60:329–345

McBride MS, Pfannkuch HO (1975) The distribution of seepage within lakebed. J Res US Geol Surv 3:505–512

McClain E, Pichel WG, Walton C (1985) Comparative performance of AVHRR multichannel sea surface temperature. J Geophys Res 90:11587–11601

McCoy CA, Corbett DR (2009) Review of submarine groundwater discharge (SGD) in coastal zones of the Southeast and Gulf Coast regions of the United States with management implications. J Environ Manag 90:644–651

Mejías M, Ballesteros J, Antón-Pacheco C, Domíngeuz JA, Garcia-Orellana J, Garcia-Solsona E, Masqué P (2012) Methodological study of submarine groundwater discharge from a kartsic aquifer in the Western Mediterranean Sea. J Hydrol 464:27–40

Michael HA, Mulligan AE, Harvey CF (2005) Seasonal water exchange between aquifers and the coastal ocean. Nature 436:1145–1148

Moore WS (1997) High fluxes of radium and barium from the mouth of the Ganges-Brahmaputra River during low river discharge suggest a large groundwater source. Earth Planet Sci Lett 150:141–150

Moore WS (1999) The subterranean estuary: a reaction zone of ground water and sea water. Mar Chem 65:111–125

Moore WS (2003) Sources and fluxes of submarine groundwater discharge delineated by radium isotopes. Biogeochemistry 66:75–93

Moore WS (2009) Submarine groundwater discharge. In: Steele JH, Thorpe SA and Turekian KK (eds) The Coastal Ocean, 2010. Oxford, The United Kingdom, 153–160

Moore WS (2010) The effect of submarine groundwater discharge on the ocean. Ann Rev Mar Sci 2:59–88

Mulligan AE, Charette MA (2006) Intercomparison of submarine groundwater discharge estimates from a sandy unconfined aquifer. J Hydrol 327:411–425

Mulligan AE, Charette MA (2009) Groundwater flow to the coastal ocean. In: Steele JH, Thorpe SA and Turekian KK (eds) The Coastal Ocean, 2010. Oxford, The United Kingdom, 143–152

Oberdorfer JA, Valentino MA, Smith SV (1990) Groundwater contribution to the nutrient budget of Tomas Bay, California. Biogeochemistry 10:199–216

Paulsen RJ, Smith CF, O'Rourke D, Wong T (2001) Development and evaluation of an ultrasonic ground water seeping meter. Ground Water 39:904–911

Peltonen K (2002) Direct groundwater flow to the Baltic Sea. Nordic Council of Ministers, Temanord, Copenhagen 78 pp

Pempkowiak J, Szymczycha B, Kotwicki L (2010) Submarine groundwater discharge (SGD) to the Baltic Sea. Rocznik Ochrony Środowiska 12:17–32

Piekarek-Jankowska H (1994) Zatoka Pucka jako obszar drenażu wód podziemnych. Wydawnictwo Uniwersytetu Gdańskiego. Gdańsk, 31–32, Poland

Piekarek-Jankowska H (1996) Hydrochemical effects of submarine groundwater discharge to the Puck Bay (Southern Baltic Sea, Poland). Geographia Polonica 67:103–119

Porubsky WP, Weston NB, Moore WS, Ruppel C, Joye SB (2014) Dynamics of submarine groundwater discharge and associated fluxes of dissolved nutrients, carbon, and trace gases to the coastal zone (Okatee River estuary, South Carolina). Geochim Cosmochim Acta 131:81–97

Povinec PP, Bokuniewicz HJ, Burnett WC, Cable J, Charette M, Comanducci JF, Kontar EA, Moore WS, Oberdorfer JA, de Oliveira J, Peterson R, Stieglitz T, Taniguchi M (2008) Isotope tracing of submarine groundwater discharge offshore Ubatuba, Brazil: results of the IAEA–UNESCO SGD project. J Environ Radioact 99:1596–1610

Rahaman W, Singh SK (2012) Sr and 87Sr/86Sr in estuaries of western India: impact of submarine groundwater discharge. Geochim Cosmochim Acta 85:275–288

Rahman MM, Lee YG, Kim G, Lee K, Han S (2014) Significance of submarine groundwater discharge in the coastal fluxes of mercury in Hampyeong Bay, Yellow Sea. Chemosphere 91:320–327

Rapaglia J, Grant C, Bokuniewicz H, Pick T, Scholten J (2015) A GIS typology to locate sites of submarine groundwater discharge. J Environ Radioact 145:10–18

Reindl A, Bolałek J (2012) Methane flux from sediment into near-bottom water in the coastal area of the Puck Bay (Southern Baltic). Oceanol Hydrobiol Stud 41:40–47

Reynolds RW, Smith TM (1994) Improved global sea surface temperature analyses using optimum interpolation. J Clim 7:929–936

Rodellas V, Garcia-Orellana J, Tovar-Sanchez A, Basterretxea G, López-Garcia JM, Sánchez-Quiles D, Garcia-Solsona E, Masqué P (2014) Submarine groundwater discharge as a source of nutrients and trace metals in a Mediterranean bay (Palma Beach, Balearic Islands). Mar Chem 160:56–66

Sadurski A (2000) Hydrogeology of the coastal aquifers. Proceeding of the 16th salt water intrusion meeting, Międzyzdroje–Wolin Island, Poland, pp 80

Santos IR, Burnett WC, Dittmar T, Suryaputra IGNA, Chanton J (2009) Tidal pumping drives nutrient and dissolved organic matter dynamics in a Gulf of Mexico subterranean estuary. Geochemica Cosmochimica Acta 73:1325–1339

Sayles FL, Dickinson WH (1990) The seep meter: a benthic chamber for the sampling and analysis of low velocity hydrothermal vents. Deep-Sea Res 88:1–13

Santos IR, de Weys J, Tait DR, Eyre BD (2013) The contribution of groundwater discharge to nutrient exports from a coastal catchment: post-flood seepage increases estuarine N/P ratios. Estuar Coasts 36:56–73

Sañudo-Wilhelmy SA, Rossi FK, Bokuniewicz H, Paulsen RJ (2002) Trace metal levels in uncontaminated groundwater of a coastal watershed: importance of colloidal forms. Environ Sci Technol 36:1435–1441

Seidel M, Beck M, Thomas R, Waska H, Suryaputra IGNA, Schnetger B, Niggemann J, Meinhard S, Thorsten D (2014) Biogeochemistry of dissolved organic matter in an anoxic intertidal creek bank. Geochemica et Cosmochimica Acta 140:418–434

Shaw RD, Prepas EE (1990a) Groundwater-lake interactions: I. Accuracy of seepage meter estimations of lake seepage. J Hydrol 119:105–120

Shaw RD, Prepas EE (1990b) Groundwater–Lake interactions II. Nearshore seepage patterns and the contribution of ground water lakes in central Alberta. J Hydrol 119:121–136

Shaw RD, Moore WS, Kloepfer J, Sochaski MA (1998) The flux of barium to the coastal waters of the southeastern USA: The importance of submarine groundwater discharge. Geochimica at Cosmochimica Acta 73:1325–1339

Sholkovitz ER, Herbolg C, Charette MA (2003) An automated dye-dilution based on seepage meter for the time-series measurements of submarine groundwater discharge. Limnol Oceanogr Methods 1:17–29

Simmons GM (1992) Importance of submarine groundwater discharge (SGWD) and seawater cycling to material flux across sediment water interfaces in marine environments. Mar Ecol Progress Ser 84:173–184

Slomp CP, Van Cappellen P (2004) Nutrient inputs to the coastal ocean through submarine groundwater discharge: controls and potential impact. J Hydrol 295:64–86

Smith AM, Cave RR (2012) Influence of fresh water, nutrients and DOC in two submarine-groundwater-fed estuaries on west of Ireland. Sci Total Environ 438:260–270

Swarzenski PW, Izbicki JA (2009) Coastal groundwater dynamics off Santa Barbara, California: combining geochemical tracers, electromagnetic seepmeters, and electrical resistivity. Estuar Coast Shelf Sci 83:77–89

Szymczycha B, Vogler S, Pempkowiak J (2012) Nutrients fluxes via submarine groundwater discharge to the Bay of Puck, Southern Baltic. Sci Total Environ 438:86–93

Szymczycha B, Miotk M, Pempkowiak J (2013) Submarine Groundwater Discharge as a source of mercury in the Bay of Puck. Water Soil Air Pollution 224. doi:10.1007/s11270-013-1542-0

Szymczycha B, Maciejewska A, Winogradow A, Pempkowiak J (2014) Could submarine groundwater discharge be a significant carbon source to the southern Baltic Sea? Oceanologia 56:327–347

Taniguchi M (1995) Change in groundwater seepage rate into Lake Biwa, Japan. Jpn J Limnol 56:261–267

Taniguchi M, Fukuo Y (1993) Continuous measurements of groundwater seepage using an automated seepage meter. Ground Water 31:675–679

Taniguchi M, Iwakawa H (2001) Measurements of submarine groundwater discharge rates by continous heat-type automated seepage meter in Osaka Bay, Japan. J Groundw Hydrol 42: 271–277

Taniguchi M, Burnett WC, Cable JE, Turner JV (2002) Investigation of submarine groundwater discharge. Hydrol Process 16:2115–2129

Taniguchi M, Burnett WC, Dulaiova H, Kontar EA, Povinec PP, Moore WS (2006) Submarine groundwater discharge measured by seepage meters in sicilian coastal waters. Cont Shelf Res 26:835–842

Thompson Reuters, Web of Knowledge. https://apps.webofknowledge.com

Travor-Sánchez A, Basterretxea G, Rodellas V, Sánchez-Quiles D, García-Orellana J, Masqué P, Jordi A, López JM, Garcia-Solsona E (2014) Contribution of groundwater discharge to the coastal dissolved nutrients and trace metal concentrations in Majorca Island: karstic vs detrital systems. Environ Sci Technol 24:11819–11827

Vacher HL (1988) Dupuit–Ghyben–Herzberg analysis of strip-island lenses. Geol Soc Am Bull 100:580–591

Valiela I, Teal JM, Volkman S, Shafer D, Carpenter EJ (1978) Nutrient and particulate fluxes in salt marsh ecosystem: tidal exchanges and inputs by precipitation and groundwater. Limnol Oceanogr 23:798–812

Valiela I, Foreman K, LaMontagne M, Hersh D, Costa J, Peckol P, DeMeo-Anderson B, D'Avanzo D, Babione M, Sham CH, Brawlej J, Lajtha K (1992) Coupling of watersheds and coastal waters: sources and consequences of nutrient enrichment in Waquoit Bay, Massachusetts. Estuaries 15:443–457

Valiela I, Bowen JL, Kroeger KD (2002) Assesment of models for estimation of land-derived nitrogen loads to shallow estuaries. Appl Geochem 17:935–953

Wang G, Wang Z, Weidong Z, Moore WS, Li Q, Yan X, Qi D, Jiang Y (2015) Net subterranean estuarine export fluxes of dissolved inorganic C, N, P, Si, and total alkalinity into the Jiulong River estuary, China. Geochemica et Cosmochimica Acta 149:103–114

Waska H, Kim G (2011) Submarine groundwater discharge (SGD) as a main nutrient source for benthic and water-column primary production in a large intertidal environment of the Yellow Sea. J Sea Res 65:103–113

Windom HL, Moore WS, Niencheski LFH, Jahrike RA (2006) Submarine groundwater discharge: a large previously unrecognized source of dissolved iron to the South Atlantic Ocean. Mar Chem 102:252–266

Wong WW, Grace MR, Cartwright I, Cook PLM (2014) Unravelling the origin and fate of nitrate in an agricultural-urban coastal aquifer. Biogeochemistry 122:343–360

Zavody AM, Mutlow CT, Llewellyn-Jones DT (1995) A radiative transfer model for sea surface temperature retrieval for the along-track scanning radiometer. J Geophys Res 100:937–952

Zekster IS, Dzyuba AV (2014) Submarine discharge into the Barents and White Seas. Environ Earth Sci 71:723–729

Zekster IS, Ivanov VA, Meskheteli AV (1973) The problem of direct groundwater discharge to the seas. J Hydrol 20:1–36

Chapter 3
Characteristic of the Baltic Sea

3.1 The Baltic Sea. General Outline

The Baltic Sea is a land locked sea located in Northern Europe. To the south, the
Baltic Sea borders the European mainland (Russia, Estonia, Latvia, Lithuania,
Poland, Germany, Denmark), while to the north–the Scandinavian Peninsula
(Finland and Sweden). The only connection to the North Sea is through the shallow
and nerrow Danish Straits and further through the Kattegat and the Skagerrak. The
Belt Sea, including the Danish Straits, is the transition zone between the Baltic Sea
with the North Sea. The Baltic Sea is one of the largest brackish water bodies in the
world with a total surface area of 415,240 km^2 (including the Danish Streids and the
Kattegat) and the volume of water equal to 21,706 km^3 (Emelyanov 1995, 2002).
The Baltic Sea is, most often, divided into several basins: the Bothnian BayX, the
Bothnian Sea, the Gulf of Finland, the Gulf of Riga, the Baltic Proper, the Danish
Sounds and the Kattegat that are separated from each other by elevations and
thresholds. The Baltic Sea has a meridional extension of more than 1500 km and a
latitudinal extension of about 650 km.

The total drainage area of the Baltic Sea is equal to 1,729,000 km^2, fourfold
larger than the sea itself (Fig. 3.1). The major Baltic Sea rivers are Neva, Vistula,
Oder, Neman, and Daugava which drain the southern and south-eastern lowlands.
River run-off plays an important role as a component of the water balance, forming
and modifying the salinity of the Baltic Sea water (Ehlin 1981; Łomnewski et al.
1985). The Baltic Sea catchment includes also a large number of lakes of post-
glacial origin (e.g. Ladoga and Onega). Due to the geographical and climatological
differences in the drainage basin the system of water courses transporting fresh
water to the sea is different in the northern and southern regions (Uścinowicz 2011).
Many rivers of variable sizes discharge water into the Gulf of Bothnia from the
Scandinavian mountains and from the flat forest areas on both sides of the gulf. In
the south flat there are only a few main rivers flowing into the Baltic Sea. The
largest rivers discharging into the Baltic Sea are the Neva flowing into the Gulf of
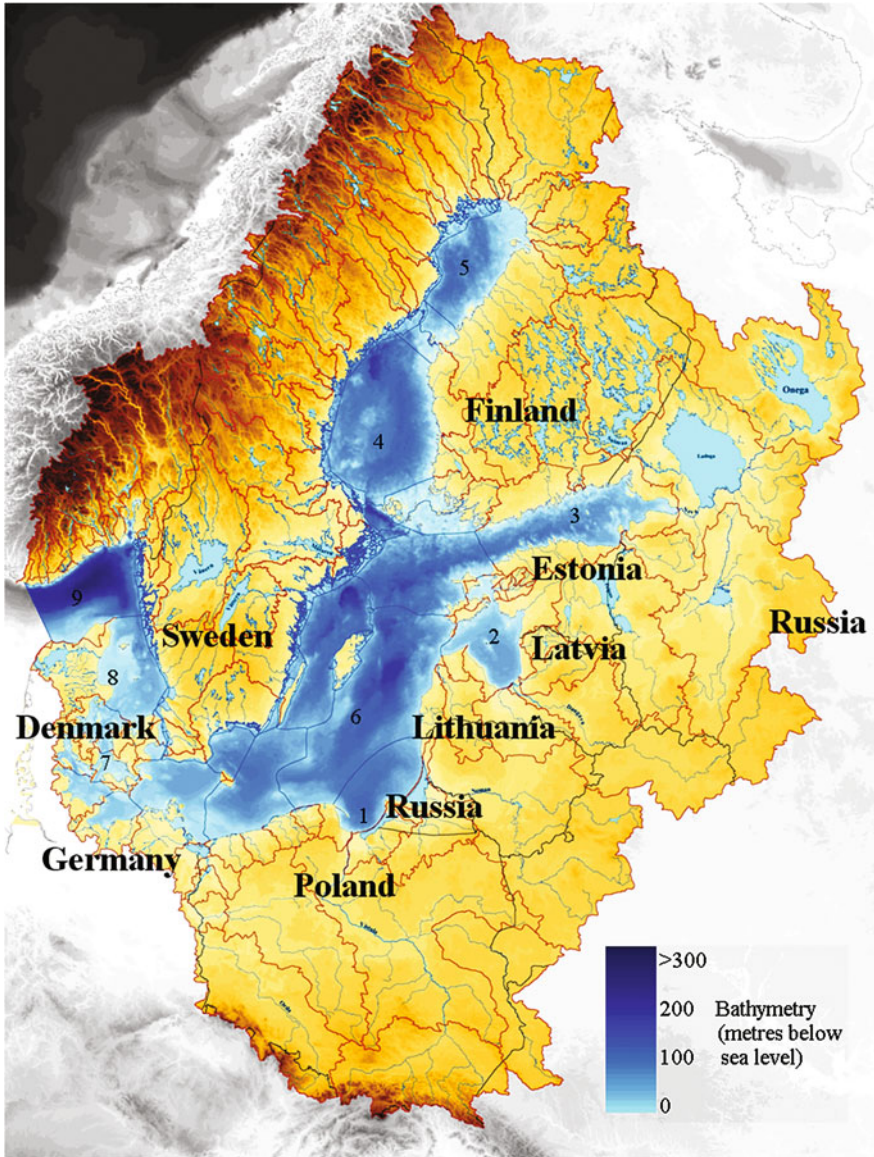
Fig. 3.1 The Baltic Sea and the sea drenage basin divided among the countries. *1* The Gdańsk Basin, *2* the Gulf of Riga, *3* the Gulf of Finland, *4* the Bothnian Sea, *5* the Bothnian Bay, *6* the Baltic Proper, *7* the Danish Straits, *8* the Kattegat, *9* the Skagerrak. Based on BALTEX-The Baltic Sea experiment website (http://www.baltex-research.eu)

Finland and the Vistula flowing into the Baltic Proper. There is a great seasonal variation in the river discharge into the Baltic Sea. The maximum run-off occurs in spring while the minimum one- during summer. The delay in the ice thawing

maxima while moving east- and north-wards has an important influence on the highest monthly run-offs. In the middle part of the Baltic Proper the maximal run-off is in April. In the Gulf of Riga, a delay of the high-water inflow until May is observed, while the Gulf of Finland the largest run-off is the highest inflow in May and June. The situation is similar in the Gulf of Bothnia, where a considerable part of the high-water inflow takes place in July. The annual minima of inflow appear in summer in the central Baltic Sea and in autumn and winter in the northern areas (Uścinowicz 2011).

Such regional differences in the times of the maxima discharge contribute to a rather steady supply of river water to the sea. As a result the outflow peak of brackish surface water from the Baltic Sea to the North Sea is diminished. The maximum of river run-off takes place in the period from April to June. The minimum value is less than 50 % of the maximum inflow and occurs in January. The total annual river run-off to the Baltic Sea has been calculated for the periods 1951–1960 and 1961–1970. The total inflow differs for the two mentioned decades by 10 km^3 a^{-1}. The difference is attributed to climatic changes resulting in variation of precipitation over the drainage basin.

The properties of the Baltic Sea are impacted by substantial, continuous fresh water inputs and the sporadic inputs of saline, North Sea water (Voipio 1981). The salinity of the Baltic Sea water varies depending on the depth and location. In the Baltic Proper surface water salinity is about 7.5. Usually, the surface water and deeper water domains are separated by stable halocline, located a depth ranging from 60 to 80 m. In the rivers mouths the surface water salinity can reach zero while in the Bothnian Bay, Gulf of Finland and Gulf of Riga the salinity is as low as 3–5. Characteristic of the Baltic Sea is a layered distribution of salinity in the vertical profile.

The Baltic Sea fills a depression into the continental crust below present sea level (Uścinowicz and Miotk-Szpiganowicz 2011; Gudelis and Jemielianov 1982). There are several forces like erosion, tectonic and glacio-isostatic processes that influence the geology, morphology and bathymetry of the Baltic Sea. The Baltic Sea continental catchment area is characterized by lowlands covered by Quaternary deposits (Uścinowicz and Miotk-Szpiganowicz 2011). The drainage area of the Baltic Sea lies within the East European Platform, the Paleozoic West European Platform and the Carpathian area. The northern part of the catchment area is covered by an outcropping crystalline bedrock of the Precambrian craton which forms the Baltic Shield covered by magmatic and metamorphic Precambrian rocks (Kramarska and Uścinowicz 2011).

Geology of the Baltic basin is described in Uścinowicz (2011). The Southern Baltic Sea is divided into two parts: the eastern and central part of the southern Baltic Sea is located within the East-European Platform (Precambrian Craton); the western part of the Baltic Sea lies within the Palaeozoic platform of Central and Western Europe (Augustowski 1987; Kaszubowski and Coufal 2008). The platforms are separated by a transcontinental zone called the Koszalin Fracture Zone. The part of the Baltic Sea located over the East-European Platform is situated between the Baltic Sea Shield in the north and north-west which consists of crystalline rock outcrops, and the Baltic syneclise which is located in the east and

south-east. The sediments from Eocene to Miocene cover older deposits along the area from Koszalin to Jastarnia (Hel Peninsula) in the east, and reach to the slopes of the Southern Middle Bank in the north (Kaszubowski and Coufal 2008). Moreover, Miocene and Oligocene sediments also occur locally near the coast of the Gulf of Gdańsk (Kramarska et al. 2002). The Paleozoic platform which is located southwest of the Teyserre-Tornquist Zone is complex in its tectonic and geological structure. Lower, rather thick Paleozoic deposits are covered by a platform of the Devonian-Carboniferous complex. In the area of the Gdańsk Basin, the sub-Pleistocene bedrock consists of Jurassic deposits lying 134–160 m b.s.l., and Cretaceous sediments (90–134 m b.s.l.) (Kaszubowski and Coufal 2008). Oligocene and Miocene sediments are found (Western part of Gdańsk Gulf) at depths of 20–100 m b.s.l. (Kaszubowski and Coufal 2008). In the area of the Słupsk Furrow, the sub-Pleistocene bedrock occurs at depths of 90–110 m b.s.l. (Kramarska and Uścinowicz 2011). However, the sub-Pleistocene surface, which consists of Silurian and Devonian deposits in the southern part of the Gotland Basin, occurs at depths of 110–120 m b.s.l. (Uścinowicz 2011). The sub-Pleistocene surface south of the Bornholm Basin and Słupsk Furrow is located at shallower depths—between 30 and 100 m b.s.l.. The upper part of the Neogene (Pleistocene and Holocene) of the southern Baltic Sea bottom includes glacial, glaciofluvial, fluvial sediments and deposits, of both terrestrial and marine origin. The thickness of this formation varies between 1 and 300 m (Uścinowicz et al. 2011). In the southern part of the Gdańsk Gulf, the deposits of the Pleistocene-Holocene cover depths spanning 50–100 m (Kaszubowski and Coufal 2008). However, the area of the coastal zone of the southern Baltic boasts a significant thickness of these deposits (50–100 m), reaching a value of 200–300 m in subglacial troughs cutting through the Pleistocene-Holocene cover. Pleistocene is represented by several glacial tills, fluvioglacial and limnoglacial accumulation sediments and also interglacial and Late Glacial barrier deposits of the Baltic Ice Lake, limnic and deltaic sediments (Uścinowicz 2011). The deposits, which build the present sea bottom of the Polish part of the southern Baltic are connected with the deglaciation of the Vistulian Glaciation and later processes of the Baltic Sea formation stages in the Late Pleistocene and Holocene. The lower parts of the Holocene sediments in deep basins are made up by Preboreal and Boreal silts and clays of the Yoldia Sea and Ancylus Lake, the upper parts were formed by Atlantic, Subboreal and Subatlantic silts and clays of the Mastogloia, Littorina and Post-Littorina seas (Kramarska and Uścinowicz 2011).

The coasts of the Baltic Sea are mainly lowlands (Peltonen 2002). The Estonian lowland stretches from Pärnu to Tallin, the rest of the coast gradually climbs reaching occasionally 100 m. The Latvian lowland occupies area within the Kurzeme Peninsula and the Gulf of Riga. The highest part does not exceed 50 m. The Lithuanian coast consists of the Pajuzio Plain, the Middle Lithuanian Lowland and the Zemaiciu and Aukstaiciu highlands (the highest parts range from 150 to 250 m). The Polish coastal region generally consists of lowlands. On the seashore sand bars were formed as a result of seawater movement. In the western end of the Bay of Puck (part of the Gulf of Gdańsk) the Hel Peninsula was formed. The dune

belt east of the Vistula sand bar separates the digressional Vistula delta from the sea. South-east of the coast lies a belt of lake lands with terrestrial moraines (reaching 300 m). The German coast consists of the North German Plain while Denmark is a lowland area with an elevation of less than 200 m. The Baltic coasts of Finland and Sweden are almost entirely lowlands, with hills in Sweden reaching a maximum of 200 m.

3.2   Baltic Proper

The bulk of the Baltic Proper lies within the Baltic Shield, part of the East European platform (Voipio 1981; Winterhalter et al. 1981). The southeastern part of the Baltic Proper forms a subsided area in the East European Platform; the Baltic Syneclise (Depression), that contains Paleozoic and Mesozoic sedimentary rocks of a considerable thickness. Southeast of Gotland the sedimentary rocks reach a thickness of 2000 m, and further southeast off the Lithuanian coast, more than 3000 m. SW of the Tornquist Line the crystalline basement occurs at a depth of 5000–7000 m. The northern part of the Baltic Proper occupies an area that consists predominantly of the exposed crystalline basement rocks of Early and Middle Proterozoic age. The term Baltic Shield is generally used for the crystalline complex that forms most of cratonic Fennoscandia.

The permanent water circulation in the Baltic Proper is very weak and is clearly related to the excess fresh-water supply. The current velocities are some few cm s^{-1} in the surface and slightly less than 1 cm s^{-1} in the deep water. Primarily the horizontal salinity distribution with a marked NE–SW inclination of the isohalines, but also to a certain extent the temperature distribution, show the long-term average circulation to be cyclonical. The influence of the Coriolis effect on the mean circulation is significant. The mean motion in the surface layer is slightly more persistent along the west coast than along the east coast due to the combined effect of outgoing river runoff and the Coriolis effect. The mean circulation contains a weak vertical shear. Although storms over the Baltic Sea are frequent and often persistent, the mean winds are generally weak and the mean circulation in the Baltic Sea appears to be mainly estuarine and thermohaline.

The western border of the Polish coastal zone lies in the Pomeranian Bay and the eastern border in the Gulf of Gdansk. The offshore border on the open-sea side may by drawn differently, depending on the criteria one applies. As far as contaminant fluxes are concerned, offshore border should enclose offshore waters affected by the land. In the Polish coastal zone it practically coincides with the extension of river run-off into the sea. This, however, depends on the river's size, the hydrological conditions in the river mouth and the wind and pressure conditions at any given time.

In this assessment, the coastal water belt is assumed to reach out to the 20 m depth contour, with the exception of the Gulf of Gdansk, where the waters of the river Vistula flow much farther out to sea, reaching the Gdansk Deep region.

3.3   The Baltic Sea-Surface Sediments and Sedimentation Processes

The following description is based on Uścinowicz (2011).

The catchment area of the Baltic Sea is covered predominantly by Pleistocene glacial and glaciofluvial deposits. These sediments are transported by rivers or directly enter the sea by coastal and partially seabed erosion. In coastal zones, the sediment material is selected and transported as a result of the effect of both wind waving and sea currents. Differentiation and distribution of the individual types of surface sediments at the sea bottom result of the activity of hydrodynamic processes, which are present especially during storms. Hydrodynamic processes that control the distribution of different types of sediments are related to the sea depth, development of the shoreline and sea-bottom relief. The shoreline development and seabed relief are of special significance for the western and northern parts of the Baltic Sea basin, where numerous islands limit free water circulation and reduce the wave base in such a way that fine-grained sediments accumulate even in shallow basins (Uścinowicz 2011).

Various hydrodynamic processes, the frequency of their occurrence, water mass movement intensity and direction, as well as the seabed relief gave rise to areas (zones) featuring dominant, specific litho-dynamic processes leading to the zonal occurrence of sediments on the bottom surface of the Baltic Proper in the southern part.

Above the pycnocline, there are sand-gravel and sand sediments. Hydrodynamics processes make the stable deposition of silt-clay sediments impossible. The contents of fractions finer than 0.063 mm are generally present in quantities lower than 1 %, and often lower than 0.5 %. The finer-grained deposits of silts and clays are usually present below the pycnocline.

Surface silt-clay sediments (i.e. the Baltic Sea olive-grey muds), containing fractions finer than 0.063 mm, are present in amounts of more than 75 %, occupying wide seabed areas in all the Baltic Sea sedimentary basins (Fig. 3.3). In the Baltic Proper, there are the following basins: Arkona, Bornholm, Gdańsk, Eastern and Western Gotland, and North Central. The present accumulation rate of the silt-clay sediments is diverse and varies from 0.5 to 2 mm/year (Pempkowiak and Szefer 1992). It is faster in the central deep-water parts of the basins than in their peripheries, and there are regional differences. Depending on oxygen conditions, there are diverse inner sedimentary structures of the deposits. In the sediments covering the sea bottom in areas where near-bottom oxygenetyd water masses occure, bioturbation is evident as the result of activity of benthic organisms, mainly *Macoma baltica* and *Mesidotea entomon.* In deeper areas of the sea bottom located below the pycnocline pycnocline, laminated sediments are deposited under anaerobic conditions, which reflects the annual sedimentary rhythmicity.

In the transition zone between the silt-clay (mud) sediments, sands and gravels, in the peripheries of the sedimentary basins, there are sand-silt deposits or mixtites, i.e. sediments composed of sand, gravel and silt grains, often associated with iron-manganese concretions. These formations prevail in the bottom areas of the

Baltic Proper, where the pycnocline approaches the sea bottom. They are distinguished by diverse grain size, including the following fractions in variable proportions: gravel (64.0–2.0 mm), sand (2.0–0.063 mm), silt (0.062–0.004 mm) and clay (<0.004). The sediments are poorly sorted. The thickness of the sand-silt sediments and mixtites is often less than 0.2 m, locally lower than 0.1 m. They are underlain by Pleistocene glacial deposits or clay sediments from early development stages of the Baltic Sea (Baltic brown clays and Baltic grey clays). Lithological features and the sonar image of the sea bottom from the area of sand-silt sediments and mixtites indicate the occurrence of bottom currents of considerable velocities. Significant are also the inner waves that are formed within the limits of the pycnocline.

Above the pycnocline, sandy and gravelly sediments prevail. Sand and sand-gravel sediments cover large areas of the sea bottom in the southern and south-eastern parts of the Baltic Proper—to the north of the coasts of Germany and Poland, and to the east of the coasts of Lithuania and Latvia. They also occupy considerable areas of the sea bottom in the coastal parts of the Belts Sea. In these sectors of the Baltic Sea, the sands and gravels of the sea bottom formed as the result of long-lasting and multiple redeposition of glacial and glaciofluvial sediments. The original features of these sediments vanished and transformed into features typical of epicontinental sea sediments. In the northern part of the Baltic Sea, i.e. in the Gulf of Finland, the Bothnian Sea and in the Bothnian Bay, sandy and sand-gravel deposits are less common. These are predominantly glaciofluvial sediments, e.g. sands and gravels of glaciofluvial deltas or eskers, currently washed out and transformed into marine sediments.

Deeper, below the storm wave base (>25–30 m), fine-grained sands dominate. They are characterized by good and very good sorting and almost symmetric and positive skewness of grain size distributions. A small thickness of the fine-grained sands, less than 2 m, indicates that they are transported probably only during extremely strong storms, and deposition of the sediments takes place periodically. According to Kolp, small ripple marks, up to 1 cm high, may occur on the sea bottom in this zone. However, it seems that more typical and more common in the area of sedimentation of fine-grained sands are biogenic structures of benthic organisms, which can be seen on the sea bottom. Among the typical are crawling and browsing traces of *Mesidotea entomon* crustaceans, and dwelling structures of Oligochaetae and *Macoma baltica* clams.

In the southern and eastern parts of the Baltic Proper, at the depths of app. 10 m to 25–30 m, medium- and coarse-grained sands, as well as gravelly sands and sandy-gravels occur most often. Those sediments are moderately sorted. Locally occurring boulders and pebbles form the residue of washed-out Pleistocene deposits. In the regions of boulders occurrence, gravel and gravelly-sand deposits are found together with very thin sand layers, often less than 20 cm in thickness, and of moderate to very poor sorting. Ripple marks are common on the sediment surface in this zone (10–30 m). Ripples with distances between crests (wave length) from 0.1 to 0.4 m and a height from 0.002 to 0.05 m occur in fine- and medium-grained sands. In coarse-grained and gravelly sands, the ripple wave length ranges from 0.5 to 1.5 m, the ripple height is from 0.08 to 0.3 m, and the crest line extends over several tens of

metres. On the sand surface, in the area of sea depths between 10 and around 30 m, in addition to ripple marks there are also large-scale bedforms, such as megaripples and sand waves of a few hundred matres long crests. Their wave length is from a few to several tens of metres and the height is from 0.5 to 2 m.

On the surfaces of gravel and gravelly-sand sediments, there are also large sand patches and bedforms similar to sand ribbons known from the North Sea and the Danish Straits, but less regular. The size of the sand patches is variable, from a few up to several hundred metres. Their shapes are often irregular, sometimes oval or elongated. These bedforms similar to sand ribbons are up to 500 m long and app. 40–50 m wide, and show variable spacing. The deposits in this zone are found within the effect of mean storm waves on the sea bottom. During strong storms, fine-grained sands migrate over the surfaces of gravelly-sand deposits as sandy waves or patches and ribbons of sands, and after multiple repositions, they leave the zone of storm wave activity.

In the coastal zone, down to a depth of app. 10 m, fine- and medium-grained sands dominate. Coarser-grained sediments occur locally on erosional sections of the coastal zone, especially at the foot of cliffs. Deposits in the coastal zone undergo frequent repositioning by waves of the surf zone. During strong storms, not only is the seashore damaged. The Pleistocene deposits, occurring at the base of marine sediments within the underwater shore slope, can also be washed out. Fine-grained sands of the coastal zone are characterized by negative skewness of grain size distribution, and good or very good sorting. Typical bedforms of the coastal zone are bars separated by troughs, canals and cones of trip currents.

The mineral composition of fine-grained (silt-clay) sediments also reflects the geology of the areas from where these components are transported into the sea. The material carried down by the rivers into the sea and that originating from erosion of Pleistocene deposits on the coasts and seabed is primary of terrigenous origin and includes quarts, feldspars, illite, chlorite, and in smaller amounts, kaolinite and carbonates. Silica of biogenic origin (diatom opal) is also found in fine-grained sediments, but it is not a considerable addition. In the Baltic Sea, other authigenic minerals, included into the sediment composition, also occur. Their formation and preservation depend on the physic-chemical conditions in the bottom and interstitial waters. Minerals such as pyrite (including hydrotroillite), kutnohorite and vivianite form under anaerobic conditions, while goethite originates under aerobic conditions (Uścinowicz 2011).

3.4 Gdańsk Bay, Bay of Puck and Pomeranian Bay

3.4.1 Gdańsk Bay

The shoreline of the Polish coast is smooth and even by comparison with the rocky, western and northern shores of the Baltic Sea. The coast consists mainly of sandy beaches and dunes; there are also a few cliffs. There are two bays—the Gulf of

Gdańsk and the Pomeranian Bay—which differ morphometrically and hydrologically from each other.

The Gulf of Gdansk receives water of the Vistula (Wisła)—the second-longest river in the Baltic drainage area (Cyberski 1992). The Gulf of Gdańsk also receives pollutants from several streams flowing through urban areas. Although their combined flow is much less than that of the Vistula, they pollute local beaches and the inshore zone of the sea. Whereas water from the Vistula usually flows farther into the Gulf, the small streams exert a direct impact on the beaches The bathymetry of the Gulf of Gdańsk is quite variable, as are the bottom sediments: the open sea side is the edge of a deep sedimentary basin- the Gdańsk Deep.

The Inner Puck Bay forms a unique basin in the western part of the Gulf of Gdansk. It is a shallow bay, isolated the rest of the Gulf by an underwater sandbar and thereby unaffected directly by the open sea.

3.4.2 *Bay of Puck*

The Bay of Puck is located in the southern part of the Baltic Sea (eastern part of the Gulf of Gdańsk). A narrow, sandy spit called the Hel Peninsula, which is 36 km long, separates the bay from the open waters of the Baltic Sea. The total area of the Bay of Puck equals 359.2 km^2. The catchment area is nearly three times larger and equals 908.8 km^2. The major rivers flowing to the Bay of Puck are Reda, Gizdepka, Płutnica, Zagorska Struga and Chylonka. The total river inflow to the Bay of Puck is equal to 0.25 km^3 year^{-1} while the average precipitation equals 0.20 km^3 year^{-1} (Cyberski and Szefler 1993). The Bay of Puck consists of an outer southeastern region, called the Outer Puck Bay or the Inner Puck Bay, with an average depth of 20.5 m, and an shallower, inner northwestern region called the Puck Lagoon with the average depth of 3.1 m. The water bodies are separated by Rybitwia Mielizna (Shallow) running from the Rewa Cape to the Hel Peninsula. During the year some parts of the shallow can protrude above the water. Water exchange between these two sections of Puck Bay mainly occurs through these passages, especially through Głębinka Narrows (Nowacki 1993). The basin is characterized by considerably larger depths and regular lowering of the bottom in the direction of the open part of the Gulf of Gdańsk, reaching the depth of 54 m near the tip of the Hel Peninsula (Cyberski and Szefler 1993). Bottom sediments of Puck Bay are very diverse; sands of various particle size, sludges, silts and organic matter (Bolałek and Graca 1996). Their distribution at the surface is distinctly related to their morphology. An average salinity in the Bay of Puck is in the range from 7.00 to 7.65 (Nowacki 1993). The surface water (0–4 m) in the Outer Puck Bay is characterised by relatively low salinity, from about 6.4 to 7, and poor transparency. The Secchi disk depth ranges from 2 to 2.5 m. In deeper water layers the salinity is higher and the water transparency is considerably better, which is proved by high values of the light beam
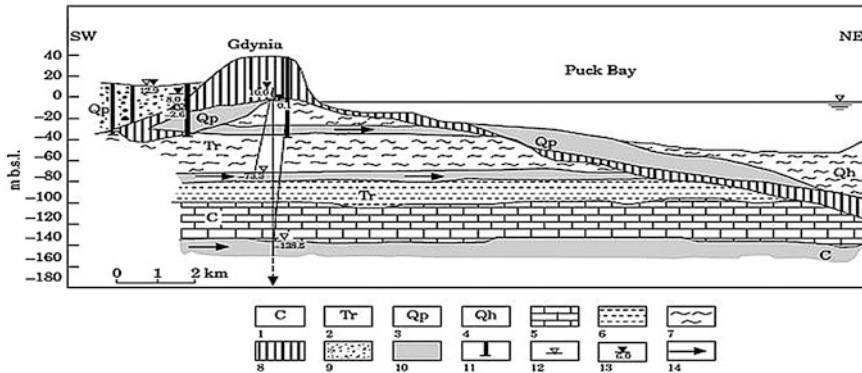
Fig. 3.2 Bay of Puck cross-section presenting hydrogeological conditions of the sediments (modified after Falkowska and Piekarek-Jankowska 1999). *1* Cretaceus, *2* tertiary, *3* quatenary-pleistocene, *4* quatenary-holocene, *5* marl, *6* clay, *7* slit, *8* boulder, *9* clay, *10* sand, *11* well, *12* top of a aquifer, *13* piezometric groundwater level, *14* direction of groundwater flow

transmission (Nowacki 1993). Maximal concentrations of Cl^- ions only infrequently exceed 5 g dm^{-3}, with average being 3.5–4.0 g dm^{-3} (Piekarek-Jankowska 1996).

The geomorphology of the Bay of Puck is quite complex. A hydrogeological section of the Bay of Puck is presented on Fig. 3.2. The Quaternary sediments located in the Bay of Puck are some 25 m thick. The Cretaceus formations lies at depth from 108 to 135 m. Seismic–acoustic investigations of the study area have imaged permeable layers of Holocene to Pleistocene sands and silts and underlying Tertiary silt layers (Piekarek-Jankowska 1994). The aquifers formed in the Tertiary forms of the Oligocene and Miocene sandy, sediments. The Hel Peninsula developed during the Pleistocene and Holocene (Piekarek-Jankowska 1994). Geomorphic landforms surrounding the Bay of Puck consist of wave-dominated sedimentary plains and dune deposits forming in micro tidal zones. Coastal erosion is the dominant source of sediments within the study area. Waves, storm surges, currents and winds drive erosion, transport, accumulation and redeposition of sediments in the coastal zone (Piekarek-Jankowska 1994).

3.4.3 Pomeranian Bay

The Pomeranian Bay is shallow and bathymetrically little differentiated. On the open-sea side, the bottom is raised forming the Odra Bank. The hydrological conditions in the Pomeranian Bay differ from those in the Gulf of Gdansk. It receives only a portion of the pollution load carried by the river Odra: on its way to the Baltic, the Odra traverses the Szczecin Lagoon, a natural purification basin. The Odra Szczecin Lagoon—Baltic hydro-geomorphological system represents quite a specific example of pollutant input to the Baltic.

3.5 Estuaries

Vistula and Odra are the two major Polish rivers. On entering the sea they from estuaries. When the wind direction is form the north, it blows seawater into both of them. The lagoons are subject to human pressure. Their basins have been heavily industrialised and urbanised for hundreds of years. There are extensive conurbations near their mouths: Gdansk, Gdynia and Sopot in the Gulf of Gdansk, and Szczecin and Swinoujscie in the Pomeranian Bay.

Between the Odra, on the western border of Poland, and the Vistula near the eastern border, there are several smaller rivers flowing into the Baltic. These rivers are significant as regards the local environmental conditions of the central coast of Poland (Fig. 3.3). Industrial and urban activities dominate in the Bays, whereas forests and arable land predominate in the hinterland of the coastal zone.

The combined population of Gdansk-Sopot-Gdynia conurbation is roughly 1 mln while this of the Szczecin–Świnoujscie area is some 0.5 mln.

3.5.1 Water Exchange Conditions

The coastal zone is influenced by the conditions in the open sea. As the seawater is generally well aerated from the surface to the bottom, there are no areas of oxygen depletion. Down to depths of ca. 20 m, wave energy moves the bottom sediments
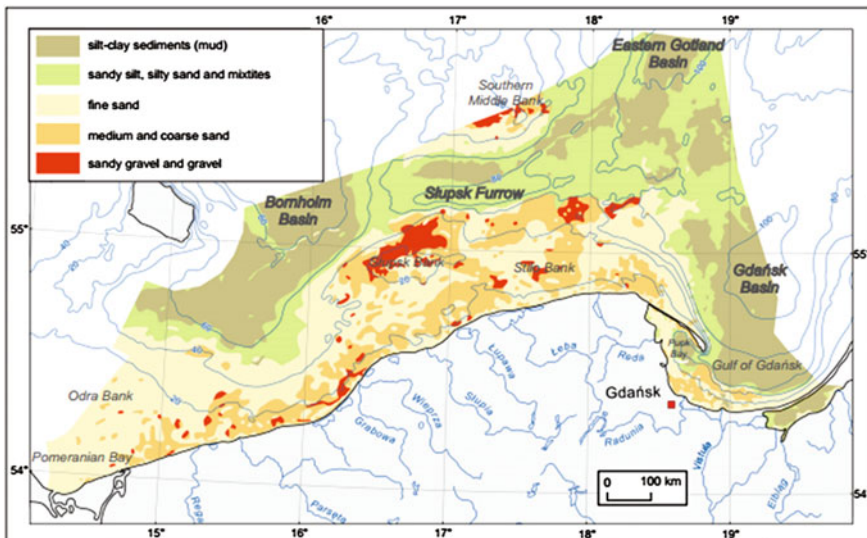
Fig. 3.3 Surface sediments in the Polish part of the Baltic Sea (based on Uścinowicz 2011; simplified)

constantly; at greater depths, bottom sands are set in motion by storms and currents in the near-bottom water layer. Resuspension of surface sediments takes place down to the depth of 50–70 m, however the the resuspension events require progressively more energy, and thus depends on frequency of storms and major storms. For this reason, there are no areas of sediment accumulation along the coast. The exception to this seems to be the Inner Puck Bay, where some accumulation of sediments may occur in its deeper parts and supplies of oxygen may become depleted during periods of prolonged ice cover.

The system of currents in the coastal zone plays a significant role in the distribution of contaminants in the sea. As in the entire Baltic, the currents in the Polish coastal zone are affected by the atmospheric conditions, but these are never persistent enough to alter the general west-east flow of the water. There are coastal morphological forms testifying to the direction of the water movement: the general shape of the shoreline, the closing of lagoons and coastal lakes, the formation of the Hel Peninsula and underwater sandbars. The velocities of currents in the Polish coastal zone rarely exceed 10 cm/s increasing only around the Hel Peninsula, when under stormy conditions they may rise to as much as 50–100 cm/s. Contaminants entering the coastal zone are transported eastwards by the prevailing surface current.

The water temperature in this area range from 18–20 °C in August to 1–2 °C in February. Ice cover usually appears in January and February and is limited to the shallowest areas. During severe winters, ice may cover the Inner Puck Bay for 2–3 months and may therefore affect the local oxygen conditions. Ice cover may also occur along the entire Polish Coast.

3.6 Bottom Sediments

Sandy shores with beaches and dunes predominate along Poland's coastline. The sandy sea floor extends into the coastal zone to a depth of about 40–50 m. Sand is easily moved by wave action, so the sea floor here is continually changing its form and depth. Sediment transport along the eastern part of the Polish shore is from west to east. To a large extent, the bottom sediments of the Polish coastal zone consist of sand, sometimes of gravel and pebbles. These sediment types do not adsorb contaminants discharged into the sea as oppose to clay-silt ones. It seems then that contaminants are transported farther from the shore and deposited in the Baltic deeps. Such a pattern causes that, substances discharged by the Vistula finish up in the Gdansk Deep, the nearest accumulation basin of fine suspended matter (Andrulewicz 1992). The meteorological and hydrological conditions and their relationship to agricultural practice in the drainage area have given rise to significant variations in the outflows of chemicals into the rivers (Niemirycz 1999). Nitrogen run-off varies markedly from season to season. Monthly nitrogen loads carried by the Vistula in various years are clearly raised in the first four months of

the year. When the snow melts during this time, freshets and swollen water-courses flush large quantities of nitrate and ammonia nitrogen. By contrast organic nitrogen run-off increases in April and May (Rybiński et al. 1992).

3.7 Characterization of Submarine Groundwater Discharge in the Baltic Sea

3.7.1 Submarine Groundwater Discharge to the Ocean

Along the continental margins rivers and submarine groundwater discharges supply nutrients, trace elements, and radionuclides to the coastal ocean, supporting coastal ecosystems and, increasingly, causing harmful algal blooms and eutrophication. Global riverine water discharge is well known but the magnitude of submarine groundwater discharge (SGD) is poorly constrained. There have been several attempts to estimate the total groundwater flux to the ocean. The first data on submarine discharge into the World Ocean are given in Garrels and Mackenzie (1971), where the submarine discharge into the World Ocean is estimated to amount to as much as up to 10 % of total river runoff (Dzhamalov et al. 1977; Zekster et al. 2007; Zverev 2009). Zekster et al. (2007) estimated fluxes of fresh groundwater into the ocean using an integrated hydrologic-hydrogeologic approach. This approach assumes that the groundwater input to rivers (m^3 km^{-1} $year^{-1}$) that drain specific hydrogeologic provinces is similar to groundwater discharge to the ocean (m^3 km^{-1} $year^{-1}$) from these provinces. They estimated that the groundwater input to the rivers, and scaled the expected discharge per kilometer of river with the shoreline length of each province to provide groundwater fluxes from each province to the ocean. This approach only includes fluxes from the upper geologic zones of the provinces (the same zones that drain into rivers) and may miss fluxes from deeper geologic zones (i.e., confined aquifers) that drain into the ocean. Zekster et al. (2007) provided a detailed list of discharge and water composition from each province into individual ocean basins. The ground-water compositions were in almost all cases <1 g L^{-1} total dissolved solids. Zekster et al. (2007) estimated a flux of fresh groundwater to the ocean of $(2.2–2.4) \times 10^{12}$ m^3 $year^{-1}$. Compared to their estimate of the world river flow (40×10^{12} m^3 $year^{-1}$), the fresh SGD component was 5–6 %, similar to other estimates (Burnett et al. 2003).

Kwon et al. (2014) used an inverse model combined with a global compilation of ^{228}Ra observations and showed that the SGD integrated over the Atlantic and Indo-Pacific Oceans between 60°S and 70°N is $(12 \pm 3) \times 10^{13}$ m^3 $year^{-1}$, which is 3–4 times greater than the freshwater fluxes into the oceans by rivers. Unlike the rivers, where more than half of the total flux is discharged into the Atlantic, about 70 % of SGD flows into the Indo-Pacific Oceans. It suggests that SGD is the

dominant pathway for dissolved terrestrial materials to the global ocean, and this necessitates revisions for the budgets of chemical elements including dissolved carbon species.

3.7.2 Groundwater Discharge to the Baltic Sea

The Baltic Sea constitute the groundwater discharge from all aquifers and multi-aquifer formations while the main groundwater recharge areas of this circulation system are located in the lakelands on morainic uplands located south of the Baltic coast (Lidzbarski 2011). Assessment of the submarine groundwater discharge to the Baltic Sea was the subject of several research projects and documentary works. Peltonen (2002) estimated the groundwater discharges from the Baltic Sea shoreline based on published studies, and also combined hydrological and hydrogeological method. From Poland and Germany the groundwater discharge was estimated to be in the range from 1.6 to 1.9 km^3 $year^{-1}$. The flux of groundwater from Sweden and Finland was 0.76 and 0.38 km^3 $year^{-1}$, respectively while the groundwater discharge from Baltic States and Russia equals approximately 1.14 km^3 $year^{-1}$. Peltonen (2002) concluded that the total groundwater discharge to the Baltic Sea is 4.4 km^3 $year^{-1}$, which is small in comparison with total river runoff (less than 1 %), however locally the groundwater contributions can be very significant.

3.7.3 Groundwater Discharge to the Eckernförde Bay (Western Baltic Sea)

Submarine groundwater discharge (SGD) from subseafloor aquifers, through muddy sediments, was studied in Eckernförde Bay (western Baltic Sea) (Schlüter et al. 2004; Scholten et al. 2015). The submarine groundwater discharge was traced by ^{222}Rn enrichment in the water column and by the chloride profiles in pore water. A considerable decrease in chloride concentrations (to levels less than 10 % of bottom water concentration) was observed within the upper few centimetres of sediment. It was observed that more than 22 % of the seafloor of the Eckernförde Bay was affected by freshwater admixture and active fluid venting. A maximal discharge rate of about 9 L m^{-2} d^{-2} was computed by modelling pore water profiles. Based on pore water data, the freshwater flow from subseafloor aquifers to Eckernförde Bay was estimated to range from 4×10^6 to 57×10^6 m^3 $year^{-1}$. Thus, 0.3–4.1 % of the water volume of the bay is replaced each year. As surface runoff by rivers is negligible in the study area, SGD is a significant pathway within the hydrological cycle of this coastal zone. High-resolution bathymetric data and side-scan sonar surveys of pockmarks, depressions up to 300 m long, were obtained by using an autonomous underwater vehicle. Steep edges, with depths increasing by

more than 2 m within 8–10 m in lateral directions, equivalent to slopes with an angle of as much as 118, were observed. The formation of pockmarks within muddy sediments is suggested to be caused by the interaction between sediment fluidization and bottom currents. Fluid discharge from glacial coastal sediments covered by mud deposits is probably a widespread, but easily overlooked, pathway affecting the cycle of methane and dissolved constituents to coastal waters of the Baltic Sea.

The submarine groundwater discharge defined as the net groundwater discharge to Eckernförde Bay was also investigated using a large-scale groundwater model (Kaleris et al. 2002). It was found that the probable range of SGD in the study area per kilometer of the land-sea interface is from 0.05 to 0.07 m^3 s^{-1}. The distribution of the groundwater outflow rates at two sea bottom sites (pockmarks) was investigated using two approaches. First, density effects were neglected. Under this condition, the resulting discharge distribution at one site is approximately uniform, whereas at the other site it is strongly non-uniform with high outflow rates at the edges of the pockmark. These differences are due to different hydraulic conductivity distributions of the aquifer. Second, the investigation by means of a density-driven flow model shows that the main effect of the saltwater is to displace the groundwater outflow from the central part of the pockmark to its edges. The approximately uniform distribution estimated by neglecting the density effects does not reflect the conditions at the sea bottom whereas the strongly non-uniform distribution does. The strongly non-uniform distribution of the outflow rates at the sea bottom indicates that the locally measured outflow rates can hardly be used for the estimation of mean outflow rates over large parts of the sea bottom.

The effluent activity from a well-known pockmark structure in Eckernförde Bay was also monitored for methane, salinity, and temperature signals in the water column intermittently over three years between 1991, 1993 and 1994 (Bussmann and Suess 1998). Groundwater discharge from an aquifer into the brackish waters of the western Baltic, dilutes bottom water salinities to values as low as 2.9 ‰. Seasurface height and the amount of precipitation preceding sampling periods by 5 days correlated significantly with the rate of groundwater discharge. Concentrations of methane in bottom water at the pockmark site were strongly influenced by seepage intensity. At two sampling sites (control and pockmark site) distinctly lower methane concentrations were observed towards the sea surface, although the entire water body of Eckernförde Bay appears to be affected by methane seeping from the sediments. This is supported by high methane concentrations above equilibrium with atmospheric methane throughout most of the year. Maximum concentration above the equilibrium value in surface waters was 2800 ‰. Methane flux from surface waters into the atmosphere follows strong seasonal variations, with maximum values in the winter (200–400 μmol m^{-2} d^{-1}). The study reveals the important role of coastal oceans in the global methane cycle, as an intense but variable source of methane of largely unknown magnitude.

3.7.4 Groundwater Discharge to the Gulf of Finland

The groundwater discharge to the Gulf of Finland was investigated of the four zones with different geological, hydrological and discharge properties by Viventsowa and Voronow (2003). The estimated groundwater discharge to the Gulf of Finland from the Russian part of the Gulf was about 0.6 km^3 year^{-1}. However, more than 50 % of the discharging groundwater value was from the southern shore of the Gulf of Finland while the smallest discharge was from the northern part of the shore.

3.7.5 Groundwater Discharge to the Southern Baltic Sea

The coastal zone of the southern Baltic Sea is distinguished by a multilevel hydrostructural system that includes Cenozoic, locally also Cretaceous and Jurassics aquifers (Lidzbarski 2011). In the vertical section of the lowland coastal zone, the multiaquifer formation reaches 250 m, and in the vicinity of Gdańsk, it increases to almost 400 m. It mostly contains usable fresh waters, with total dissolved solids (TDS) <1 g dm^{-3}. Apart of fresh water, there is also mineralised water that locally fill the whole of the water bearing deposits. Lidzbarski (2011) characterized the groundwater water types entering the southern Baltic Sea. The Jurrasic multiaquifer formation occurs in the western part of the coast and they are mostly HCO$_3$–Ca–Mg type waters. In the other regions of the western coast, the Jurassic waters are highly mineralised and used for curative purposes. These are Cl–Na or Cl–Ca type, bromide-iodide- boron ferruginous brines. Their TDS reaches 65 g dm^{-3}, and the content of chloride ion is even up to 40 g dm^{-3}. The Cretaceous multiaquifer formation occurs in the western and central coast and characterize with elevated salinity and TDS content from 0.8 to 10 g dm^{-3}. These are Cl–HCO$_3$–Na type waters, and, at lower chloride concentrations, HCO$_3$–Cl–Ca–Na–Mg type waters. In the eastern coast, near Gdańsk, the Cretaceous waters form an extensive aquifer developed in the Santonian and Coniacian sands. This reservoir is also widespread under the bottom of the Gulf of Gdańsk and reaches the Hel Peninsula. The Cretaceous aquifer contains low-mineralised groundwater of HCO$_3$–Na type, and, more rarely, of HCO$_3$–Ca type. High concentrations of the fluoride ion are also a specific feature of these waters, reaching even 5 g dm^{-3} in some places. West of the Vistula River mouth, the Cretaceous waters lose their usable character, and their TDS reaches 10 g dm^{-3}. Hydrodynamically, it ought to be recognised that the Upper Cretaceous aquifer in the Gdańsk region and under the sea bottom of the Gulf of Gdańsk conducts artesian waters. The vector of hydrostatic pressures is directed upward and the final drainage basis for these waters is situated in the sea bottom sediments of the Gulf of Gdańsk and Puck Bay. The Paleogene and Neogene multi aquifer formations occur almost on the entire Polish coast of the Baltic Sea, excluding depressions (troughs) in the Quaternary basement. The

Miocene multiaquifer formation occurs locally and consists of two or even three aquifers lying at the depth of 10–100 m. The Quaternary multiaquifer formation is the most widespread in the Baltic Sea coastal zone.

Estimation of groundwater discharge to the Baltic Sea from the territory of Poland was made by Kryza and Kryza (2006). The geological construction and hydrogeological conditions were characterised on the basis of regional elaboration and numerous publications. A hydrogeological schema was prepared for area of water supply of the waterside zone of the sea. Four main aquifers were assigned and their parameters were characterized. Along cross-section above 500 km analytic counts of groundwater to the Baltic Sea were executed. Forming zons of groundwater direct inflow to the Baltic Sea numeric models for four representative areas ware constructed. Obtained effects of counts of direct inflow according to the two methods are comparable. The total value of calculated groundwater discharge to the Baltic Sea was about 398,000 $m^3 d^{-1}$. The individual equal module was on average 793 $m^3 d^{-1}$.

The groundwater discharge to the Bay of Puck was mainly indicated by salinity changes of seafloor water layer. It is said that about 50 % of sediments in the Bay of Puck are impacted by groundwater discharge (Piekarek-Jankowska 1994). The identified groundwater impacted areas are located: in the inner part of the Bay of Puck (the western part of the inner Bay of Puck from Płutnica river estuary to the mouth of the Reda valley and in the outer part of the Bay of Puck (in the middle part of the reservoir) (Piekarek-Jankowska 1994). In the groundwater impacted areas the hydrological structure of water showed certain abnormalities e.g. salinity decreased in the bottom water. The differences in salinity between surface and bottom water reach from 0.3 to 0.5 (Piekarek-Jankowska 1996). In the same study Piekarek-Jankowska (1996) measured composition of oxygen and hydrogen isotopes to identify the origin of fresh water in the marine sediments. These isotopes were also analysed in the bottom water and in the groundwater from the Quaternary and Tertiary coastal aquifers. Due to the mixing of groundwater and seawater already in the sediment, less abundant in heavy isotopes, the values of δ18O and δD are shifted towards the negative pole as compared with the typical composition of marine bottom water.

The anomalies in macro components distribution in pore water profiles in groundwater impacted areas were also identified by Bolałek (1992). Figure 3.4 presents the pore water depth profiles of chloride, carbonate and sulphate ions, sodium, potassium, magnesium and calcium. The samples were collected at two study sites located in the Bay of Puck: st.5 represents a groundwater non-impacted area located in the outer part of the Bay of Puck, off Jastarnia while st.15 characterizes a groundwater impacted area located in inner part of the Bay of Puck, in the Płutnica river estuary.

The differences of sodium, chloride, potassium, magnesium bicarbonate and sulphate anions distribution in both areas are clearly visible. In pore water profiles of station 5 diffusion of sodium and chloride ions from bottom seawater can be observed. The vertical distribution of sodium concentrations in pore water shows similar characteristics to those observed in chlorides indicating seawater intrusion
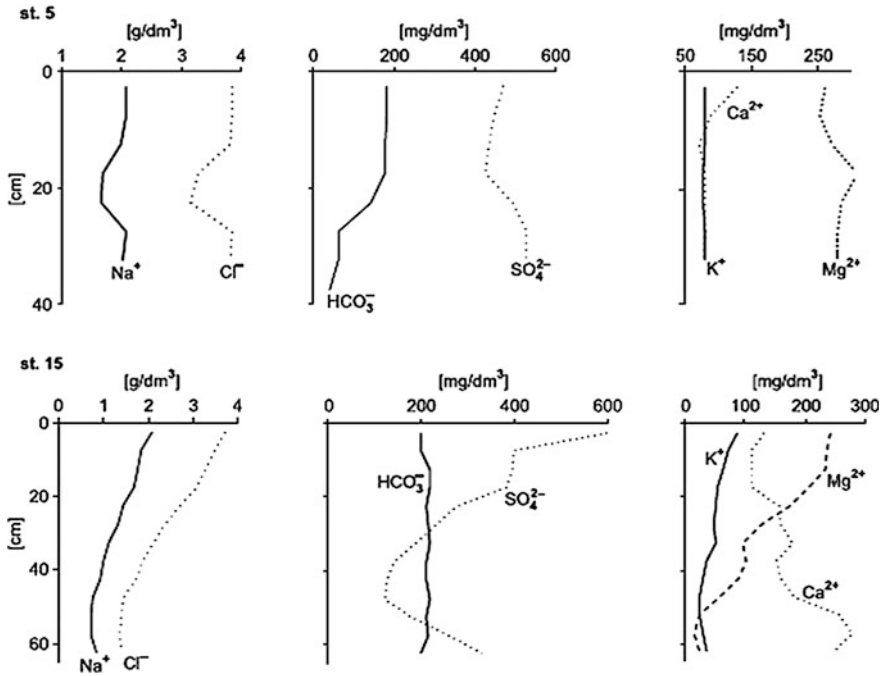
Fig. 3.4 The macro ions composition of pore water in the Bay of Puck. St.5 corresponds to the groundwater non-impacted area, while st.15 corresponds to groundwater impacted area (modified from Bolałek 1992)

into the sediment. In pore water st.15 profiles the decrease of chloride concentrations was attributed to both: the process of diffusion and discharge of groundwater. Thus, groundwater is characterized by different chemical composition in comparison to seawater. The process leads to a cation exchange. The concentration of calcium in pore water increases while that of magnesium, sodium and potassium decreases (st.15). The bicarbonate ion concentrations slightly increase in a groundwater impacted area (st.15) in comparison to a decrease in a groundwater non-impacted area (st.5) which is also caused by the mixing groundwater and recirculated seawater. The significant decrease of sulphate ions at st.15 in comparison to st.5 can be caused by bacterial mediated reduction and bicarbonate ions forming during the process. Similar pore water observations had been made by Piekarek-Jankowska (1994). The lowest concentration of chloride in the pore water was equal to 0.37 g L^{-1} while the highest value equaled 4.24 g L^{-1}. Falkowska and Piekarek–Jankowska (1999) showed an unusual vertical distribution of temperature and salinity in the seawater column in the groundwater impacted area located in the Gulf of Gdańsk and the Bay of Puck. Along the marine side of the Hel Peninsula lower salinity values were also recorded during upwelling events (Matciak et al. 2002).

References

Andrulewicz E (1992) Introduction. In: Trzosinska A (ed) Marine pollution—an assessment of the effects of pollution in the Polish coastal area of the Baltic Sea 1984–1989, 2, National Scientific Committee on Oceanic Research PAN, Gdańsk, pp 5–21

Augustowski B (1987) Bałtyk Południowy, Gdańskie Towarzystwo Nakowe, Wydział V Nauk o Ziemi, Zakład Narodowy imienia Ossolińskich

Bolałek J (1992) Ionic macrocomponents of interstitial water of Puck Bay. Oceanologia 33: 131–158

Bolałek J, Graca B (1996) Ammonia nitrogen at the water-sediment interface in the Puck Bay (Baltic Sea). Estuar Coast Shelf Sci 43:776–779

Burnett WC, Bokuniewicz HJ, Huettel M, Moore WS, Taniguchi M (2003) Groundwater and pore water inputs to the coastal zone. Biogeochemistry 66:3–33

Bussmann I, Suess E (1998) Groundwater seepage in Eckernförde Bay (Western Baltic Sea): effect on methane and salinity distribution of the water column. Cont Shelf Res 18:1795–1806

Cyberski J (1992) Hydrological factors—river outflow from Poland. In: Trzosinska A (ed) Marine pollution—an assessment of the effects of pollution in the Polish coastal area of the Baltic Sea 1984–1989, 2, National Scientific Committee on Oceanic Research PAS, Gdańsk, pp 53–67

Cyberski J, Szefler K (1993) Klimat Zatoki i jej zlewiska: Zatoka Pucka. Edited by Korzeniewski K. Fundacja Rozwoju Uniwersytetu Gdańskiego, Gdańsk, Poland, pp 14–39

Dzhamalov RG, Zektser IS, Meskheteli AV (1977) Groundwater flow to the seas and the world ocean. Moscow Nauka (PublishingHouse), Moscow

Ehlin U (1981) Hydrology of the Baltic Sea. In: Voipio A (ed) The Baltic Sea. Elsevier Oceanography Series, Amsterdam-Oxford-New York, pp 123–133

Emelyanov E (1995) Baltic Sea: geology, geochemistry, paleoceanography, pollution. Shishov Institute of Oceanology Russian Academy of Sciences, Atlantic Branch Baltic Ecological Institute of Hydrosphere Academy of Natural Sciences, Kaliningrad, Russia, 494 pp

Emelyanov E (2002) Geology of the Gdańsk Basin, Baltic Sea. Yantarny skaz, Kaliningrad 2002, 494 pp

Falkowska L, Piekarek-Jankowska H (1999) Submarine seepage of fresh groundwater: disturbance in hydrological and chemical structure of the water column in the Gdańsk Basin. J Mar Sci 56:153–160

Garrels RM, Mackenzie FT (1971) Evolution of sedimentary rocks. Norton, NY

Gudelis W, Jemielianow J (1982) Geologia Morza Bałtyckiego. Wydawnictwo Geologiczne, Warszawa 1982, 412 pp

Kaleris V, Lagas G, Marczinek S, Piotrowski JA (2002) Modelling submarine groundwater discharge: an eample from Western Baltic Sea. J Hydrol 265:76–99

Kaszubowski LJ, Coufal R (2008) Preliminary engineering-geological division of the Baltic Sea bottom (Polish part) in the light of geological maps of the Baltic and seismoacoustic research. In: 11th Baltic Sea geotechnical conference, Gdańsk, Poland, pp 1–19

Kramarska R, Uścinowicz Sz (2011) An outline of the gelologic structure of the Baltic Sea catchment area: geochemistry of Baltic Sea surface and sediments. In: Uścinowicz Sz (ed) Polish Geological Institute-National Research Institute, Warsaw, Poland, pp 17–20

Kramarska R, Sz Uścinowicz, Zachowicz J (2002) Kenozoik południowego Bałtyku wybrane problemy. Summary: Cainozoic of the Southern Baltic-selected problems. Przegląd Geologiczny 50:709–716

Kryza J, Kryza H (2006) The analytic and model estimation of the direct groundwater flow to Baltic Sea on the territory of Poland. Geologos 10:154–165

Kwon EY, Kim G, Primeau F, Moore WS, Cho H-M, DeVries T, Sarmiento JL, Charette M, Cho Y-K (2014) Global estimate of submarine groundwater discharge based on an observationally constrained radium isotope model. Geophys Res Lett 41:8438–8444. doi:10.1002/2014GL06157

Lidzbarski M (2011) Groundwater discharge in the Baltic Sea Basin: geochemistry of Baltic Sea surface and sediments. In: Uścinowicz Sz (ed) Polish Geological Institute-National Research Institute, Warsaw, Poland, pp 138–145

Łomniewski K, Mańkowski W, Zaleski J (1985) Morze Bałtyckie. PWN, Warszawa 1975, 507 pp

Matciak M, Urbański J, Piekarek-Jankowska H, Szymelfenig M (2002) Presumable groundwater seepage influence on the upwelling events along the Hel Peninsula. Oceanogr Stud 30:125–132

Niemirycz E (1999) Dopływ zanieczyszczeń z rzekami, In: Warunki środowiskowe w Polskiej strefie Bałtyku południowego w 1998 roku, Eds. B.Cyberska, Z. Lauer, and A. Trzosinska, Instytut Meteorologi i Gospodarki Wodnej, Gdynia 1999, pp 217–231

Nowacki J (1993) Termika, zasolenie i gęstość wody. In: Korzeniewski K (ed) Zatoka Pucka. Fundacja Rozwoju Uniwersytetu Gdańskiego, Gdańsk, Poland, pp 79–112

Peltonen K (2002) Direct groundwater inflow to the Baltic Sea. TemaNord, Nordic Councils of Ministers, Copenhagen, Holand, 79 pp

Pempkowiak J, Szefer P (1992) Origin, sources and concentrations of selected heavy metals in the southern Baltic biota, Bull Sea Fish Inst Gdynia 1:29–32

Piekarek-Jankowska H (1994) Zatoka Pucka jako obszar drenażu wód podziemnych. Wydawnictwo Uniwersytetu Gdańskiego. Gdańsk, Poland

Piekarek- Jankowska H (1996) Hydrochemical effects of submarine groundwater discharge to the Puck Bay (Southern Baltic Sea, Poland). Geographia Pol 67:103–119

Rybiński J, Niemirycz E, Makowski Z (1992) Pollution load. In: Trzosinska A (ed) Marine pollution—an assessment of the effects of pollution in the Polish coastal area of the Baltic Sea 1984–1989, 2, National Scientific Committee on Oceanic Research PAS, Gdańsk, pp 21–53

Schlüter M, Sauter EJ, Andersen CA, Dahlgaard H, Dando PR (2004) Spatial distribution and budget for submarine groundwater discharge in Eckernförde Bay (Western Baltic Sea). Limnol Oceanogr 49:157–167

Scholten J, Kreuzburg M, Knoeller K, Rapaglia J, Schlüter M, Schubert M (2015) Submarine groundwater discharge controlled by wind: an example from Eckernförde Bay, Southwestern Baltic Sea. Geophys Res Abs, 17: EGU2015–6830

Uścinowicz Sz (2011) An outline of the history of the Baltic Sea: geochemistry of Baltic Sea surface and sediments. In: Uścinowicz Sz (ed) Polish Geological Institute-National Research Institute, Warsaw, Poland, pp 70–73

Uścinowicz Sz, Miotk-Szpiganowicz G (2011) The Baltic Sea: location, division and catchment area: geochemistry of Baltic Sea surface and sediments. In: Uścinowicz Sz (ed) Polish Geological Institute-National Research Institute, Warsaw, Poland, pp 13–17

Uścinowicz Sz, Kramarska G, Miotk-Szpiganowicz G (2011) Quatenary cover of the Baltic Sea: geochemistry of Baltic Sea surface and sediments. In: Uścinowicz Sz (ed) Polish Geological Institute-National Research Institute, Warsaw, Poland, pp 73–76

Viventsowa EA, Voronow AN (2003) Groundwater discharge to the Gulf of Finland (Baltic Sea): ecological aspects. Environ Ecol 45:221–225

Voipio A (1981) The Baltic Sea. Elsevier, Amsterdam, 418 pp

Winterhalter B, Floden T, Ignatius H, Axberg S, Niemisto L (1981) Geology of the Baltic Sea. In: Voipio A (ed) The Baltic Sea, Elsevier Oceanography Series. Amsterdam-Oxford-New York, pp 1–117

Zekster IS, Everett LG, Dzhamalov RG (2007) Submarine groundwater. CRC Press, Boca Raton, The United States, 512 pp

Zverev VP (2009) Water in the Earth. Nauchniy mir (Publishing House), Moscow

Chapter 4
Research on Submarine Groundwater Discharge in the Baltic Sea

SGD has been recognized as an important pathway of material transport from land to the marine environment. Despite numerous studies as regards hydraulic fluxes and chemical composition of groundwater seeping to the coastal ocean much remains to be done to characterize SGD impact on the coastal marine environment. The Baltic Sea is an example of a region highly influenced by a variety of human activities that affect the ecosystem. SGD is a source introducing dissolved substances into the Baltic Sea that has not been quantified so far. Little is known regarding the concentrations and fluxes of chemical substances in groundwater discharged to the Baltic Sea and chemical reactions that control their flux into the coastal ecosystem. There are no studies concerning the importance of geochemical transformations in determining SGD-derived metals, nutrients, dissolved organic carbon and dissolved inorganic carbon fluxes to the Baltic Sea. Within 2009–2014 a major study was carried out aimed at quantification of SGD chemical composition and fluxes to the Baltic Sea (Pempkowiak et al. 2010; Szymczycha et al. 2012, 2013, 2014; Szymczycha 2015). The study was centered at the Bay of Puck, southern Baltic Sea, and other locations along the coast of Poland.

4.1 Aims, Scope and General Characteristics

4.1.1 Aims of the Study

The most important of the study objective was to examine the magnitude of the groundwater flow into the study area, located in the Bay of Puck, southern Baltic Sea including consideration of possible seasonal changes. The location of the study area was chosen as it is an exemplary groundwater impacted area based on a literature report (Piekarek-Jankowska 1996; Pempkowiak et al. 2010) and one of the results of the COSA- project (Huettel et al. 2004). The studies of groundwater composition in the neighborhood of the study area (Pruszkowska and Przewłócka 2007) indicate that consistent concentrations of major ions in groundwater collected by means of land based piezometers, within two–three month long periods are typical of the Bay of Puck coastline, where the study area is located. Pomerania is a

typical area of the southern Baltic Sea coast, i.e. an area dominated by agriculture. Little is known about groundwater discharges along the Baltic coast, both in terms of flux intensity and location. However, the geological structure of the Baltic Sea indicates that seeps occur mainly along the southern and eastern coasts of the sea, which are densely populated and dominated by agriculture. Lidzbarski (2011) indicates that the Bay of Gdańsk, and consequently the Bay of Puck might be the most important discharge areas in the Baltic Sea. Thus the study area might well prove to be typical to regional SGD.

The second objective was to examine and measure the concentrations of nitrates ions, nitrites ions, ammonium ions, phosphates ions, dissolved organic carbon, dissolved inorganic carbon, lead, cadmium, cobalt, manganese, copper, nickel, lead, chromium and mercury in the groundwater seeping to the study area located in the Bay of Puck, seawater and pore water, bearing in mind possible seasonal concentrations variability.

The third objective of the study was to examine the distribution and speciation of the measured chemical constituents in the groundwater impacted area. For this purpose the mixing process between groundwater and seawater was studied in order to define the processes influencing the speciation of selected constituents.

Finally, the fourth and last objective was to determine the fluxes of selected chemical substances into the study area and establish the importance of SGD derived loads of these substances as a component of their total input to the study area. The seepage meter method combined with the end-member method and the measured water components concentrations were used to calculate fluxes. Furthermore, the results were scaled up for the whole Bay of Puck and Baltic Sea, based on literature groundwater fluxes and concentrations measured within this study.

4.1.2   Description of the Study Area and Sampling

The main study area is situated in the Bay of Puck (H), a shallow part of the Gulf of Gdańsk in the southern Baltic Sea (Fig. 4.1) and in this manuscript will be called study area. The additional study sites were situated along the Polish coast at Międzyzdroje (M), Kołobrzeg (K), Łeba (Ł), Władysławowo (W). These locations were selected in accordance with literature reports indicating areas that were expected to be impacted by groundwater (Kryza and Kryza 2006). This additional sampling campaign was carried out in order to investigate chemical substances concentrations in seeping water collected at locations other than the main study area—the Bay of Puck. The obtained results together with results obtained in the Bay of Puck were used to calculate chemical substances fluxes to the Baltic Sea.

The study area in the Bay of Puck equals some 9200 m^2 and is located off the Hel Peninsula (Pempkowiak et al. 2010; Szymczycha et al. 2012). A narrow, sandy peninsula is mostly recent alluvial and littoral zone of Holocene sediments from 10 to 100 m in thickness (Korzeniowski 1993). The Bay of Puck, which is a part of the
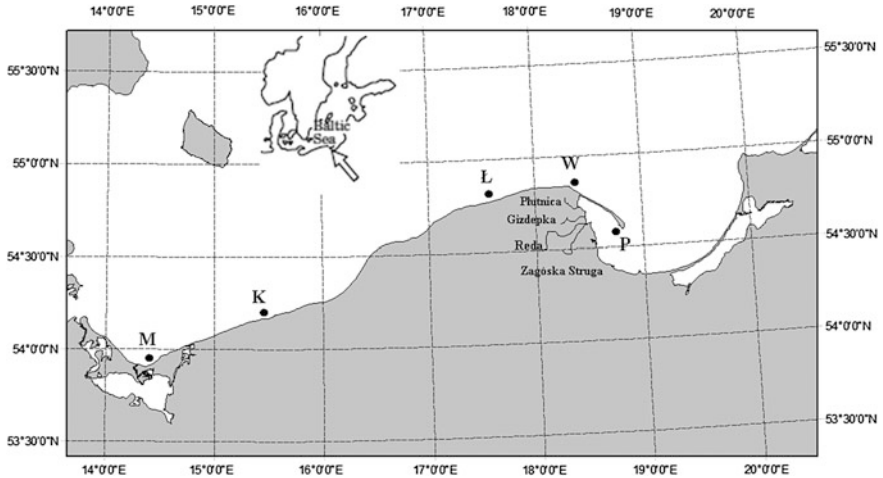
Fig. 4.1 A map of the Baltic Sea showing the location of the study areas: the Bay of Puck (*P*), Międzyzdroje (*M*), Kołobrzeg (*K*), Łeba (*Ł*), Władysławowo (*W*) and sampled rivers: Reda, Zagórska Struga, Płutnica and Gizdepka

Gulf of Gdansk is a shallow, sandy, wave-dominated bay, well known for its high eutrophication rates due to anthropogenic impact (Huzarska et al. 2013; Kotwicki et al. 2014). The sediments of the study area are influenced by seepage of groundwater (Piekarek-Jankowska 1996; Pempkowiak et al. 2010; Szymczycha et al. 2012, 2013, 2014; Kotwicki et al. 2014). Similar conditions were found in other sampling areas located along southern part of the semi-enclosed, non-tidal Baltic Sea. This region generally consists of lowlands. On the seashore sand bars were formed as a result of seawater movement. South-east of the coast lies a belt of lake lands with terrestrial moraines (reaching 300 m). The coast of the Wolin Island consists of alternating sections of cliffs and barrier ridges overtopped by dunes. The cliffs are mainly built up of Pleistocene deposits (tills, melt water deposits such as kames). The maximum height above mean sea level (MSL) of the polish cliffs is 115 m on Wolin Island.

Sampling The sampling campaigns were carried out in the following periods: 31.08–3.09.2009, 2–6.11.2009, 28.02–1.03.2010, 5–7.05.2010, 10–17.07.2013 and 22–27.06.2014.

Measurements of pore water salinity as a groundwater tracer were used for determining SGD site within the Bay of Puck. This method is commonly employed and leads to a successful identification of SGD location and rate (Millham and Howes 1994; Rapaglia 2007). The pore water salinity distribution from the study area at two depths: 5 and 25 cm into sediments, is presented in Fig. 4.2. The isolines were plotted by means of the Surfer software on the basis of salinity values. Yellow colour corresponds to low salinity while red colour—to high salinity. The groundwater impacted (GI) and groundwater non-impacted (GNI) zones can be
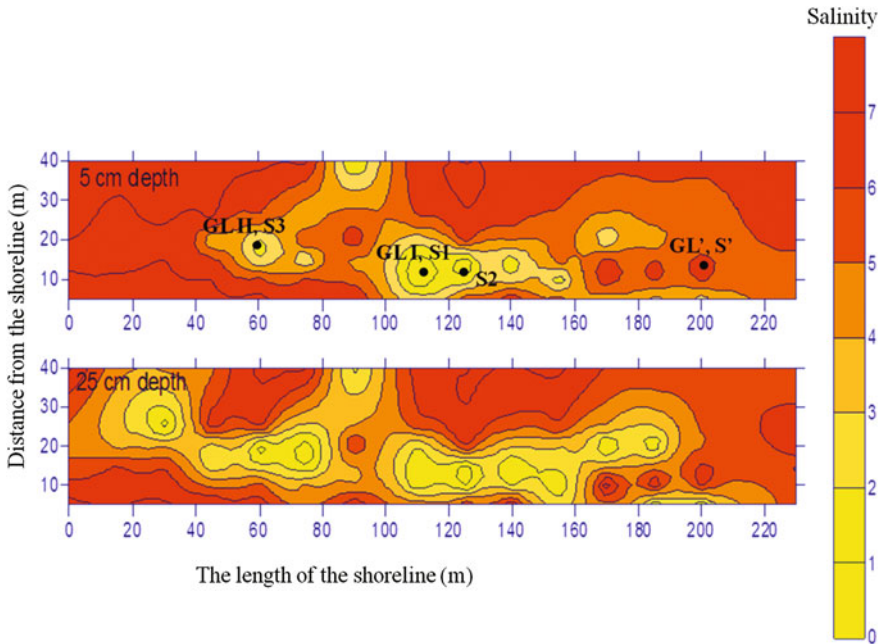
Fig. 4.2 Salinity distribution in sediment pore water samples collected at 5 cm and 25 cm depth on 31.08.2009. GL I, GL II and GL′ correspond to positions of groundwater lances while S1, S2, S3 and S′ correspond to seepage meter positions (Szymczycha et al. 2012)

clearly distinguished. Those with low salinity are attributed to groundwater discharge. It is a common phenomena for groundwater impacted areas that the pore water salinity varies substantially due to groundwater flux variations. Basing on salinity distribution (Fig. 4.2) the representative sampling points were selected for collecting pore water samples and groundwater seepage. In the Bay of Puck two separate seepage water discharge points located at close proximity (Groundwater lance I—GL I and Groundwater lance II—GL II) were sampled once a day. Groundwater lances were used to extract water from sediment. After 24 h, from inserting the device, samples of pore water were collected twice a day from several depths (0, 4, 8, 12, 16, 24, 30 cm) below sediment- water interface, by means of syringes. Filtered (0.45 µm, syringe-driven, membrane filters) pore water samples were collected from each depth. Water samples were transferred into polyethylene bottles, previously washed with 2 M nitric acid and rinsed with MilliQ water, transported to laboratory and analyzed.

Whereas at Międzyzdroje (M), Kołobrzeg (K), Łeba (Ł), Władysławowo (W) one groundwater lance was implemented for sampling groundwater impacted area.

Moreover in the Bay of Puck seepage meters (S1, S2, S3 and S′) consisted of a polyethylene (PTE) chamber with one end open, while the other end had a sample

port with PTE collector. Groundwater seeping through the sediment flew up into the a PTE collector. The change of water volume in the collector over a measured time interval provided the water flux intensity.

In the course of each sampling campaign seawater samples 50 cm above the sea floor were also collected. In May 2010; July 2013 and June 2014 sediment pore water samples from P, M, K, Ł, W without apparent groundwater discharge (GNI) were collected. In 2009 and 2010 samples of river water were collected from rivers close to the mouth: the Reda (0.6 km from mouth), the Zagórska Struga (0.1 km from mouth), the Płutnica (0.2 km from mouth), and the Gizdepka (0.2 km from mouth).

Water samples for additional parameters were collected directly into the vials and salinity, pH and oxidation-reduction potential (ORP) measurements were made with a multimeter (WTW Multi 3400i Multi-Parameter Field Meters) right after samples collection.

Quantification of SGD Seepage water fluxes were measured using seepage meters. Seepage meters, by measuring seepage flow across an isolated portion of the sediment-water interface, provide the most direct method of quantifying SGD (Burnett et al. 2006). Seepage water flowing through the sediment displace water trapped in the chamber forcing it up through the port into the PTE bag. The change in volume of water in the bag, over a measured time interval, provides the seepage water flux. Rosenberry (2008) claimed that SGD measurements made by means of seepage meters provide results within a 10 % error margin of true seepage rates. Combing the seepage meter method with the end-member method allows the estimation of the proportion of groundwater flux in seepage fluxes (Szymczycha et al. 2012). The measured salinity of the collected samples varied in the range from 3.7 to 6.5 (Table 4.1). The groundwater fraction in the collected samples was calculated using the end-member method (Burnett et al. 2006), and finally groundwater flux was calculated as a ratio of collected groundwater fraction and the device surface area divided by time. In short the end-member method is based on mass balance:

$$V_S = V_G + V_{SW}$$
$$S_S V_S = S_G V_G + S_{SW} V_{SW}$$

where S and V are the salinity and volume. Subscripts S, G, SW represent respectively: collected sample, groundwater and seawater. Using the above two equations and the measured values of S_S, S_G, S_{SW}, V_S, the two unknowns, namely V_G, V_{SW} were calculated (Szymczycha et al. 2012).

This combination method uses sensitive and precise measurements of end-member compositions to receive groundwater and seawater contributions to seepage fluxes. Salinity of seepage water samples, seepage water fluxes and groundwater fluxes are presented in Table 4.1. Measurements were taken three times per each seepage meter location during four sampling campaigns: September 2009; November 2009; February 2010 and May 2010. In the course of each

Table 4.1 Seepage water fluxes and groundwater discharge to the study area

Date	Location	Salinity of seepage water	Fluxes (L d^{-1} m^{-2})		Groundwater discharge seasonal average ± SD
			Seepage water	Groundwater	
September 2009	S1	5.6 ± 0.5	84.0 ± 3.6	23.7 ± 1.1	25.8 ± 2.4
	S2	5.2 ± 0.6	89.7 ± 3.4	25.6 ± 0.5	
	S3	4.1 ± 0.4	64.4 ± 2.4	28.5 ± 1.1	
November 2009	S1	6.5 ± 0.7	187.1 ± 7.0	18.7 ± 0.5	18.4 ± 5.4
	S2	6.1 ± 0.6	150.4 ± 5.7	23.6 ± 0.7	
	S3	6.3 ± 0.7	99.9 ± 3.8	15.8 ± 0.9	
February 2010	S1	5.6 ± 0.6	10.2 ± 0.4	2.3 ± 0.1	3.0 ± 2.1
	S2	4.7 ± 0.5	15.1 ± 0.6	5.4 ± 0.2	
	S3	5.8 ± 0.6	7.1 ± 0.3	1.4 ± 0.1	
May 2010	S1	3.7 ± 0.4	7.3 ± 0.3	3.7 ± 0.1	3.6 ± 0.1
	S2	6.5 ± 0.7	36.7 ± 1.4	3.7 ± 0.1	
	S3	5.9 ± 0.6	19.3 ± 0.7	3.6 ± 0.1	

Seepage water samples were collected and salinity was measured three times per each sampling location (S1, S2, S3) during four sampling campaigns: September 2009; November 2009; February 2010 and May 2010

sampling campaign the measured values of seepage water fluxes were stable at each of the sampling locations. Variations of the obtained results did not exceed 5 %. However, the differences in seepage water fluxes between the locations (S1, S2, S3) during each sampling campaign were significant. In February 2010 the relative standard deviation (RSD) of the obtained average groundwater flux reached the highest value, equal to 70 % of the average. Moreover, the data indicate that fluxes in February 2010 and May 2010 where lower than fluxes measured in September 2009 and November 2009. Thus, the measured fluxes of seepage water differ both by sampling location and season. One reason for this is the varying contribution of recirculated seawater to the seepage water. Seawater contributions to seepage fluxes ranged between 4 L d^{-1} m^{-2} in February 2010 to 44 L d^{-1} m^{-2} in November 2010. Thus, groundwater discharge contributed less than recirculated seawater to seepage water fluxes. However, the basic purpose for groundwater flux variation is varying supply of recharging rainwater. The annual groundwater discharge was approximated at 12.1 ± 10.3 L d^{-1} m^{-2}. This, rather large, standard error for the annual average of the groundwater flux into the study area is caused by seasonal differences in groundwater discharge into the study area (Table 4.3). The average SGD turned out to be well correlated with the average monthly precipitation characteristic of the area (Cyberski and Szefler 1993). A close relation between SGD and precipitation was also reported in a study off the west coast of Ireland (Smith and Cave 2012). Other studies indicate that SGD rates from shallow aquifers can also vary seasonally due to changes in precipitation (Cable et al. 1997; Capone and

Slater 1990). Thus, it can be assumed that groundwater discharge rate in the study area depend strongly on precipitation.

The groundwater discharges calculated by means of the seepage meters method combined with the end-member method were used to calculate the total groundwater discharge rate to the Bay of Puck. The total groundwater drainage area of the Bay of Puck equals 200 km^2—some 56 % of total surface area of the Bay of Puck (359.2 km^2) (Piekarek-Jankowska 1994). The average groundwater discharge is equal to 0.9 ± 0.8 km^3 year^{-1}. Piekarek-Jankowska (1994) calculated that total groundwater discharge to the Bay of Puck equals 0.03 km^3 year^{-1}. The results can be used to estimate the ratio of "active" and "inactive" areas of the seafloor as regards to SGD. The groundwater flux obtained during this study is 30 times higher than that obtained by Piekarek-Jankowska (1994). As the Bay of Puck seafloor is characterized by areas of seepage water discharge and areas with no discharge, using the total surface area of the Bay of Puck and the measured SGD flux in an "active" site, for calculating SGD could have led to overestimation.

4.1.3 The Studied Properties of Seeping Water

Units. Molar units

1. Molarity = moles per litre of solution = M

   - Commonly used terms include:

     mM = millimolar = millimoles per litre = 10^{-3} mol per litre
     μM = micromolar = micromoles per litre = 10^{-6} mol per litre
     nM = nanomolar = nannomoles per litre = 10^{-9} mol per litre
     pM = picomolar = picomoles per litre = 10^{-12} mol per litre
     fM = femtomolar = femtomoles per litre = 10^{-15} mol per litre
     aM = attomolar = attomoles per litre = 10^{-18} mol per litre

2. Molality = moles per kilogram of solvent = m

   - No longer in common use except in some computer programs that calculate distribution of chemical species concentration units for aqueous solutions, gases, and solids

3. Moles per kilogram of solution

   - The preferred usage in geochemistry, if not in marine chemistry, about 1.024 smaller than M in case of seawater (S = 35 ‰)

4. Normality = moles of charge equivalents per litre of solution (analogous to molarity, except that it refers to charge, Comes from acidity, i.e. moles H$^+$/L

   - Can also use equivalents per kg of solution (eq/kg)

5. g-atom/L = mole/L (a gram-atom is a mole)
6. Mole fraction (used for mixtures of gases and for solid solutions) = n1/n1 +
   n2 + n3

Mass concentration units

1. wt% = "weight percent" (actually, mass percent) = g per 100 g

   • Used for solids

2. ‰ = parts per thousand = g/kg for liquids and solids = mL/L for gas mixtures
3. Per mil = parts per thousand

   • Term is analogous to "percent"
   • Is used extensively for isotopic analyses—specifies the deviation from an
     isotopic standard reference material (SRM)

4. ppm = parts per million = μg/g or mg/kg for liquids and solids = μL/L for
   mixtures of gases = ppmv

   • "ppm" is commonly used for solids, whereas "mg/kg" is generally preferred
     for liquids

5. ppb = parts per billion = ng/g or μg/kg
6. mg/L = milligrams per litre

   • commonly used for solutions

Salinity Salinity is defined as a sum of inorganic salts present in 1 kg of sea water.
Interestingly, proportions of specific ions in sea water are always the same, which
can be understood if salinity differences are caused by either evaporating fresh
water or adding fresh water from rain. Freezing and thawing temperatures of sea-
water are affected by salinity concentration. Originally, salinity was measured by
evaporating water from sea-water. Up to 1980 salinity was calculated from chlo-
rinity largely measured using titration. Titration with silver nitrate was used to
determine the concentration of halide ions (mainly chlorine and bromine) to give a
chlorinity (Knudsen method). The chlorinity was then multiplied by a factor 1.83 to
account for all other constituents. The resulting 'Knudsen salinities' are expressed
in parts per thousand (ppt or ‰). The use of electrical conductivity measurements to
estimate the ionic content of seawater led to the development of the so-called
practical salinity scale 1978-PSS-78 (UNESCO 1981). Salinities measured using
PSS-78 do not have units. The 'unit' of PSU (denoting *practical salinity unit*) is
sometimes added to PSS-78 measurements, however this is officially discouraged
(Millero 1993). A sample of seawater with a chlorinity of 19.37 ppt will have a
Knudsen salinity of 35.00 ppt, a PSS-78 practical salinity of about 35.0. The
electrical conductivity of this water at a temperature of 15 °C is 42.9 mS/cm.

Salinity (along with temperature) affects the density and thus stability of the
water column. This in turn profoundly affects many biological processes in the
upper ocean and coastal seas. Saltier water is more dense and thus tends to sink

below fresher water. Oceanographers can identify where a water mass comes from just by noting its salt content and temperature. Salinity affects marine organisms because the process of osmosis transports water towards a higher concentration through cell walls. A fish with a cellular salinity of 1.8 % will swell in fresh water and dehydrate in salt water. So, saltwater fish drink water copiously while excreting excess salts through their gills. Freshwater fish do the opposite by not drinking but excreting copious amounts of urine while losing little of their body salts.

The salinity of sea water (usually 3.5 %) is made up by all the dissolved salts shown in Table 4.2. Marine plants (seaweeds) and many lower organisms have no mechanism to control osmosis, which makes them very sensitive to the salinity of the water in which they live.

According to the salinity of the sea several water types can be distinguished (Table 4.3). The salinity of *euhaline* seas is 30–35. *Brackish seas* or waters have salinity in the range of 0.5–29 and *metahaline seas* from 36 to 40. These waters are all regarded as *thalassic* because their salinity is derived from the ocean and defined as *homoiohaline* if salinity does not vary much over time (essentially constant). Highly saline water, from which salts crystallize (or are about to), is referred to as *brine*.

Reduction potential Reduction potential is also called redox potential, oxidation/reduction potential (ORP, pE, ε). Reduction potential of an aqueous solution characterizes the transfer of electrons between chemical species. The reduction potential indicates how strongly electrons are transferred to/from species

Table 4.2 The main salt ions that make up 99.9 % of all contents of sea water (S = 34.7 ‰)

Chemical ion	Valence	Molecular weight	Concentration		
			ppm, mg/kg	%	mmol/kg
Chloride Cl	−1	35.453	19,345	55.03	546
Sodium Na	+1	22.990	10,752	30.59	468
Sulfate SO_4	−2	96.062	2701	7.68	28.1
Magnesium Mg	+2	24.305	1295	3.68	53.3
Calcium Ca	+2	40.078	416	1.18	10.4
Potassium K	+1	39.098	390	1.11	9.97
Bicarbonate HCO_3	−1	61.016	145	0.41	2.34
Bromide Br	−1	79.904	66	0.19	0.83
Borate BO_3	−3	58.808	27	0.08	0.46
Strontium Sr	+2	87.620	13	0.04	0.091
Fluoride F	−1	18.998	1	0.003	0.068

Table 4.3 Water types according to salinity ranges

Types of saline water			
Fresh water	Brackish water	Saline water	Brine
<0.05 %	0.05–3 %	3–5 %	>5 %
<0.5 ‰	0.5–30 ‰	30–50 ‰	>50 ‰

in solution. It does not characterize the amount of electrons available for oxidation or reduction, in much the same way that pH does not characterize the buffering capacity. Thus the red-ox potential is a measure of the tendency of a chemical species to acquire electrons and thereby be reduced. Reduction potential is measured in volts (V), or millivolts (mV). Each species has its own intrinsic reduction potential; the more positive the potential, the greater the species' affinity for electrons and tendency to be reduced. ORP is a common indicator of for water quality.

In aqueous solutions, the reduction potential is a measure of the tendency of the solution to either gain or lose electrons when it is subject to change by introduction of a new species. A solution components with a higher (more positive) reduction potential than the new species will have a tendency to gain electrons from the new species (i.e. to be reduced by oxidizing the new species) and a solution with a lower (more negative) reduction potential will have a tendency to lose electrons to the new species (i.e. to be oxidized by reducing the new species). Because the absolute potentials are difficult to accurately measure, reduction potentials are defined relative to a reference electrode. Reduction potentials of aqueous solutions are determined by measuring the potential difference between an inert sensing electrode in contact with the solution and a stable reference electrode connected to the solution by a salt bridge (van Loon and Duffy 2011).

The sensing electrode acts as a platform for electron transfer to or from the reference half cell. It is typically platinum, although gold and graphite can be used. The reference half cell consists of a redox standard of known potential. The standard hydrogen electrode (SHE) is the reference from which all standard redox potentials are determined and has been assigned an arbitrary half cell potential of 0.0 mV. However, it is fragile and impractical for routine laboratory and field use. Therefore, other more stable reference electrodes such as silver chloride and saturated calomel (SCE) are commonly used because of their more reliable performance.

Although measurement of the reduction potential in aqueous solutions is relatively straightforward, many factors limit its interpretation, such as effects of solution temperature and pH, irreversible reactions, slow electrode kinetics, non-equilibrium, presence of multiple redox couples, electrode poisoning, small exchange currents and inert redox couples. Consequently, practical measurements seldom correlate with calculated values. Nevertheless, reduction potential measurement has proven useful as an analytical tool in monitoring changes in a system rather than determining their absolute value.

In fact, it is possible to define pE, the logarithm of electron concentration in a solution, which will be directly proportional to the redox potential (Stumm and Morgan 1981). Sometimes pE is used as a unit of reduction potential instead of Eh, for example in environmental chemistry. If we normalize pE of hydrogen to zero, we will have the relation pE = 16.9 Eh at room temperature. This point of view is useful for understanding redox potential, although the transfer of electrons, rather than the absolute concentration of free electrons in thermal equilibrium, is how one usually thinks of redox potential. Theoretically, however, the two approaches are equivalent.

In the field of environmental chemistry, the reduction potential is used to determine if oxidizing or reducing conditions are prevalent in water or sediments, and to predict the states of different chemical species in the water, such as dissolved metals. pE values in water range from -12 to 25; the levels where the water itself becomes reduced or oxidized, respectively (van Loon and Duffy 2011).

The reduction potentials in natural systems often lie comparatively near one of the boundaries of the stability region of water. Aerated surface water, rivers, lakes, oceans, rainwater and acid mine water, usually have oxidizing conditions (positive potentials). In places with limited air supply, such as submerged soils, swamps and marine sediments, reducing conditions (negative potentials) are the norm. Intermediate values are rare and usually a temporary condition found in systems moving to higher or lower pE values (van Loon and Duffy 2011).

In environmental situations, it is common to have complex non-equilibrium conditions between a large number of species, meaning that it is often not possible to make accurate and precise measurements of the reduction potential. However, it is usually possible to obtain an approximate value and define the conditions as being in the oxidizing, unoxic, or reducing regime (van Loon and Duffy 2011). In a given system there is a strong dependence of ORP on pH. The dependence is often presented as a diagram, called a Pourbaix diagram. It shows thermodynamically stable species of a given element as a function of Eh and pH (Fig. 4.3).

pH of seawater An important property of aqueous solutions is pH because it affects chemical and biochemical properties such as chemical reactions, equilibrium conditions, and biological toxicity of dissolved species (Bates 1982; Dickson 1984; Herczeg et al. 1985; Millero et al. 2009b). The pH of seawater is a key quantity for the calculation of fossil fuel carbon dioxide transfer into the oceans and of the

Fig. 4.3 Pourbaix diagram for manganese
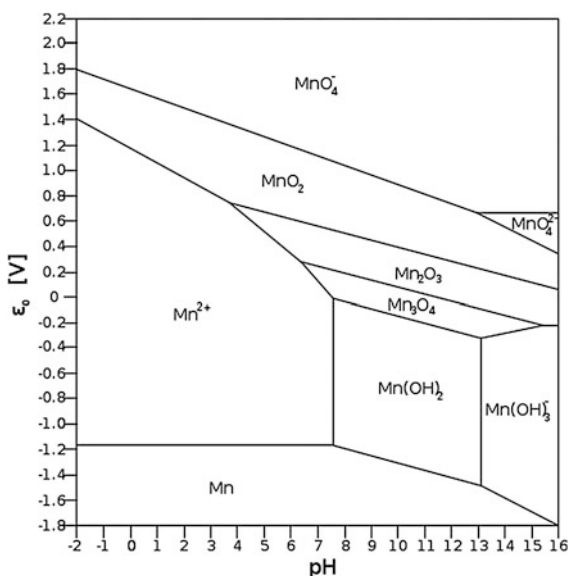
potential dissolution of calcareous organisms that constitute a sink for the carbon dioxide.

$$pH = -\log_{10}[H^+]$$

The pH of a solution is a measure of the molar activity (concentration) of hydrogen ions in the solution and as such is a measure of the acidity or basicity of the solution. The letters pH stand for "power of hydrogen" and the numerical value is defined as the negative base 10 logarithm of the molar activity of hydrogen ions:

The measurement of the pH of a sample can be done by measuring the cell potential of that sample in reference to a standard hydrogen electrode. This procedure would give a value of zero for a "one" Molar solution of H^+ ions, so that defines the zero of the pH scale. The cell potential for any other value of H^+ concentration can be obtained with the use of the Nernst equation. For a solution at 25 °C this gives:

$$E_{cell} = -0.0592 \log_{10}[H^+]$$

or

$$pH = E_{cell}/0.0592$$

For this expression, a base change from the natural log to the base 10 logarithm was made in the Nernst equation.

In practice, the pH is not usually measured in this way because it requires hydrogen gas at standard pressure, and the platinum electrode used in the standard hydrogen electrode is easily fouled by the presence of other substances in the solution. Fortunately, other practical electrode configurations can be calibrated to read the H^+ ion concentration. Laboratory pH meters are often made with a glass electrode consisting of a silver wire coated with silver chloride immersed in dilute hydrochloric acid. The electrode solution is separated from the solution to be measured by a thin glass membrane. The potential which develops across that glass membrane can be shown to be proportional to the hydrogen ion concentrations on the two surfaces. In the measurement instrument, a cell is made with the other electrode commonly being a mercury-mercury chloride electrode. The cell potential is then linearly proportional to the pH and the meter can then be calibrated to read directly in pH. Solution that is neither acidic nor basic is neutral.

The pH scale measures how acidic or basic a solution is. It ranges from 0 to 14. A pH of 7 is neutral. A pH less than 7 is acidic, and a pH greater than 7 is basic. Each whole pH value below 7 is ten times more acidic than the next higher value. For example, a pH of 4 is ten times more acidic than a pH of 5 and 100 times (10 times 10) more acidic than a pH of 6. The same holds true for pH values above 7, each of which is ten times more alkaline—another way to say basic—than the next lower whole value. For example, a pH of 10 is ten times more alkaline than a pH of 9.

Pure water is neutral, with a pH of 7.0. When chemicals are mixed with water, the mixture can become either acidic or basic. Vinegar and lemon juice are acidic substances, while laundry detergents and ammonia are basic.

Especially important for seawater pH are acid–base systems that are functions of pH. With the increasing uptake of fossil fuel CO_2 into the oceans, the effect of a decrease in pH is important to consider at this time (Marion et al. 2009; Millero et al. 2009b). According to Dickson (1984): "The field of pH scales and the study of proton-transfer reactions in seawater is one of the most confused areas of marine chemistry".

Waters with high algal growth can show a diurnal change in pH. When algae grow and reproduce they use CO_2. This reduction causes the pH to increase. This increase in pH may exceed 8.5, especially during the spring when nutrients are readily available. Therefore, if conditions are favorable for algal growth (sunlight, warm temperatures), the water will be more alkaline. Maximum pH usually occurs in late afternoon, and pH will decline at night when cellular respiration adds CO_2 to water. Because algal growth is restricted to light penetrating zones, pH can vary with depth in lakes, estuaries, bays and sea water.

Oxygen All animal life in the ocean, from most of bacteria, zooplankton to fish, requires oxygen to live. Oxygen enters the ocean in two main ways. It diffuses into the ocean surface from the atmosphere, and it is produced by plants in the sea during photosynthesis. The amount of oxygen in the water is controlled by the temperature, as well as by the levels of animal respiration and plant photosynthesis. Oceanographers can use oxygen measurements to determine rates of photosynthesis and animal respiration in the sea on a large scale.

Oxygen is measured by sensors and by analyzing water samples collected with chemical methods. Since oxygen is a gas that can easily escape from sea water, it is the first element to be analyzed when samples are collected. The chemicals are added that bind to the oxygen molecules. This is followed by an oxygen titrator to determine the amount of oxygen in each sample, and the result is recalculated to concentration of oxygen in seawater.

Concentrations of oxygen in seawater are most often given in mg dm^{-3} or cm^3 dm^{-3}. When compared to the maximum concentration at equilibrium, the relative concentration are given (%). Saturation concentrations of oxygen depend on temperature (Csat. = 10 cm^3 dm^{-3} at 20 °C), while relative concentration may change in the range from 350 % to −20 %. The negative value indicates that reduced species (e.g. H_2S) occure in water and give the amount of oxygen required to oxidize the reduced species.

Nutrients Plants in the ocean require nutrients to grow. The most important nutrients for phytoplankton growth in seawater are nitrate and phosphate. Some types of phytoplankton, called diatoms, also require the nutrient silicate, which they use to build their cell walls. Some "micro-nutrients" are needed too, but in smaller amounts. Iron is an important micronutrient. The main nutrients for plant growth are nitrogen (N as in nitrate NO_3^-, nitrite NO_2^-, ammonia NH_4^+), phosphorus (P as phosphate PO_4^{3-}) and potassium (K) followed by sulfur (S), magnesium (Mg) and calcium (Ca). Iron (Fe) is an essential component of enzymes and is copiously available in soil, but not in sea water (0.0034 ppm) in areas distant from land. This makes iron an essential nutrient for plankton growth. Plankton organisms (like

diatoms) that make shells of silicon compounds furthermore need dissolved silicon (SiO_2) which at 3 ppm can be also limiting. Nutrients are present in a dissolved form in seawater. Plants in the surface waters of the ocean take up these dissolved nutrients during photosynthesis. Once taken up by a plant we say the nutrients are in particle form. When the plants die they are decomposed and mineralized by marine bacteria. This returns the nutrients to a dissolved form that the plants can once more use. The plants may also be consumed by zooplankton, which digest the plants organic matter and also return the nutrients to a dissolved state.

Because light only penetrates a few hundred meters into the open ocean and just several maters in estuaries, no plants grow in the ocean's permanently dark depths. Thus there are no plants in these regions to remove nutrients from the water, and the ocean's deeper waters tend to be enriched in nutrients compared to its surface waters. A phenomenon called upwelling brings nutrients from the ocean depths to the sunlit surface waters where they can be used by plants. In some areas of the world's oceans (like the Sargasso Sea) nutrients are not replenished continually, and plants can sometimes use them up completely. These regions thus become nutrient-poor "ocean deserts" during certain seasons of the year.

Seawater for nutrient analysis is usually collected from research vessels or ships of opportunity (e.g., ferry boats, fishing boats, coast guard or navy vessels). The reference method for measuring nutrients in the following (including storage and pre-treatment) is presented in Grasshoff (1976) "Methods of Seawater Analysis".

Sea water contains microorganisms and other suspended matter of different composition. In some cases, these particles bias the measurement of the nutrient in the soluble phase. The suspended matter can be removed either by filtration or centrifugation. Unnecessary manipulation of the sample should be avoided, but in particle-rich waters (e.g., coastal waters, during plankton blooms), filtration or centrifugation may become necessary. It is important that the procedure used for filtration/centrifugation has been validated. Filtration in closed systems with a neutral gas is recommended. Centrifugation is especially advisable for samples destined for ammonia determination. If a sample containing particles is not filtered, the turbidity causes light scattering which can bias a colorimetric measurement. In this case, a turbidity blank should be carried out by measuring light absorption of the sample before adding the colour-forming reagents.

Special attention must be paid to possible nutrient sample contamination generated in the course of collecting. Wastewater discharged from wash basins, showers, and toilets contains significant amounts of phosphorus and nitrogen compounds and, therefore, can contaminate the surface waters to be sampled. For this reason, the water sampler must be deployed far from wastewater outlets, even if no sewage is discharged at the time of sampling. Although most modern ships are equipped with special sewage tanks, they are often emptied at sea owing to a lack of appropriate reception facilities in ports. Phosphorus and nitrogen compounds are secreted from human skin. However, touching of the sampler and the sample bottles by hands does not cause problems unless the sample comes into contact with the outer surface of the sampler or sample bottle. This is something that should never happen since the outer surfaces cannot be kept free of contamination on-board a

ship. In view of the potential for contamination, the analyst should preferably supervise the collection of samples. The written instructions for the collection of samples should include the precautions to be taken when a sub-sample is transferred to the storage container. The instructions must include the details of the essential record of the sample: station location, station code, depth of sampling, date, time, etc., and the identity of the person responsible for sampling.

The stability of nutrients in seawater samples depends strongly on the season and the location from which the samples were taken. Nutrients in seawater samples are generally unstable. Grasshoff (1976) recommends that ammonia and nitrite are measured no later than one hour after sampling. Samples for nitrate, phosphate, and silicate should preferably be analysed within six hours after sampling, and no later than ten hours. If for practical reasons samples cannot be analysed within these time limits, the corresponding data should be flagged if stored in databases, unless the storage method has been validated. Samples should be stored protected from light and refrigerated. Plastic bottles must be used if silicate is measured. New sample bottles sometimes adsorb nutrients onto their walls. The new bottles, if necessary, should be cleaned with phosphate-free detergent, rinsed generously with distilled/deionized water, and left filled with sea water containing nutrients for a few days. Then checks for adsorption of nutrients onto the walls or losses due to transformation to another chemical form should be carried out. Sample bottles should always be rinsed with the seawater sample from the sampler before they are filled. As regards ammonia determination, glassware for ammonia should always be cleaned with dilute hydrochloric acid. If samples cannot be analysed within the above-mentioned time limits, the following methods of storage can be recommended:

Silicate—0–4 °C protected from light. Do not freeze (polymerization may occur).
Nitrite—Freezing or 0–4 °C protected from light. Do not acidify (rapid decomposition).
Ammonia—No known preservation methods are applicable.
Nitrate—Freezing.
Total nitrogen—Freezing or 0–4 °C protected from light. Do not acidify (enhanced risk of contamination).
Phosphate—Freezing or acidification.
Total phosphorus—Freezing or acidification with sulphuric acid, store at 0–4 °C, protected from light.

The addition of mercury or chloroform is an alternative preservation method for all nutrients except ammonia. However, these chemicals can affect the reaction kinetics, especially with automated methods, and this effect should be evaluated by the laboratory. The same chemical preservation of calibrants and quality controls can compensate for this effect. The use of mercury should be minimized and optimum disposal procedures should be ensured. These preservation methods are all second choice to immediate analysis. They should, as mentioned, be validated by each laboratory, taking into account the concentration levels, storage time and environment, differences in sample matrices, and the analytical method of the laboratory. Since no preservation method for nutrients can, at present, be

recommended for general use, each laboratory must validate its storage methods for each nutrient before they are used routinely.

The choice of an analytical method should be based on the following criteria:

- the method should measure the desired constituent, i.e., be adequately specific, with accuracy sufficient to meet the data needs in the presence of interferences normally encountered in natural samples;
- the method should be sufficiently simple and rapid to permit routine use for the examination of large numbers of samples.

Dissolved Organic Carbon (DOC) and Particulate Organic Carbon (POC)

Dissolved and suspended organic substances addressed as organic matter cause that sea water is not just a solution of inorganic salts. Organic matter plays a key role in a variety of natural, physical and biological, processes occurring in the marine environment, especially in the shelf seas like the Baltic Sea, where its concentration is substantial (Kuliński and Pempkowiak 2008). These include O_2 depletion, formation of complexes with both organic and inorganic compounds and thus facilitating downward transport of chemical substances (C, N, P, heavy metals, organic pollutants) in the water column. Organic matter is responsible for chemical and physical properties of sea water like sea-color and light-availability in water column, absorbing, refracting, dispersing or reflecting light in sea water (Dera 1992; Hedges 2002). In order to completely understand the carbon cycle in the sea, it is important to understand changes in the amount of both dissolved organic carbon (DOC) and particulate organic carbon (POC). DOC and POC, both fractions can be separated by seawater filtering through, for example, 0.4 µm glass-fiber filters. DOC is an important source of nutrition for marine bacteria. Most of the organic carbon in the sea is in a dissolved form.

Aquatic organic matter is commonly divided into particulate organic matter—POM and dissolved organic matter—DOM. Both fractions are important components in the carbon cycle. POM in the marine environment is composed of phytoplankton, zooplankton, bacteria and dead organic material (detritus) while dissolved organic matter comprises molecules of both high and low molecular weight. Both, POM and DOM, can originate from internal and external (river run-off, atmosphere, sediments) sources (Emerson and Hedges 2008). Organic matter is measured, most often, as organic carbon which constitute some 45 % of organic matter (Chester 2003). In the oceans, concentration of organic carbon is less than 1,5 mg/dm³, in coastal areas it amounts to as much as 6 mg/dm³.

POC and DOC concentration in the Baltic Sea have been a subject of interest for many years (Pempkowiak et al. 1984; Kulinski and Pempkowiak 2008; Dzierzbicka-Glowacka et al. 2010, 2011).

Concentrations of DOC and POC in the Baltic seawater have been reported in the range 3.2–7.7 mgC/dm³, while in pore-water of bottom sediments they amount to some 12 mgC/dm³ (Grzybowski and Pempkowiak 2003; Kuliński and Pempkowiak 2011) and 0.1–1.4 mgC/dm³ (Burska et al. 2005; Kuliński and Pempkowiak 2011), respectively. It is reported that POC and/or DOC concentrations fluctuate seasonally

(Burska et al. 2005) and change vertically (Kuliński and Pempkowiak 2008). Mathematical modelling indicate POC and DOC concentrations dependence on light, water temperature and nutrient availability (Dzierzbicka-Glowacka et al. 2010; Almroth-Rosell et al. 2011). Organic substances are exchanged horizontally— through Danish Straits with the North Sea (Thomas et al. 2003; Kuliński and Pempkowiak 2011). Concentration of organic carbon depends upon distance from the land—costal and estuarial areas are more abundant in organic matter than open sea (Witek et al. 1997; HELCOM 2005a, b). Plankton activity may contribute to large seasonal fluctuations of both POC and DOC (Dzierzbicka-Glowacka et al. 2011). Although numerous studies have been carried out regarding organic carbon concentration and its dynamics in the Baltic Seawater, factors affecting its spatial and temporal distribution still, largely, lack quantification. For example no knowledge was developed as to differences of carbon concentration in different subbasins of the Baltic Sea. As changes of organic matter concentration, both particular and dissolved are to be expected in the near future (Dzierzbicka-Glowacka et al. 2011) base knowledge regarding this important component of seawater is of primary importance.

Dissolved inorganic carbon (DIC) The carbonate system of seawater is the primary buffer for the acidity of water, which determines the reactivity of most chemical components and solids (Emerson and Hedges 2008). The carbonate system of the ocean plays a key role in controlling the pressure of carbon doxide in the atmosphere, which helps to regulate the temperature of the planet. The formation rate of the most prevalent authigenic mineral in the environment, $CaCO_3$, is also a major sink for dissolved carbon in the long term global carbon balance.

The total concentration, CT, for inorganic carbon in seawater is called dissolved inorganic carbon (DIC).

The total dissolved inorganic carbon in a sea water sample:

$$DIC = [CO_2] + \left[HCO_3^-\right] + \left[CO_3^{2-}\right]$$

can be measured directly by acidifying the sample, extracting the CO_2 gas that is produced and measuring its amount.

4.2 Research on Salinity, pH, ORP, Nutrients, Metals, Dissolved Organic Carbon and Dissolved Inorganic Carbon Distribution in SGD Impacted Area

4.2.1 Salinity Distribution

Salinity (Burnett et al. 2006) and the concentration of chloride ions (Piekarek-Jankowska 1994) are good tracers of fresh and saline water in the marine environment. This is because chloride ions do not form insoluble compounds with

other macro components and they do not participate in the process of absorption. Moreover, their concentrations in the marine environment do not depend on the chemical or biochemical composition of sediments. Pore water salinity concentration is usually associated with chloride concentration in seafloor water. The change in chloride concentrations in pore waters stems from the processes of diffusion, migration induced by compaction and SGD (Bolałek et al. 2011). Intrusion of seawater into sediments plays an important role in shallow areas (Massel et al. 2005; Szymczycha et al. 2012). In groundwater impacted areas in the Southern Baltic Sea: Bay of Puck (Falkowska and Piekarek-Jankowska 1999) and Eckernfőorde Bay (Schlüter et al. 2004) a variability in the salinity of pore water was observed.

Piekarek-Jankowska (2007) indicated that at the depth of 50 cm below water-sediment interface, the pore water chloride concentration at the groundwater impacted area of the Bay of Puck is in a range between 0.37 and 4.24 g L^{-1}. Moreover, she identified the groundwater impact on seawater by measuring seafloor water salinity. The salinity of seafloor water in a groundwater impacted area was lower than salinity in a groundwater non-impacted area by 0.1–0.2.

Pore water salinity profiles collected at sites GL I, GLII and GL′ are presented in Fig. 4.4. Generally, in the GI-areas pore water profiles present a decrease of salinity with depth. For September 2009 pore water profiles GLI 2.09.09 and GLI 3.09.09 show salinity decreases from 7.1 to 3.3 and 2.8, respectively. The GLII 2.09.09 and GLII 3.09.09 pore water profiles show salinity decreases from 7.1 to 1.0 and 1.1, respectively. For November 2009 pore water profile GLI 4.11.09 presents a decrease of salinity from 7.1 to 4.0, while the pore water profile GLI 5.11.09 shows a salinity decrease from 7.1 to 5.2. Pore water profiles GLII 4.11.2009 and GL II 5.11.09 display salinity declines from 7.0 to 2.8 and 2.1, respectively. For February 2010 pore water profile GLI 28.02.10 presents a decrease of salinity from 7.3 to 2.3 while pore water salinity profile GLI 1.03.10 shows a salinity decrease from 7.0 to 1.0. Pore water profiles GLII 28.02.10 and GLII 1.03.10 show salinity declines from 7.0 to 1 and 0.3, respectively. For May 2010 pore water profiles GLI 5.05.10 and GLI 6.05.10 showed salinity decreases from 7.1 to 0.4 and 0.5, respectively, while both pore water profiles GLII 5.05.10 and GLII 6.05.10 showed a salinity decrease from 7.1 to 1.8. In the GNI-area the salinity profile was nearly constant and oscillated around 7.0. The shape of this pore water salinity profile is impacted by seawater percolation into the sediment.

The shapes of the salinity profiles in the GI-area depend on several processes. In each of the pore water salinity profiles the seawater intrusion into the sediment occurs regardless of the intensity of groundwater discharge. Similar pore water salinity (chloride concentration) profiles were found in groundwater impacted areas in the Gulf of Gdańsk (Pazdro and Kozerski 1990) and in the Bay of Puck (Bolałek 1992).

Many studies have shown that salt-water intrusion into the sediments is possible together with groundwater circulation (f.e. Massel 2001; Massel et al. 2005). In a tideless sea, like the Baltic Sea, the groundwater discharge can be controlled by the dynamics of surface waves. Especially in shallow water where waves propagate
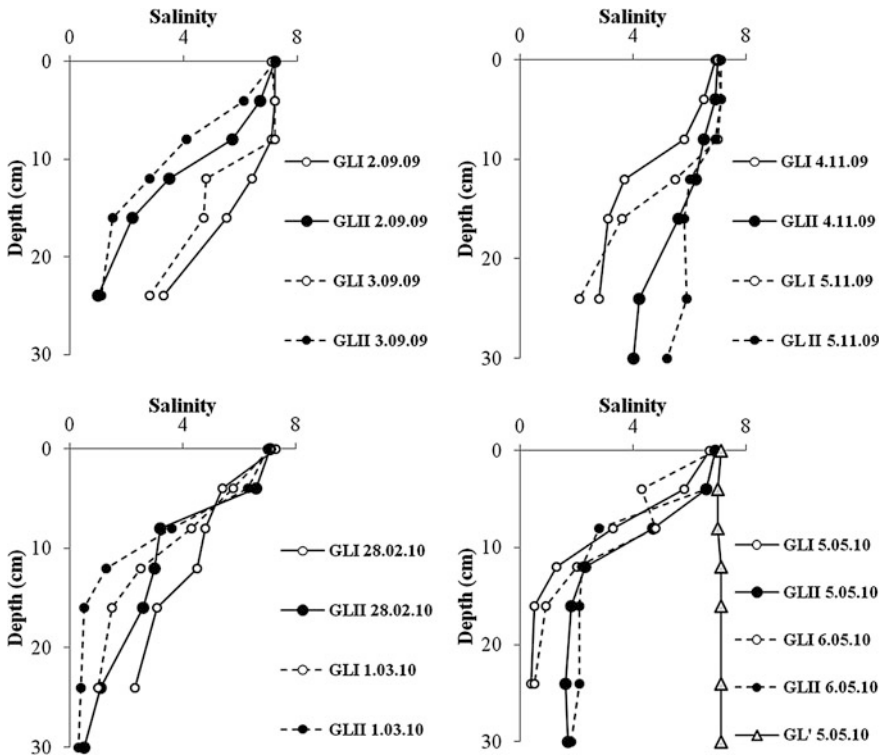
Fig. 4.4 The pore water salinity profiles. The samples were collected during four sampling campaigns: September 2009; November 2009; February 2010 and May 2010. Sixteen pore water profiles represent the groundwater impacted area (*hollow symbols* represent GLI location and *solid symbols* represent GLII location), while one profile is attributed to groundwater non-impacted area (*triangle symbols* represent GL′ location)

towards the shore and become steeper (Massel et al. 2005). As a result mixing between seawater and groundwater occurs in the surfacemost sediment layer. Generally, in the GI-area the uppermost 15 cm thick sediment layer below the water-sediment interface represents the mixing zone between seawater and groundwater. In some profiles the mixing zone is even deeper reaching down to 24 cm below the water-sediment interface (GLI 4.11.09 and GLI 5.11.09) or even 30 cm below water-sediment interface (GLII 4.11.09 and GLII 5.11.09). Below the groundwater-seawater mixing zone, lies the layer of sediment that contains groundwater. In most cases it is difficult to separate seepage water and groundwater as salinity profiles do not often show steep gradient. Thus, it was necessary to adopt boundaries dividing the zones. It was assumed that the salinity of pore water equal or lower than 0.5 is characteristic of groundwater, salinity of pore water in the range of 0.6–6.9 is attributed to seepage water and salinity of pore water higher than 7.0 is attributed to seawater. The assumption was based on direct measurements in the

course of the study and literature data concerning salinity and chloride concentrations in groundwater and seawater in the study area (Piekarek-Jankowska 1994; Bolałek 1992).

4.2.2 The Sediment Pore Water pH

Pore water profiles of chemical constituents are commonly used to identify the predominant reactions taking place in aquatic sediments (Charette et al. 2005; Beck et al. 2007). Amongst the chemical parameters that are measured routinely, oxygen concentration, oxidation-reduction potential and pH are particularly informative (Bolałek et al. 2011).

Figure 4.5 presents the pore water pH profiles (changes of pH with increasing sediment dept). The GLI and GLII profiles present similar trends in pore water
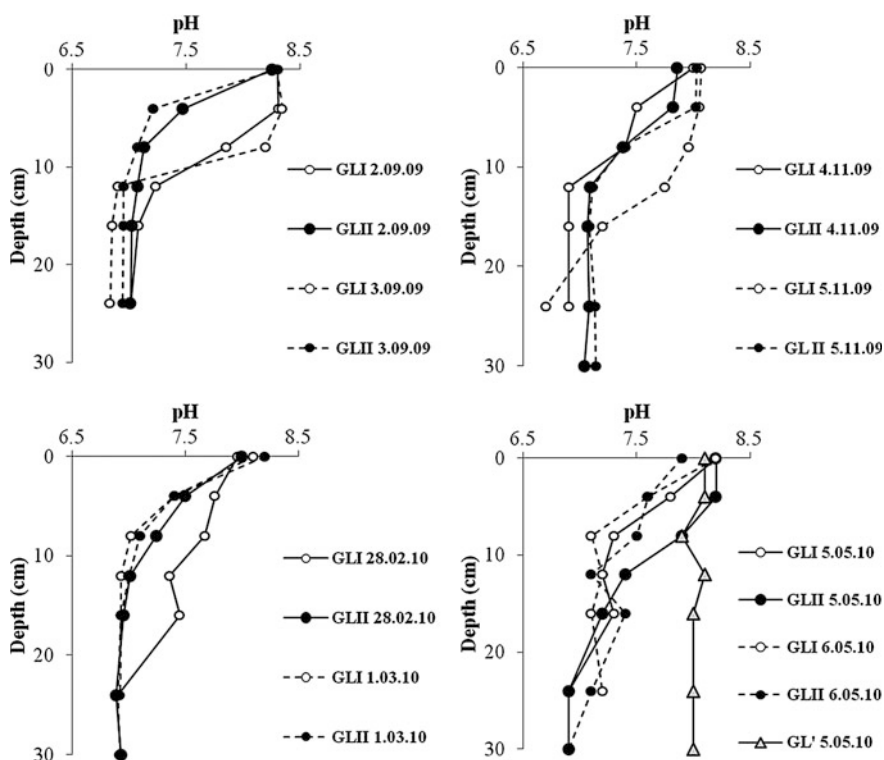
Fig. 4.5 The pore water pH profiles. The samples were collected during four sampling campaigns: September 2009; November 2009; February 2010 and May 2010. Sixteen pore water profiles represent the groundwater impacted area (*hollow symbols* represent GLI location and *solid symbols* represent GLII location), while one profile is attributed to groundwater non-impacted area (*triangle symbols* represent GL′ location)

salinity profiles. In the GI-area pore water profiles show a decrease of pH with depths while in the GNI-area the pH of pore water is rather constant, and oscillates about 8. Pore water profiles: GLI 2.09.09 and GLI 3.09.09 show a decrease of pH from 8.3 to 7.0 and 6.8, respectively. The GLII 2.09.09 and GLII 3.09.09 pore water profiles indicate a pH decrease from 8.3 to 7.0 and 6.9, respectively. In pore water profile GLI 4.11.09 pH declines from 8.0 to 6.8, while in pore water profile GLI 5.11.09 pH decreases from 8.1 to 6.7. Pore water profile GLII 4.11.2009 shows a pH decrease from 7.9 to 7.0 while pore water profile GLII 5.11.2009 shows a pH drop from 8.0 to 7.1. For February 2010 both pore water profiles GLI 28.02.10 and GLII 28.02.10 indicate a decrease of pH from 8.0 to 6.9 while pore water profiles GLII 28.02.10 and GLII 1.03.10 show a pH decline from 8.1 and 8.0 to 6.9, respectively. For May 2010 pore water profiles GLI 5.05.12 and GLI 6.05.10 present a pH decrease from 8.2 to 6.8 and 7.8, respectively. In pore water profile GLII 5.05.10 pH decreases from 8.2 to 7.2 while in pore water profile GLII 6.05.10 pH declines from 7.9 to 6.9.

The shapes of pore water pH profiles, similarly to the shapes of pore water salinity profiles, depend on seawater intrusion and groundwater flux. The pH of seawater equals 8.1 ± 0.1, while the pH of groundwater equals 7.2 ± 0.3. Thus, the process of seawater and groundwater end-members mixing results in the decrease of pH with the increasing depth in sediments. The differences between the shapes of the profiles are clearly visible. Thus, the shape of the pH pore water profiles depends on seawater intrusion and the intensity of groundwater discharge.

4.2.3   The Sediment Pore Water ORP

The presence or absence of oxygen in the environment is known to grately influence biota. It also conditions a range of red-ox reactions including both inorganic (Mn, Fe) and organic species. A measure of oxygen abundance/depletion is the so called oxidation-reduction or red-ox potential, often abbreviated as Eh or ORP. ORP can change in the range from −400 mV (reducing environment), through 150 mV (unoxic envirnment), to 400 mV (fully oxic envirnment). The ORP values can also determine the oxidation conditions within sediments. Oxidized sediment is characterized by ORP in the range from 0 to 400 mV, while reducing sediment has ORP below the range of −150 mV (Jørgensen 2006). The "oxidation-reduction condition" in the sediment pore water impacts biological and chemical processes there.

In Fig. 4.6 pore water ORP profiles are presented. ORP decreases in all the profiles including both GI-area and GNI-area. A usual red-ox profiles in the study area are interpreted as follows: close to the sediment surface, dissolved oxygen is abundant as it is transported from sea water into sediment either by molecular diffusion or as a result of biological processes. Thus, the ORP values in the
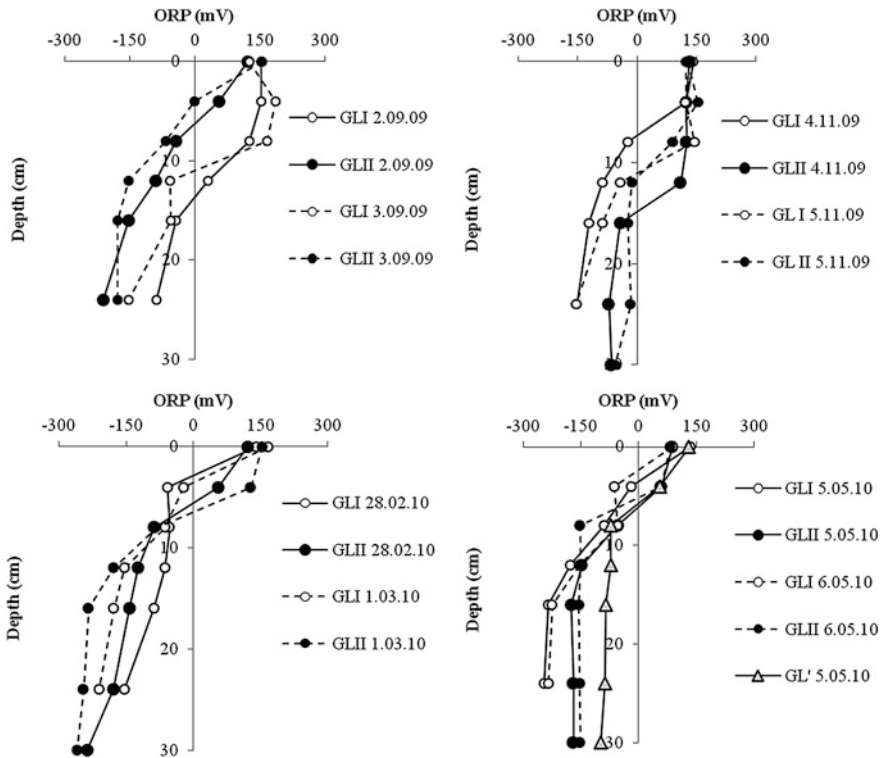
Fig. 4.6 The pore water ORP profiles. The samples were collected during four sampling campaigns: September 2009; November 2009; February 2010 and May 2010. Sixteen pore water profiles represent the groundwater impacted area (*hollow symbols* represent GLI location and *solid symbols* represent GLII location), while one profile is attributed to groundwater non-impacted area (*triangle symbols* represent GL′ location)

uppermost layer are characterized with positive values; below this zone follows a zone where manganese(IV) oxides in the solid phase serve as electron acceptors; next nitrate serves as an electron acceptor; in the deeper part of the sediment iron (III) oxides or iron(III) hydroxides in the solid phase of the sediment act as electron acceptors; after that, dissolved sulphate serves as an electron acceptor and finally, the reaction with the lowest ORP values is methane fermentation. In pore water profiles of the study area (Fig. 4.6) steep gradients of ORP occur at varying depths indicating the zone where intensive red-ox reactions lead to depletion of oxygen followed by Mn(IV) and Fe(III).

Thus, in the anoxic zone iron and manganese occur in dissolved, reducing forms (Mn II, Fe II), while in the oxic zone- as oxidized insoluble forms (Mn IV and Fe III). In the GI- area the profiles show lower ORP values than in the GNI-area. Thus, in the GI-area, ORP is influenced by geondwater discharge and its rates.

4.2.4   Nutrients Distribution

The inorganic compounds of nitrogen, phosphorous and silica (nitrates, nitrites, orthophosphates and orthosilicates) are the major nutrients, the so called macronutrients, in the aquatic environment. There are also various minor elements [e.g. Fe(II), Cu(II), Zn(II)] which are important for plant growth; these are called micronutrients. Micronutrients seldom limit the primary production in the coastal areas of the world ocean. On the other hand macronutrients do limit the primary production. The input of anthropogenic nitrogen and phosphorous to the coastal zone significantly impacts the nitrogen and phosphorous cycles there. High loads of nutrients are especially important in semi-enclosed or enclosed water reservoirs. The Baltic Sea is one of the biggest semi-enclosed, brackish seas and is vulnerable to nitrogen and phosphorous loads (HELCOM 2009). Once nitrogen and phosphorus have reached the Baltic Sea, they will remain there for a considerable time causing substantial alteration to primary productivity. The only sinks are outflow to the North Sea, burial in the sediments and, for nitrogen-denitrification. The main nutrient sources are river discharge and atmospheric deposition. So far nutrients fluxes via SGD have not been assessed in the Baltic Sea although in other study areas they are equal to, or exceed those from surface runoff (Kroeger et al. 2007; Leote et al. 2008; Kim et al. 2011).

Concentrations of nitrates, nitrites, ammonium, phosphates measured in collected water samples are presented in Table 4.4. Nutrient concentrations were measured in the study area, groundwater wells, nearby streams and rivers. Collecting samples for nutrient analyses from groundwater wells and rivers posed no difficulties. Collecting seepage water samples was more complex. Seepage meters are not well suited for this purpose due to the excess time required for sample collection. Therefore, groundwater lances were applied for collecting seepage water and groundwater samples (Szymczycha et al. 2012).

The yearly seawater averages were equal to 3.0 ± 1.0 μmol L^{-1} NO_3^-, 0.6 ± 0.2 μmol L^{-1} NO_2^-, 3.4 ± 1.9 μmol L^{-1} NH_4^+, 3.4 ± 0.3 μmol L^{-1} PO_4^{3-}. Seasonal variations of the measured nutrient concentrations in surface seawater were caused by spring and summer blooming of phytoplankton.

Seawater nitrate and nitrite concentrations were similar or slightly higher than those in the uppermost pore water layer as pore water there is freshly introduced seawater. The ammonium concentrations and phosphate concentrations were similar or slightly lower.

Their annual averages in pore water (salinity exceeding 6.9) were equal to 1.8 ± 0.3 μmol L^{-1} NO_3^-, 0.5 ± 0.1 μmol L^{-1} NO_2^-, 4.8 ± 1.1 μmol L^{-1} NH_4^+, 1.9 ± 1.1 μmol L^{-1} PO_4^{3-}. Nitrate concentrations and nitrite concentrations in seepage water samples were lower than in seawater while ammonium concentrations and phosphates concentrations were higher than in seawater. The annual average concentrations in seepage water (salinity in the range from 0.6 to 6.9) equaled 0.7 ± 0.6 μmol L^{-1} NO_3^-, 0.3 ± 0.1 μmol L^{-1} NO_2^-, 40.8 ± 25.0 μmol L^{-1} NH_4^+, 38.5 ± 18.2 μmol L^{-1} PO_4^3. Groundwater samples (pore water salinity lower

Table 4.4 Nutrients concentrations in the water samples collected during six sampling campaigns: September 2009; November 2009; February 2010; May 2010; April 2011 and August 2011

Sampling Campaign	Sample type		No of samples	Concentrations (µmol L⁻¹)			
				NO_3^- Average ± SD (min–max)	NO_2^- Average ± SD (min–max)	NH_3^+ Average ± SD (min–max)	PO_4^{3-} Average ± SD (min–max)
September 2009	Seawater		3	2.1 ± 0.1 (1.9–2.2)	0.7 ± 0.1 (0.5–0.8)	1.7 ± 0.1 (1.6–1.8)	3.1 ± 0.1 (2.9–3.0)
	Pore water	Seawater $S^a > 7$	8	1.6 ± 0.1 (1.4–1.6)	0.5 ± 0.1 (0.4–0.6)	3.7 ± 0.3 (3.4–4.0)	1.8 ± 0.2 (1.6–2.1)
		Seepage water $0.6 > S > 6.9$	15	0.5 ± 0.2 (0.2–0.9)	0.2 ± 0.1 (0.1–0.4)	68.0 ± 28.9 (14.6–108.0)	37.9 ± 18.6 (4.6–67.1)
		Groundwater $S < 0.5$	–	–	–	–	–
	Seepage water from seepage meters		3	0.9 ± 0.3 (0.6–1.2)	0.3 ± 0.1 (0.1–0.4)	59.4 ± 4.0 (55.6–63.7)	25.1 ± 6.5 (19.3–31.5)
	Groundwater from well in Hel		1	0.9	0.1	5.8	6.1
November 2009	Seawater		3	3.5 ± 0.3 (3.1–3.6)	0.4 ± 0.1 (0.3–0.4)	3.1 ± 0.4 (2.3–3.4)	3.5 ± 0.3 (3.2–3.7)
	Pore water	Seawater $S > 7$	6	2.2 ± 0.4 (1.8–2.1)	0.6 ± 0.1 (0.5–0.6)	5.6 ± 0.4 (5.0–5.9)	1.4 ± 1.4 (0.7–3.5)
		Seepage water $0.6 > S > 6.9$	21	1.1 ± 1.0 (0.2–2.5)	0.6 ± 0.1 (0.1–0.6)	34.0 ± 18.7 (6.5–55.8)	35.9 ± 15.9 (12.4–55.8)
		Groundwater $S < 0.5$	–	–	–	–	–
	Groundwater from well in Hel		1	0.8	0.2	6.4	7.2

(continued)

Table 4.4 (continued)

Sampling Campaign	Sample type		No of samples	Concentrations (µmol L⁻¹)			
				NO$_3^-$ Average ± SD (min–max)	NO$_2^-$ Average ± SD (min–max)	NH$_3^+$ Average ± SD (min–max)	PO$_4^{3-}$ Average ± SD (min–max)
February 2010	Seawater		3	4.1 ± 0.3 (3.5–4.4)	0.9 ± 0.1 (0.7–0.9)	5.3 ± 0.2 (5.1–5.5)	2.2 ± 0.1 (2.0–2.3)
	Pore water	Seawater S > 7	3	2.4 ± 0.5 (2.1–2.9)	0.53 ± 0.1 (0.52–0.54)	6.0 ± 0.6 (6.1–6.6)	3.1 ± 1.4 (1.9–4.5)
		Seepage water 0.6 > S > 6.9	19	0.7 ± 0.2 (0.5–1.0)	0.2 ± 0.1 (0.2–0.3)	35.4 ± 15.6 (3.4–58.2)	45.8 ± 14.2 (11.8–61.3)
		Groundwater S < 0.5	6	0.2 ± 0.1 (0.2–0.3)	0.2 ± 0.1 (0.2–0.3)	55.1 ± 2.1 (53.0–57.4)	60.1 ± 0.1 (59.6–60.4)
	Groundwater from well in Hel		1	0.9	0.4	8.4	10.2
May 2010	Seawater		3	2.1 ± 0.1 (2.0–2.2)	0.5 ± 0.1 (0.4–0.5)	2.9 ± 0.1 (2.8–2.9)	3.2 ± 0.6 (2.4–3.8)
	Pore water	Seawater S > 7	2	(2.0–2.2)	(0.2–0.3)	(2.0–2.1)	(3.7–3.9)
		Seepage water 0.6 > S > 6.9	21	0.7 ± 0.6 (0.1–1.7)	0.2 ± 0.2 (0.1–0.2)	31.4 ± 20.1 (2.2–53.6)	37.6 ± 18.3 (8.6–59.1)
		Groundwater S < 0.5	3	0.2 ± 0.1 (0.1–0.2)	0.2 ± 0.1 (0.1–0.2)	54.1 ± 1.7 (51.2–52.3)	60.6 ± 0.2 (60.4–60.8)
	Groundwater from wells[b]		5	0.9 ± 0.7 (0.1–2.1)	0.3 ± 0.3 (0.1–0.6)	4.4 ± 3.0 (2.0–9.6)	5.2 ± 3.1 (2.7–10.5)
	Water from rivers[c]		4	16.0 ± 2.3 (14.0–18.9)	1.3 ± 0.3 (1.0–1.6)	2.8 ± 0.7 (2.1–3.4)	7.2 ± 2.9 (4.1–9.1)

(continued)

Table 4.4 (continued)

Sampling Campaign	Sample type		No of samples	Concentrations (μmol L^{-1})			
				NO$_3^-$ Average ± SD (min–max)	NO$_2^-$ Average ± SD (min–max)	NH$_3^+$ Average ± SD (min–max)	PO$_4^{3-}$ Average ± SD (min–max)
April 2011	Seawater S > 7		1	0.9	0.3	2.8	0.7
	Pore water	Groundwater S < 0.5	1	0.3	0.1	48.6	66.4
August 2011	Seawater S > 7		1	0.4	0.3	1.3	0.3
	Pore water	Groundwater S < 0.5	1	0.1	0.1	51.0	61.2

[a]S is salinity

[b]Groundwater onshore wells: Reda I, II, III, Władysławowo, Hel

[c]Rivers: Reda, Zagórska Struga, Gizdępka and Płutnica

than 0.5) were characterized by the lowest nitrate concentrations and nitrite concentrations and the highest ammonium and phosphate concentrations. The annual groundwater averages equaled 0.2 ± 0.1 µmol L^{-1} NO_3^-, 0.1 ± 0.1 µmol L^{-1} NO_2^-, 55.2 ± 2.3 µmol L^{-1} NH_4^+, 60.3 ± 0.4 µmol L^{-1} PO_4^{3-}. The high standard deviation characteristic of ammonium concentrations is caused by unusually high ammonium concentrations measured in September 2009.

Generally, ammonium concentration and the phosphate concentration were significantly higher in groundwater than in seawater. In a coastal lagoon barrier in southern Brazil, Nienchesky et al. (2007) also showed that groundwater is enriched in ammonium, but contained only slightly elevated levels of phosphate. The ranges of ammonium and phosphate levels in groundwater samples from their study however were lower than those reported here. A study by Lee et al. (2009) of the Masan Bay, a site recognized as the most eutrophic embayment in Korea, reported similar inorganic nitrogen concentrations to those reported here. The phosphate concentrations in groundwater samples from the Lee et al. (2009) study, however were approximately ten times lower than those reported here. The phosphate concentrations reported here also exceed those measured at seepage locations in other studies (Leote et al. 2008; Lee et al. 2009).

Nutrient concentrations in groundwater wells were in a range characteristic to seawater. Annual averages were equal to 0.9 ± 0.1 µmol L^{-1} NO_3^-, 0.3 ± 0.1 µmol L^{-1} NO_2^-, 6.3 ± 1.7 µmol L^{-1} NH_4^+, 7.2 ± 2.2 µmol L^{-1} PO_4^{3-}. It can be assumed that when groundwater percolates through the sediments chemical processes influence nutrient concentrations. Therefore, nutrient concentrations measured in groundwater wells are different from those measured some 15 cm below the water-sediment interface. Nutrient concentrations in river water were equal to 16.0 ± 2.3 µmol L^{-1} NO_3^-, 1.3 ± 0.3 µmol L^{-1} NO_2^-, 2.8 ± 0.7 µmol L^{-1} NH_4^+, 7.2 ± 2.9 µmol L^{-1} PO_4^{3-}. These low concentrations may result from the seasonal fractionation.

Pore water nutrient profiles are presented in Figs. 4.7, 4.8, 4.9 and 4.10. Sixty four pore water nutrient profiles represent the GI-area, while four pore water nutrient profiles represent the GNI-area. Generally, within all the concentration profiles two trends can be distinguished. Nitrate concentrations and nitrite concentrations decrease with sediment depth while phosphate and ammonium concentrations increase with sediment depth.

In September 2009 nitrate concentrations in pore water profiles decreased with sediment depth from 1.6 ± 0.1 µmol L^{-1} to 0.3 ± 0.1 µmol L^{-1}. Nitrite concentrations decreased from 0.5 ± 0.1 µmol L^{-1} to 0.1 ± 0.1 µmol L^{-1}.

Ammonium concentrations increased with sediment depth from 3.6 ± 0.4 µmol L^{-1} to 92.7 ± 11.0 µmol L^{-1}. Phosphate concentrations increased with sediment depth from 1.8 ± 0.2 µmol L^{-1} to 53.9 ± 10.2 µmol L^{-1}.

In November 2009 nitrate concentrations in pore water profiles decreased with sediment depth from 2.1 ± 0.1 µmol L^{-1} to 0.2 ± 0.1 µmol L^{-1}. Nitrite concentrations decreased from 0.6 ± 0.1 µmol L^{-1} to 0.2 ± 0.1 µmol L^{-1}. Ammonium concentrations increased with sediment depth from 5.3 ± 0.4 µmol L^{-1} to
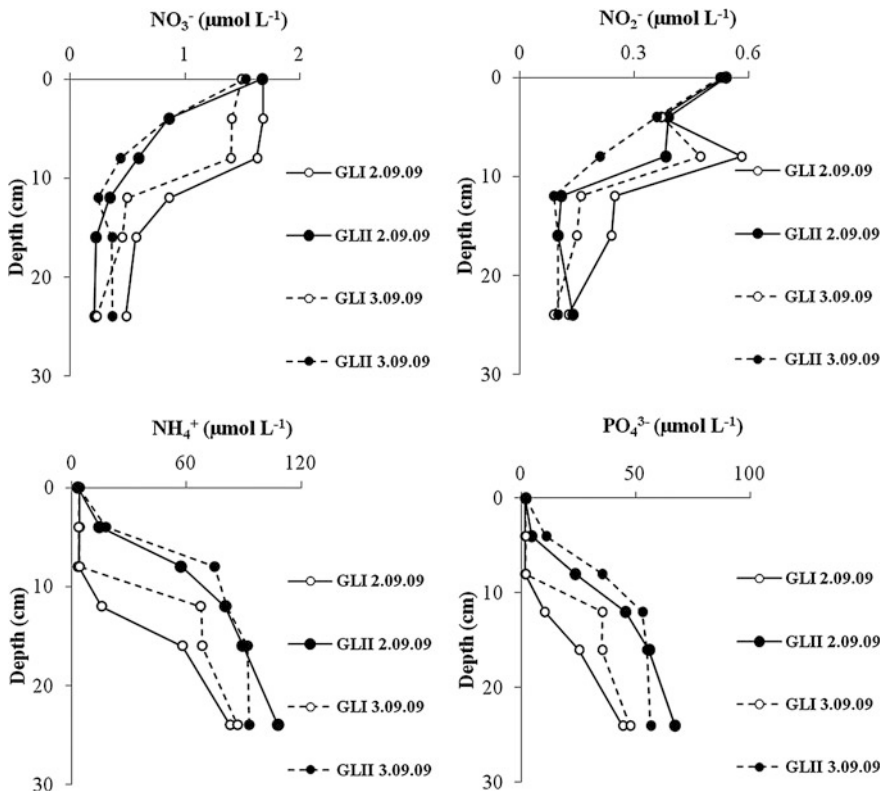
Fig. 4.7 The pore water nutrients profiles. The samples were collected in the GI-area in September 2009. The *hollow symbols* represent the concentrations of samples collected at the GLI location while *solid symbols*—at the GLII location. The *solid lines* represent samples collected on the first day of sampling while *dotted lines* represent samples collected on the second day of sampling

45.3 ± 0.4 μmol L^{-1}. Phosphate concentrations increased with sediment depth from 2.5 ± 2.7 μmol L^{-1} to 47.4 ± 7.0 μmol L^{-1}.

In February 2010 nitrate concentrations in pore water profiles decreased with sediment depth from 2.0 ± 0.1 μmol L^{-1} to 0.2 ± 0.1 μmol L^{-1}. Nitrite concentrations decreased from 0.5 ± 0.1 μmol L^{-1} to 0.2 ± 0.1 μmol L^{-1}. Ammonium concentrations increased with sediment depth from 5.9 ± 0.6 μmol L^{-1} to 54.1 ± 3.7 μmol L^{-1}. Phosphate concentrations increased with sediment depth from 3.1 ± 1.4 μmol L^{-1} to 59.8 ± 0.5 μmol L^{-1}. In May 2010 in the GI-area nitrate concentrations in pore water profiles decreased with sediment depth from 1.8 ± 0.1 μmol L^{-1} to 0.2 ± 0.1 μmol L^{-1}. Nitrite concentrations decreased from 0.3 ± 0.1 μmol L^{-1} to 0.1 ± 0.0 μmol L^{-1}. Ammonium concentrations increased with sediment depth from 2.9 ± 0.6 μmol L^{-1} to 53.6 ± 2.8 μmol L^{-1}.
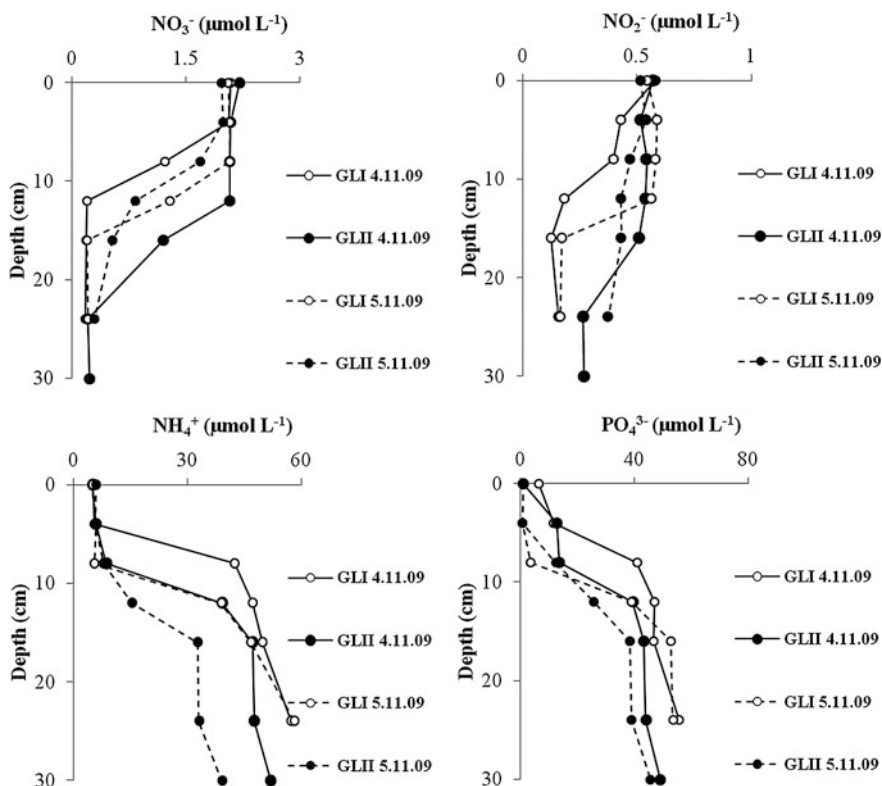
Fig. 4.8 The pore water nutrients profiles. The samples were collected in the GI-area in November 2009. The *hollow symbols* represent the concentrations of samples collected at the GLI location while *solid symbols* at the GLII location. The *solid lines* represent samples collected on the first day of sampling while *dotted lines* represent samples collected on the second day of sampling

Phosphate concentrations increased with sediment depth from 3.2 ± 0.6 µmol L^{-1} to 58.5 ± 3.2 µmol L^{-1}. The nitrate and nitrite concentrations in pore water profiles in the GNI-area smoothly decrease along with sediment depth. At approximately 24 cm depth below the water-sediment interface the nitrate concentrations and nitrite concentrations are similar to concentrations that occurred in the GI-area at 12 cm depth below water-sediment interface.

The pore water phosphate profile in the GNI-area is generally flat in comparison with the profiles in the GI-area. Small phosphate concentrations are characteristic of oxygenated sediments (Jørgensen 2006). The increase of phosphate concentrations at deeper sediment layers is visible as the reductive conditions limit phosphate adsorption and lead to dissolution on iron and manganese phosphates (Graca and Bolalek 2011).
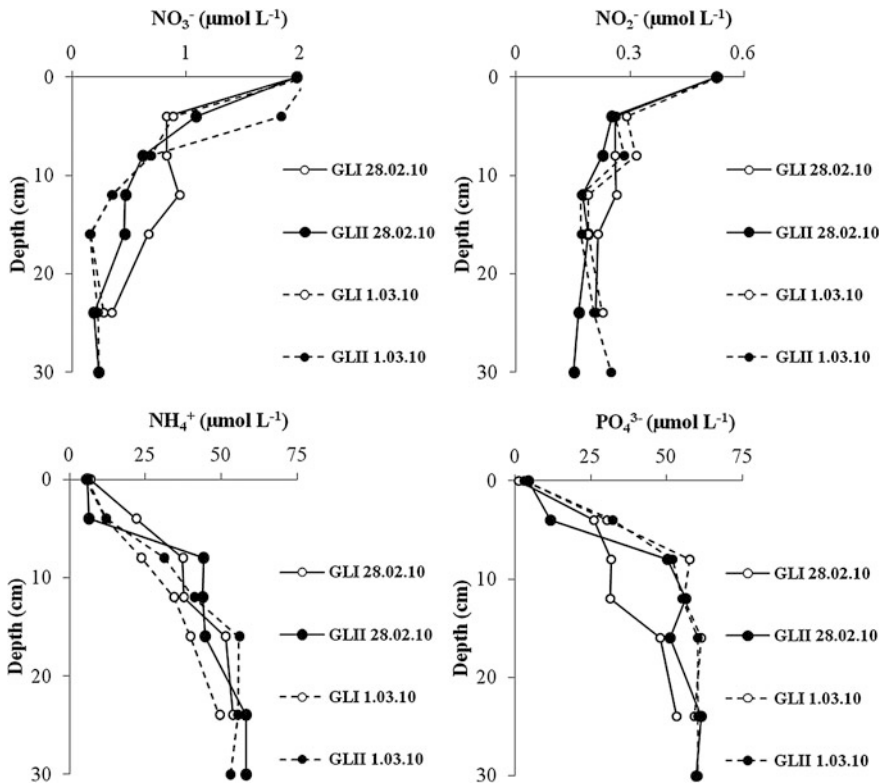
Fig. 4.9 The pore water nutrients profiles. The samples were collected in the GI-area in February 2010. The *hollow symbols* represent the concentrations of samples collected at the GLI location while *solid symbols*—at the GLII location. The *solid lines* represent samples collected on the first day of sampling while *dashed lines* represent samples collected on the second day of sampling

Ammonium concentrations similarly to phosphate concentrations increase with sediment depth but not as rapidly as in the GI-area indicating more oxic conditions in the sediments. The differences between the GI-area and the GNI-area are clearly visible.

4.2.5 *Dissolved Organic and Inorganic Carbon Distribution*

The carbon cycle is one of the most important biogeochemical cycles regarding the flow of matter and energy in the environment. The main constituent of the carbon cycle is carbon dioxide (CO_2). A significant increase of carbon dioxide in the atmosphere has been observed recently. Fossil fuel burning is responsible for CO_2
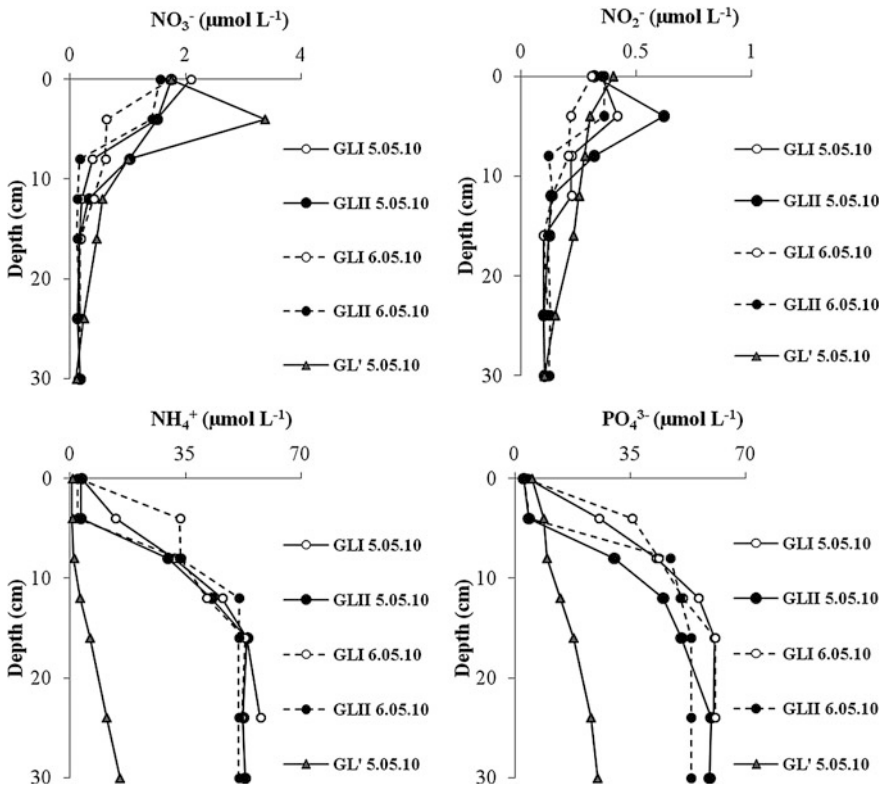
Fig. 4.10 The pore water nutrients profiles. The samples were collected both from the GI-area and GNI-area in May 2010. The *hollow symbols* represent the concentrations of samples collected in the GI-area at the GLI location while *solid symbols*—at the GLII location. The *triangle symbols* represent concentrations of samples collected in GNI-area at the location GL'. The *solid lines* represent samples collected on the first day of sampling while dashed lines represent samples collected on the second day of sampling

increase which results in global warming and seawater acidification (Chen and Borges 2009; IPCC 2007).

Takahashi et al. (2009) calculated that almost 35 % of anthropogenic CO_2 emission is absorbed by seas and oceans and almost $^1/_3$ of this load is absorbed by shelf seas. It has been proposed that shelf seas, including the Baltic Sea, are responsible for approximately 20 % of marine organic matter production and about 80 % of the total organic matter load deposited into marine sediments (Borges 2005). Some recent findings question earlier estimations regarding carbon dioxide sequestration, at least for selected coastal seas (Kuliński and Pempkowiak 2012). One of the possible reasons is that a significant pathway of material exchange between land and ocean i.e. SGD had been neglected (Szymczycha et al. 2014). Although data concerning carbon concentrations and fluxes via SGD are limited (Cai et al. 2003; Santos et al. 2009; Moore 2010; Liu et al. 2012), it is obvious that

SGD must be considered an important carbon source for the marine environment. It can be especially important for shelf seas, which play a significant role in the global matter and energy transfer between land, ocean and atmosphere (Thomas et al. 2009).

Table 4.5 presents dissolved inorganic carbon and dissolved organic carbon concentrations in the GI-area (seawater, pore water)—in groundwater wells and in nearby streams and rivers.

Dissolved carbon concentrations in seawater were rather stable over time. The annual averages of DIC concentrations and DOC concentrations in seawater equaled 20.8 ± 0.5 mg L^{-1} and 4.1 ± 0.1 mg L^{-1}, respectively. These DIC and DOC concentrations are well within ranges reported earlier for seawater (Pempkowiak 1983; Kuliński and Pempkowiak 2012). Seawater DIC and DOC concentrations were similar or slightly lower than in pore water defined as seawater (salinity exceeding 7.0). Annual averages of DIC and DOC concentrations in pore water defined as seawater were equal to 21.2 ± 1.2 mgl L^{-1} DIC, 4.1 ± 0.2 mgl L^{-1} DOC. The measured concentrations are close to results obtained earlier (Bełdowski and Pempkowiak 2003). DIC concentrations and DOC concentrations in seepage water were higher than in seawater. The annual seepage water DIC and DOC concentrations equaled 48.5 ± 19.4 mg L^{-1} and 5.2 ± 0.8 mg L^{-1}, respectively. Groundwater samples were characterized by the highest DIC concentrations and DOC concentrations. Groundwater averages (including all the sampling campaigns) were equal to 64.5 ± 15.0 mg L^{-1} for DIC, and 5.8 ± 0.5 mg L^{-1} for DOC. High standard deviation of the DIC average is typical of seasonal DIC variations in groundwater (Szymczycha et al. 2014). Relatively high concentrations of DIC compared to, for example, rivers (Kuliński and Pempkowiak 2011) that discharge in the region were measured in the groundwater at the study site. The content of carbonates within geological structures of the Baltic Sea continental drainage area is much higher than in the drainage area covering the Scandinavian Peninsula. The Baltic Sea is a land locked sea, and thus covers an area of geological structures similar to the land surrounding it (Lidzbarski 2011). The south-western part of the Baltic Sea, where the study is located, lies on the Paleozoic West European Platform separated from the East European Platform by the Teisseyre-Tornquist Fault Zone. The northern part of the Baltic Sea lies within the Baltic Shield, while the southern part is situated on the East European Platform. The study area is located on a sediment layer consisting of dolomites, calcites, limestones, syrrulian clays, and silts with dolomites abundant in carbonates. The reason for a higher DIC concentration in groundwater is thus the geological structure of the southern Baltic Sea. Other possibilities here are the reduction-oxidation processes of the system. The groundwater is anoxic (Szymczycha et al. 2013), and so organic matter oxidation occurs through sulphate reduction and methane production. Both these processes lead to an increase in carbonate presence in the system and explain higher alkalinity and carbon concentrations in "continental" rivers entering the sea along the southern coast compared with rivers draining the Scandinavian Peninsula. The results of DIC concentrations and DOC concentrations indicate that groundwater discharge is a source of DIC and DOC to coastal waters. Similar conclusions

Table 4.5 Dissolved inorganic carbon (DIC) and dissolved organic carbon (DOC) concentrations in the water samples collected during six sampling campaigns: September 2009; November 2009; February 2010; May 2010; April 2011 and August 2011

Sampling campaign	Sample type		No of samples	Concentartions µmol L^{-1}	
				DIC Average ± SD (min–max)	DOC Average ± SD (min–max)
September 2009	Seawater		3	20.0 ± 1.1 (18.9–21.1)	4.2 ± 0.1 (4.1–4.2)
	Pore water	Seawater S^a > 7	8	20.6 ± 1.4 (18.8–22.9)	4.2 ± 0.2 (4.0–4.6)
		Seepage water 1 > S > 6.9	15	52.8 ± 17.2 (20.0–74.9)	4.9 ± 0.7 (4.0–6.4)
		Groundwater S < 0.5	–	–	–
	Well groundwater from Hel		1	55.5	0.1
November 2009	Seawater		3	21.2 ± 0.3 (20.1–21.2)	4.0 ± 0.1 (4.0–4.1)
	Pore water	Seawater S > 7	6	22.1 ± 0.7 (1.8–2.1)	4.0 ± 0.0 (0.5–0.6)
		Seepage water 0.6 > S > 6.9	21	51.4 ± 20.9 (22.3–83.6)	4.6 ± 0.7 (4.0–6.3)
		Groundwater S < 0.5	–	–	–
	Well groundwater from Hel		1	55.4	0.1
February 2010	Seawater		3	21.3 ± 0.2 (21.3–21.5)	4.1 ± 0.2 (4.0–4.1)
	Pore water	Seawater S > 7	3	21.6 ± 0.7 (20.9–21.5)	4.0 ± 0.1 (4.0–4.1)
		Seepage water 0.6 > S > 6.9	19	37.4 ± 6.8 (26.5–47.8)	5.7 ± 0.6 (4.8–6.1)
		Groundwater S < 0.5	6	47.2 ± 0.5 (46.7–47.8)	5.8 ± 0.2 (5.6–6.4)
	Well groundwater from Hel		1	54.8	0.2
May 2010	Seawater		3	21.1 ± 0.1 (21.0–21.2)	4.0 ± 0.0 (4.0)
	Pore water	Seawater S > 7	2	(21.3–21.6)	(4.0–4.1)
		Seepage water 0.6 > S > 6.9	21	51.8 ± 24.0	5.1 ± 0.8
		Groundwater S < 0.5	3	84.0 ± 0.8 (83.4–85.1)	6.8 ± 0.1 (6.6–7.0)

(continued)

Table 4.5 (continued)

Sampling campaign	Sample type		No of samples	Concentartions μmol L^{-1}	
				DIC Average ± SD (min–max)	DOC Average ± SD (min–max)
	Groundwater from wells[b]		5	48.8 ± 6.2 (41.8–55.6)	2.1 ± 2.5 (0.3–5.0)
	Water from rivers[c]		4	42.7 ± 7.2 (38.0–59.1)	4.5 ± 1.3 (3.2–5.9)
April 2011	Seawater S > 7		1	20.9	4.0
	Pore water	Groundwater S < 0.5	1	83.0	6.7
August 2011	Seawater S > 7		1	20.4	4.0
	Pore water	Groundwater S < 0.5	1	77.3	5.4

[a]S is salinity
[b]Groundwater wells: Reda I,II,III, Władysławowo, Hel
[c]Rivers: Reda, Zagórska Struga, Gizdepka and Płutnica

regarding the role of SGD in the carbon cycle were drawn by Smith and Cave (2012). Their research demonstrated the impact of groundwater discharge on dissolved organic matter in the Irish coastal waters (Kinvara Bay and Auginish Bay). They established that DOC concentrations in groundwater were equal to 5.4 mg L^{-1}, which is slightly smaller than DOC concentration measured in this study.

In the northern South China Sea Liu et al. (2012) researched the impact of submarine groundwater discharge on the carbonate system. The results obtained indicated that the groundwater is enriched with DIC. The mean value reported by Lie et al. (2012) was 5.1 mmol L^{-1}, 1.3 times lower than in the groundwater discharged to the Bay of Puck. Dissolved carbon concentrations in samples from groundwater wells were similar to those measured in seawater. The annual averages equaled 53.6 ± 3.2 mg DIC L^{-1} and 0.6 ± 0.5 mg DOC L^{-1}. The DIC and DOC concentrations in rivers were equal to 42.7 ± 7.2 mg L^{-1} and 4.5 ± 1.3 mg L^{-1}, respectively.

Pore water dissolved carbon profiles, obtained during four sampling campaigns, are presented in Figs. 4.11 and 4.12. Thirty two pore water dissolved carbon profiles represent the GI-area, while two pore water profiles represent the GNI-area. Generally, within all the sampling campaigns DIC concentrations and DOC concentrations increase with sediment depth in the GI-area. In September 2009 DIC concentrations in pore water profiles increased with sediment depth from 20.2 ± 0.9 mg L^{-1} to 69.2 ± 3.8 mg L^{-1}. DOC concentrations increased from 4.0 ± 0.0 mg L^{-1} to 5.5 ± 0.1 mg L^{-1}, well within ranges reported for sea water (Kuliński and Pempkowiak 2008).
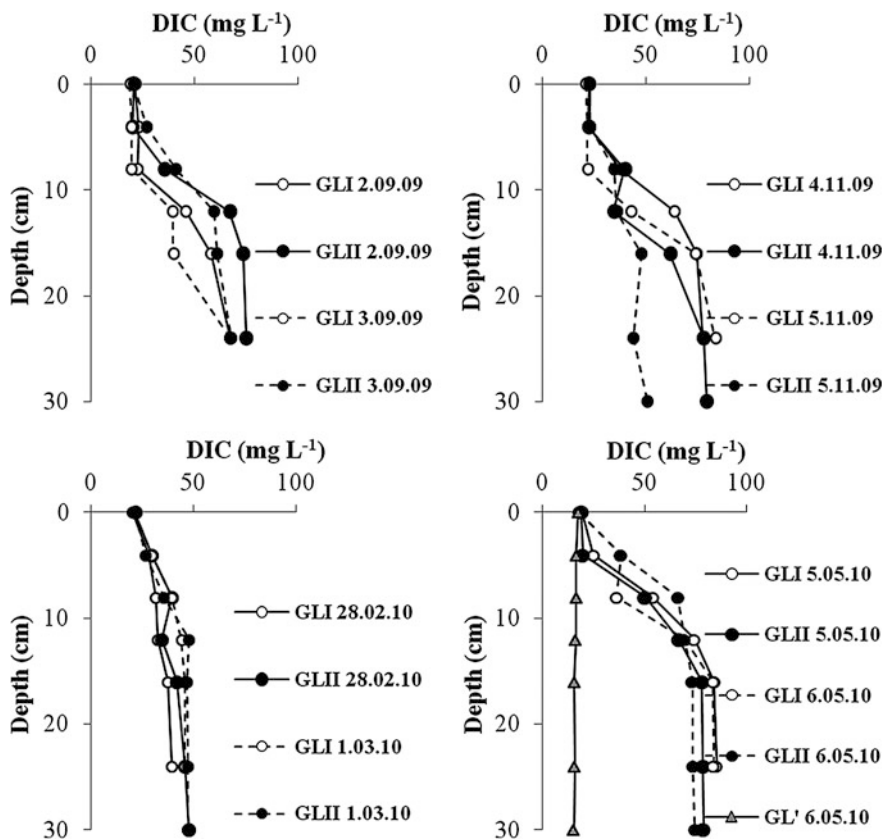
Fig. 4.11 Pore water dissolved inorganic carbon (DIC) concentration profiles. The samples were collected during four sampling campaigns (September 2009; November 2009; February 2010; May 2010). The *hollow symbols* represent the concentrations of samples collected in the GI-area at the GLI location while *solid symbols*—at the GLII location. The *triangle symbols* represent concentrations of samples collected in GNI-area at the location GL′. The *solid lines* represent samples collected on the first day of sampling while *dashed lines* represent samples collected on the second day of sampling

In November 2009—they increased from 21.0 ± 0.7 mg L^{-1} to 45.0 ± 3.9 mg DIC L^{-1} and from 4.1 ± 0.2 mg L^{-1} to 5.3 ± 0.9 mg DOC L^{-1}, while In February 2010 DIC concentrations in pore water profiles increased with sediment depth from 20.2 ± 0.9 mg L^{-1} to 69.2 ± 3.8 mg L^{-1}. DOC concentrations increased from 4.0 ± 0.0 mg L^{-1} to 6.0 ± 0.3 mg L^{-1}. In May 2010 in the GI area DIC and DOC concentrations increased with sediment depth from 18.6 ± 0.7 mg L^{-1} to 80.6 ± 4.8 mg L^{-1} and 4.1 ± 0.1 mg L^{-1} to 6.5 ± 0.5 mg L^{-1}, respectively.

The shapes of the pore water profiles in the GI-area can be explained by the intrusion of seawater into the sediments (Szymczycha et al. 2012) as different concentrations of DIC and DOC are characteristic of both the system end-members (groundwater and seawater).
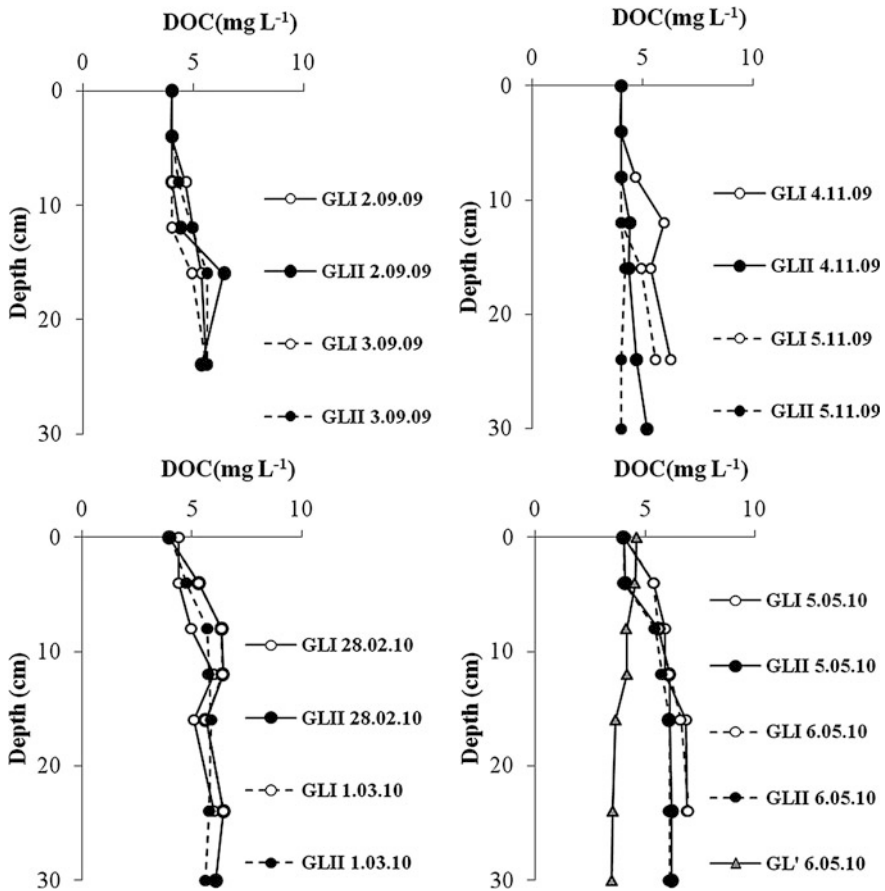
Fig. 4.12 Pore water dissolved organic carbon (DOC) concentration profiles. The samples were collected during four sampling campaigns (September 2009; November 2009; February 2010; May 2010). The *hollow symbols* represent the concentrations of samples collected in the GI-area at the GLI location while *solid symbols*—at the GLII location. The *triangle symbols* represent concentrations of samples collected in GNI-area at the location GL′. The *solid lines* represent samples collected on the first day of sampling while *dashed lines* represent samples collected on the second day of sampling

Decreases of DIC and DOC concentrations towards the subsurface sediment layer were caused by groundwater–seawater mixing as seawater is characterized by lower DIC and DOC concentrations in comparison to groundwater. The seawater intrusion depth depends on hydrodynamic conditions at the time of sampling and groundwater discharge rate. Pore water DIC and DOC profiles in the GNI-area indicated constant concentrations as oppose to profiles in the GI-area. The differences between DIC and DOC pore water profiles in GI-area and GNI-area are apparent. The groundwater discharge has a significant impact on dissolved carbon pore water concentrations.

4.2.6   Distribution of Trace Metals

The increasing concentrations of heavy metals in the environment signify a serious threat to human health, living resources, and ecological systems. Mobile and soluble heavy metal species are not biodegradable and tend to accumulate in living organisms, causing various diseases and disorders. Heavy metal contamination exists in aqueous waste streams of many industries and, frequently, surroundings of military bases. The soils surrounding polluted areas pose a risk of surface water and groundwater contamination (Sprynskyy et al. 2006).

Studies concerning metal cycling in groundwater impacted areas are limited. There is no available data concerning metal concentrations and fluxes via SGD into the Puck Bay, into the Gdańsk Basin, or into the entire Baltic Sea. The results of this study represent metal concentrations in the groundwater-seawater mixing zone, processes occurring on mixing groundwater and seawater zone and finally, metal fluxes via SGD into the Bay of Puck.

Concentrations of lead, cadmium, cobalt and manganese are presented in Table 4.6 while concentrations of copper, nickel, zinc and chromium in Table 4.7. Seawater and pore water samples were collected in the GI-area. Metal concentrations in seawater were rather stable in the course of time. The annual seawater averages were equal to 0.04 ± 0.01 nmol L^{-1} Pb, 0.4 ± 0.1 nmol L^{-1} Cd, 1.6 ± 0.5 nmol L^{-1} Co, 0.03 ± 0.01 µmol L^{-1} Mn, 18.9 ± 1.4 nmol L^{-1} Cu, 21.2 ± 0.5 nmol L^{-1} Ni, 1.5 ± 0.2 nmol L^{-1} Zn, 2.1 ± 0.4 nmol L^{-1} Cr. Metal concentrations in seawater are in the concentration ranges reported for the Bay of Gdańsk (Pempkowiak et al. 2000). Seawater copper concentrations and nickel concentrations were similar or slightly higher than in pore water defined as seawater while concentrations of lead, cadmium, cobalt, manganese, zinc and chromium were similar or slightly lower. Annual averages for pore water defined as seawater were equal to 0.05 ± 0.01 nmol L^{-1} Pb, 0.5 ± 0.1 nmol L^{-1} Cd, 1.4 ± 0.5 nmol L^{-1} Co, 0.04 ± 0.01 µmol L^{-1} Mn, 18.5 ± 1.6 nmol L^{-1} Cu, 21.4 ± 0.4 nmol L^{-1} Ni, 1.5 ± 0.2 nmol L^{-1} Zn, 2.0 ± 0.4 nmol L^{-1} Cr. Copper concentrations and nickel concentrations in seepage water samples were lower than in seawater while concentrations of lead, cadmium, cobalt, manganese, zinc and chromium were higher than in seawater. Annual average concentrations for seepage water equaled 0.3 ± 0.2 nmol L^{-1} Pb, 1.3 ± 0.4 nmol L^{-1} Cd, 5.0 ± 0.9 nmol L^{-1} Co, 1.6 ± 0.1 µmol L^{-1} Mn, 7.3 ± 3.1 nmol L^{-1} Cu, 16.4 ± 1.8 nmol L^{-1} Ni, 15.3 ± 4.4 nmol L^{-1} Zn, 7.5 ± 2.2 nmol L^{-1} Cr. Groundwater samples are characterized by the lowest concentrations of nickel and copper, and the highest concentrations of lead, cadmium, cobalt, manganese, zinc and chromium. Annual groundwater average concentrations equaled 1.2 ± 0.1 nmol L^{-1} Pb, 2.5 ± 0.1 nmol L^{-1} Cd, 8.7 ± 0.1 nmol L^{-1} Co, 2.6 ± 0.1 µmol L^{-1} Mn, 0.7 ± 0.1 nmol L^{-1} Cu, 5.1 ± 0.2 nmol L^{-1} Ni, 33.1 ± 0.6 nmol L^{-1} Zn, 18.4 ± 0.1 nmol L^{-1} Cr. The concentrations of the trace elements in groundwater are one (Pb, Cd, Co, Zn) or two (Mn) orders of magnitude higher than in seawater. Ni and Cu concentrations similarly to Hg concentrations (Szymczycha et al. 2013)

Table 4.6 Dissolved lead, cadmium, cobalt and manganese concentrations in the study area

Sampling campaign	Sample type		No of samples	Concentrations			
				nmol L⁻¹			µmol L⁻¹
				Pb	Cd	Co	Mn
September 2009	Seawater		3	0.04 ± 0.01 (0.03–0.04)	0.4 ± 0.1 (0.4–0.5)	0.8 ± 0.1 (0.7–0.8)	0.04 ± 0.01 (0.03–0.05)
	Pore water	Seawater S > 7	8	0.03 ± 0.01 (0.02–0.04)	0.4 ± 0.1 (0.3–0.5)	0.8 ± 0.1 (0.8–0.9)	0.04 ± 0.03 (0.03–0.07)
		Seepage water 0.6 > S > 6.9	15	0.4 ± 0.2 (0.1–0.8)	1.2 ± 0.7 (0.2–2.2)	5.1 ± 1.8 (1.8–7.2)	1.7 ± 0.7 (0.5–2.6)
		Groundwater S < 0.5	–	–	–	–	–
November 2009	Seawater		3	0.03 ± 0.01 (0.02–0.04)	0.3 ± 0.1 (0.2–0.3)	1.3 ± 0.1 (1.2–1.3)	0.03 ± 0.01 (0.02–0.03)
	Pore water	Seawater S > 7	6	0.04 ± 0.01 (0.03–0.04)	0.3 ± 0.1 (0.2–0.3)	1.2 ± 0.1 (1.1–1.3)	0.02 ± 0.01 (0.01–0.03)
		Seepage water 0.6 > S > 6.9	21	0.3 ± 0.2 (0.1–0.5)	0.8 ± 0.6 (0.2–2.0)	3.6 ± 2.1 (1.2–6.9)	1.4 ± 0.6 (1.0–2.4)
		Groundwater S < 0.5	–	–	–	–	–
February 2010	Seawater		3	0.04 ± 0.01 (0.03–0.04)	0.4 ± 0.1 (0.1–0.5)	2.0 ± 0.1 (1.9–2.0)	0.04 ± 0.01 (0.03–0.05)
	Pore water	Seawater S > 7	3	0.05 ± 0.01 (0.04–0.05)	0.5 ± 0.4 (0.1–0.9)	2.0 ± 0.3 (1.7–2.3)	0.04 ± 0.01 (0.02–0.05)
		Seepage water 0.6 > S > 6.9	19	0.6 ± 0.3 (0.1–1.2)	1.6 ± 0.6 (0.4–2.5)	5.6 ± 1.8 (2.5–8.5)	1.7 ± 0.8 (0.4–2.7)
		Groundwater S < 0.5	6	1.2 ± 0.1 (1.1–1.2)	2.5 ± 0.0 (2.5–2.5)	8.7 ± 0.0 (8.7–8.7)	2.7 ± 0.1 (2.6–2.8)

(continued)

Table 4.6 (continued)

Sampling campaign	Sample type		No of samples	Concentrations			
				nmol L^{-1}			µmol L^{-1}
				Pb	Cd	Co	Mn
May 2010	Seawater		3	0.06 ± 0.01 (0.05–0.06)	0.6 ± 0.1 (0.5–0.6)	1.5 ± 0.2 (1.3–1.6)	0.04 ± 0.01 (0.03–0.04)
	Pore water	Seawater S > 7	2	(0.05–0.06)	(0.5–0.6)	(1.4–2.1)	(0.02–0.05)
		Seepage water 0.6 > S > 6.9	21	0.06 ± 0.04 (0.1–1.2)	1.6 ± 0.7 (0.1–2.5)	5.5 ± 2.2 (1.9–8.7)	1.6 ± 0.8 (0.1–2.6)
		Groundwater S < 0.5	3	1.2 ± 0.1 (1.1–1.2)	2.5 ± 0.0 (2.5–2.5)	8.7 ± 0.0 (8.7–8.7)	2.6 ± 0.1 (2.6–2.7)
April 2011	Seawater S > 7		1	0.04	0.4	2.1	0.02
	Pore water	Groundwater S < 0.5	1	1.2	2.4	8.6	2.7
August 2011	Seawater S > 7		1	0.03	0.4	2.0	0.02
	Pore water	Groundwater S < 0.5	1	1.3	2.5	8.7	2.5

Table 4.7 Dissolved copper, nickel, zinc and chromium concentrations in the study area

Sampling campaign	Sample type		No of samples	Concentrations (nmol L^{-1})			
				Cu	Ni	Zn	Cr
September 2009	Seawater		3	19.7 ± 0.1 (19.6–19.9)	21.6 ± 0.4 (21.4–22.1)	1.5 ± 0.1 (1.5–1.6)	1.5 ± 0.1 (1.4–1.5)
	Pore water	Seawater S > 7	8	19.6 ± 0.3 (19.2–19.9)	21.6 ± 0.5 (21.2–22.6)	1.5 ± 0.3 (1.1–1.9)	1.5 ± 0.2 (1.3–1.8)
		Seepage water 0.6 > S > 6.9	15	5.3 ± 6.9 (1.6–16.8)	16.7 ± 4.7 (9.1–21.1)	15.3 ± 10.6 (3.2–30.6)	7.5 ± 4.7 (2.7–16.0)
		Groundwater S < 0.5	–	–	–	–	–
November 2009	Seawater		3	19.5 ± 0.1 (19.3–19.6)	21.6 ± 0.1 (21.5–21.7)	1.6 ± 0.1 (1.5–1.7)	1.8 ± 0.1 (1.8–1.9)
	Pore water	Seawater S > 7	6	19.5 ± 0.3 (19.3–19.8)	21.5 ± 0.2 (21.3–21.8)	1.6 ± 0.3 (1.2–1.9)	1.8 ± 0.1 (1.7–1.9)
		Seepage water 0.6 > S > 6.9	21	11.7 ± 5.2 (2.1–18.7)	18.9 ± 3.7 (7.9–21.2)	9.2 ± 7.9 (2.9–9.4)	4.3 ± 1.9 (2.4–8.2)
		Groundwater S < 0.5	–	–	–	–	–
February 2010	Seawater		3	18.8 ± 0.2 (18.6–19.0)	21.5 ± 0.1 (21.4–21.6)	1.7 ± 0.1 (1.6–1.8)	2.1 ± 0.1 (2.0–2.2)
	Pore water	Seawater S > 7	3	18.8 ± 1.1 (17.6–19.9)	21.5 ± 0.2 (21.3–21.8)	1.7 ± 0.4 (1.1–1.9)	2.1 ± 0.3 (1.8–2.4)
		Seepage water 0.6 > S > 6.9	19	5.1 ± 4.6 (0.7–16.1)	14.7 ± 4.3 (6.7–19.9)	19.4 ± 10.9 (3.0–33.6)	9.1 ± 5.0 (2.9–18.4)
		Groundwater S < 0.5	6	0.6 ± 0.1 (0.4–0.7)	5.4 ± 0.5 (5.1–6.1)	33.5 ± 0.4 (33.1–33.8)	18.3 ± 0.2 (18.1–18.5)

(continued)

Table 4.7 (continued)

Sampling campaign	Sample type		No of samples	Concentrations (nmol L^{-1})			
				Cu	Ni	Zn	Cr
May 2010	Seawater		3	16.1 ± 0.1 (16.0–16.2)	20.9 ± 0.1 (20.8–21.0)	1.2 ± 0.0 (1.2–1.2)	2.5 ± 0.1 (2.4–2.5)
	Pore water	Seawater S > 7	2	(15.8–16.4)	(20.6–21.0)	(1.2–1.2)	(2.4–2.6)
		Seepage water 0.6 > S > 6.9	21	6.9 ± 6.5 (0.6–13.5)	15.4 ± 5.3 (5.7–20.5)	17.3 ± 11.7 (2.1–33.7)	8.9 ± 5.1 (2.4–18.8)
		Groundwater S < 0.5	3	0.7 ± 0.1 (0.6–0.8)	5.1 ± 0.6 (4.8–5.8)	33.6 ± 0.2 (33.4–33.8)	18.4 ± 0.1 (18.3–18.5)
April 2011	Seawater S > 7		1	19.5	20.5	1.6	2.5
	Pore water	Groundwater S < 0.5	1	0.6	4.9	32.9	18.4
August 2011	Seawater S > 7		1	19.7	20.8	1.6	2.3
	Pore water	Groundwater S < 0.5	1	0.7	5.1	32.3	18.3

were smaller in groundwater than in seawater indicating a seawater as a source of these trace elements in the system. It was determined that groundwater discharged to the study site is enriched with lead, cadmium, cobalt, manganese, zinc and chromium.

Thus, the flux of groundwater influences metal concentrations in pore water. Selected metal concentrations (lead, cadmium, cobalt, manganese, zinc and chromium) are higher in the groundwater-seawater mixing zone as a result of groundwater flow. On the other hand, groundwater is low in nickel and copper, thus decreases their concentrations in the groundwater-seawater mixing zone and in seawater.

Groundwater discharge not only influences other seawater properties: salinity, pH and ORP, but changes several metals distribution in seawater, because it is enriched with, or depleted of, some metals. The phenomena are a subject of modification due to reastions occurring in the mixing zone of ground water and seawater.

As a result other processes parallel to mixing cause metal speciation changes in the groundwater discharge area. Studies concerning SGD carried out by Jeong et al. (2012) identified groundwater enrichment in manganese and cobalt concentrations comparable to this study. Moreover, similar distribution of copper concentrations and nickel concentrations were identified by Beck et al. (2007) in the West Neck Bay. They suggested that seawater is enriched with copper and nickel. Moreover, Beck et al. (2010) indicated copper enrichment in seawater and lead enriched in groundwater in the Great South Bay.

Studies concerning mercury concentrations in seepage water and their impact on the marine ecosystem have indicated the ecological and geochemical importance of SGD. In this respect some of the recent studies indicated enriched concentrations of mercury in SGD impacted areas (Lee et al. 2011; Ganguli et al. 2012).

In the Bay of Puck ranges of dissolved mercury concentrations in the water samples collected in the study area within five sampling campaigns (November 2009; February 2010; May 2010; April 2010; August 2011) are presented in Table 4.8. The measured dissolved mercury concentrations were in a relatively wide range (0.5–6.4 ng L^{-1}). The concentrations of dissolved mercury in seawater

Table 4.8 The dissolved mercury concentrations measured in water samples collected within five sampling campaigns (November 2009; February 2010; May 2010; April 2011; August 2011)

Sample type		Salinity	HgT_D concentrations (ng L^{-1})		
			Number of samples	Range (low–high)	Average
Seawater		S > 7	18	4.4–6.4	5.4
Pore water	Seawater	S > 7	11	3.2–5.3	4.1
	Seepage water	0.6 < S < 6.9	61	0.5–4.9	2.2
	Groundwater	S < 0.5	15	0.5–1.2	0.7
Groundwater from wells		S < 0.5	7	0.5–3.3	1.1

covered the range from 4.4 to 6.4 ng L^{-1}. Comparable concentrations were measured earlier in the seawater of the Gulf of Gdańsk, and the Bay of Puck (Boszke 2005; Bełdowski et al. 2009). The Bay of Puck is under the influence of nearby industrial and urban areas of Gdynia and Gdańsk. This means the presence of atmospheric mercury (Boszke 2005), and point sources. As a consequence concentrations of mercury in the waters of the Bay of Puck were much greater than concentrations in waters of the open Baltic Sea (Pempkowiak et al. 1998). Generally, dissolved mercury concentrations in the groundwater and seepage water ranged from 0.5 to 4.9 ng L^{-1}. Mercury concentrations in the water samples collected in the wells located on the Hel Peninsula were lower than 3.3 ng L^{-1}.

The trace metals concentrations (Pb, Cd, Zn, Cr, Mn, Co, Ni, Cu) in the pore water are presented as the pore water depths profiles in Fig. 4.13. The results represents the metals concentrations from groundwater impacted area (solid circles) and groundwater not impacted area (hollow circles). The errors bars represent the variation of the metals concentrations in the cause of time.

The concentrations of dissolved metals in the groundwater not impacted area generally slightly increased (Cd, Zn, Cr, Co, Mn) with sediments depths or were constant (Pb, Ni, Cu). The lead pore water concentrations were constant at every depth and similar to those in seawater. Concenttrations of Cd, Co, Zn and Mn were slightly higher than those in seawater, but again constant. Concentrations of Cu did not change much with sediment depth, while Ni concentrations slightly decreased with sediment depth, however they did not exceed concentrations characteristic of groundwater. Concentrations of Cr slightly increased with sediment depth but, similarly to Ni, did not exceed concentrations characteristic of groundwater. The pore water concentrations in the groundwater nonimpacted areas were comparable with the seawater averages which were equal to 0.04 ± 0.01 nmol L^{-1} Pb, 0.4 ± 0.1 nmol L^{-1} Cd, 1.6 ± 0.5 nmol L^{-1} Co, 0.03 ± 0.01 μmol L^{-1} Mn, 18.9 ± 1.4 nmol L^{-1} Cu, 21.2 ± 0.5 nmol L^{-1} Ni, 1.5 ± 0.2 nmol L^{-1} Zn, 2.1 ± 0.4 nmol L^{-1} Cr. Metal concentrations in seawater were in the concentration ranges reported for the Bay of Gdańsk and the southern Baltic Sea (Pempkowiak et al. 2000).

Generally, within all the sampling campaigns in the groundwater impacted areas two trends in the trace metals pore water profiles can be distinguished (Fig. 4.11). The concentrations of the most of the investigated metals (Pb, Cd, Zn, Cr, Co, Mn) increased with the sediment depths. This indicates significantly higher concentrations of dissolved metals in groundwater than in seawater. At the same time, the concentrations of Ni and Cu dropped with sediment depths. The concentration gradients near the sediment surface the steepest due to the fact that seawater is enriched in these elements in comparison to pore water and consequently to groundwater. The concentrations of the all measured trace elements were comparable between the sampling campaigns. No significant seasonal change in trace metals concentrations was detected in the cause of the study. The shapes of the profiles can be further elucidated by gradient of ionic strength, the redox potential shifts, and complexity of dissolved organic matter.
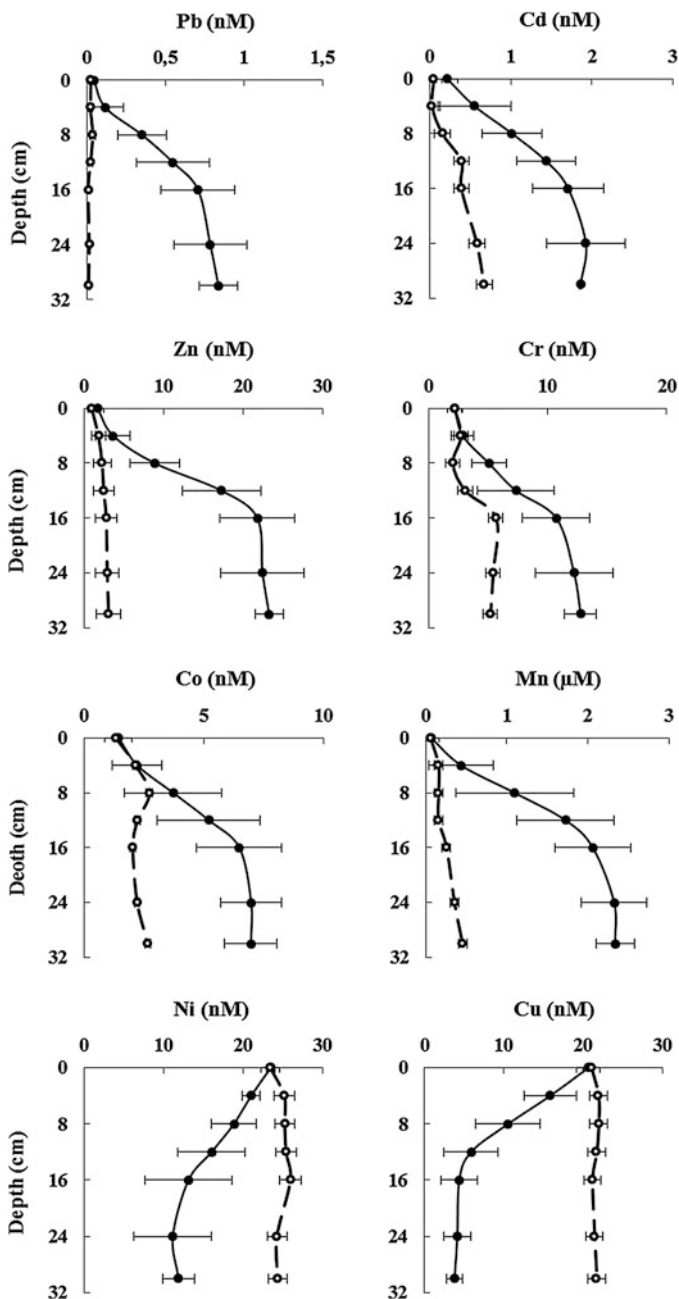
Fig. 4.13 The average trace metals profiles in the sediments pore water obtained for groundwater impacted areas (GI)—*solid circles* and groundwater not-impacted (GNI)—*hollow symbols*. The samples were collected in the following periods: 31.08–3.09.2009, 2–6.11.2009, 28.02–1.03.2010, 5–7.05.2010, 10–17.07.2013 and 22–27.06.2014 by means of groundwater lances
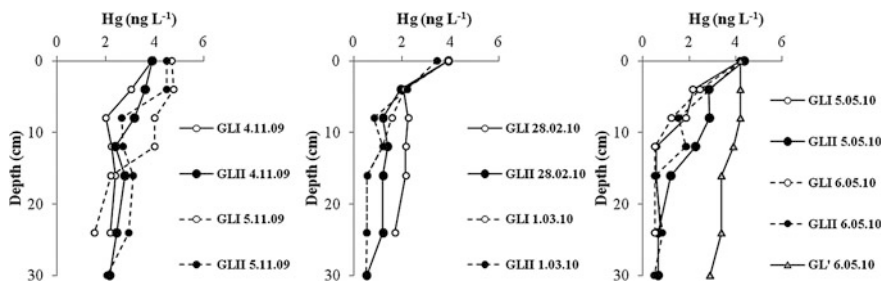
Fig. 4.14 The pore water dissolved mercury profiles. The samples were collected during the following sampling campaigns: November 2009; February 2010 and May 2010. The *hollow symbols* represent GLI location while *solid symbols* GL II location. The *triangle symbols* are attributed to the groundwater non-impacted area. The *solid lines* represent samples collected on the first day of sampling while *dashed lines* represent samples collected on the second day of sampling

Figure 4.14 presents dissolved mercury depth profiles. The average dissolved mercury concentrations decreased from 4.1 ± 0.3 ng L^{-1} to 1.0 ± 0.5 ng L^{-1} in November 2009. In February 2010 dissolved mercury concentration decreased from 4.2 ± 0.4 ng L^{-1} to 0.6 ± 0.1 ng L^{-1}, while in May 2010 dissolved mercury concentrations decreased from 4.3 ± 0.5 ng L^{-1} to 0.9 ± 0.3 ng L^{-1}. The average dissolved mercury concentrations and standard deviations were calculated from measured dissolved mercury concentrations in definite sampling campaign. The standard errors of the average concentrations indicated substantial variations of dissolved mercury. The average concentrations of dissolved mercury in groundwater were much lower than those in seawater. Thus, the GI profiles show the decrease of dissolved mercury concentrations downward in sediment pore water which is caused by the mixing groundwater and seawater. The seawater is characterized by higher mercury concentration than groundwater. Dissolved mercury concentrations were set by seawater intrusion into the sediment. On the other hand GNI profiles also present the decrease of dissolved mercury concentrations with depth, however in this case the minimum values do not exceed those from GI-area. The distribution of mercury in the GI-area showed greater mercury concentrations in seawater and lower- in groundwater.

4.3 The Processes Influencing Chemical Substances Concentrations in the Groundwater Impacted Area

4.3.1 Conservative Mixing

The relation between salinity and chloride concentrations is linear (Fig. 4.15). Thus, salinity can be regarded as a conservative peropery of water. The determination coefficient equals 0.9872. The obtained results confirm that salinity can be used as a
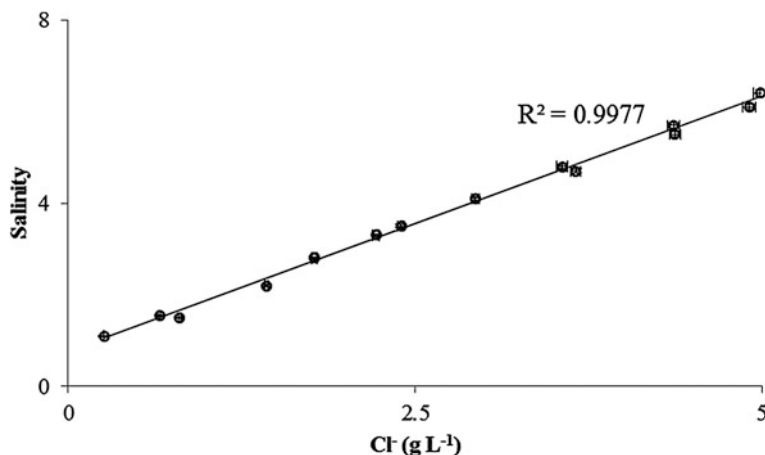
Fig. 4.15 The dependence between salinity and chloride concentrations

groundwater tracer. Hence, during subsequent sampling campaigns salinity measurements were carried out directly in collected samples instead of chloride concentration analyses in the laboratory.

As salinity is a conservative property of water (Bolałek 1992), the dependences between salinity and other water constituents in the mixing zone of groundwater and seawater define if the selected constituents are conservative or nonconservative components of water under conditions that prevail in the mixing zone.

The results indicate that whenever a dependence between salinity and a given constituent is linear, a conservative type of mixing is responsible for either decreasing or increasing concentration of the constituent. Obviously the increasing concentration of the constituent on reising salinity means that the element concentration in seawater is larger than that in the groundwater and vice versa. Thus conservarive mixing can be regarded as dilution of seawater or dilution of groundwater with the other end member.

4.3.2   Unconservative Mixing

Dependences between nutrients and salinity are presented in Figs. 4.14 and 4.15 (NO_3^- vs. salinity and NO_2^- vs. salinity) and in Figs. 4.16 and 4.17 (NH_4^+ vs. salinity and PO_4^{3-} vs. salinity). In the figures conservative mixing line represents the case when mixing groundwater with seawater resulted in a conservative relationship between salinity and the selected nutrient. Solid symbols indicate the end-members. The end-member characteristics are given as annual averages of the nutrient concentrations measured in seawater and groundwater. The standard deviations marked as error bars characterize seasonal changes of the measured concentrations and salinity. Figure 4.16 presents nitrate concentrations versus salinity. When mixing
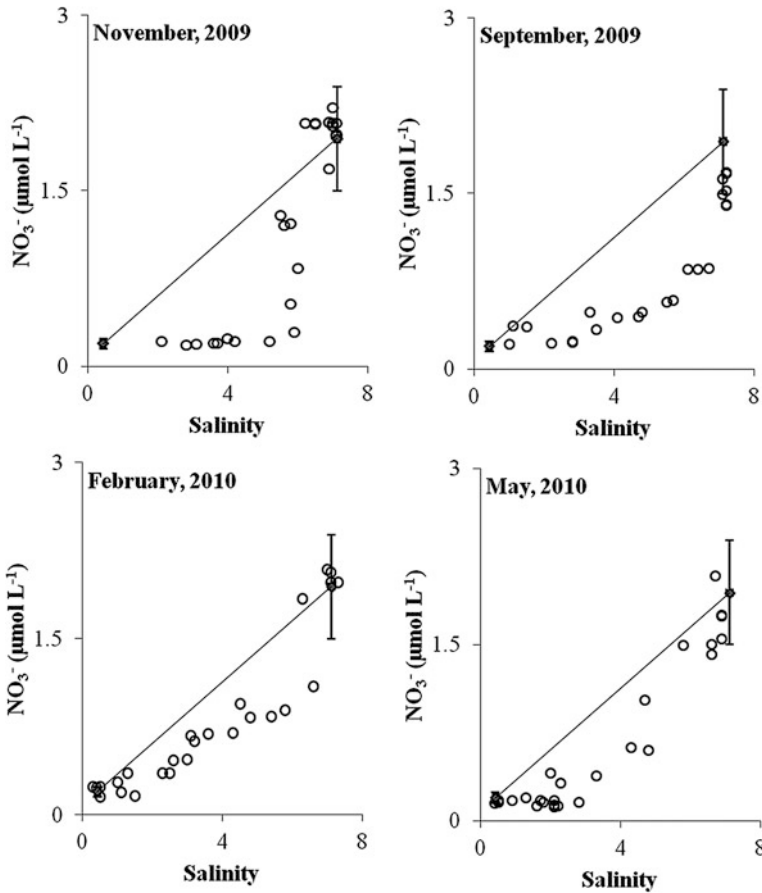
Fig. 4.16 The dependences between nitrate concentrations and salinity in the pore water profiles in the GI-area (September 2009; November 2009; February 2010 and May 2010). *Solid lines* represent nitrates concentrations changes under conservative mixing of groundwater with seawater, while *solid symbols* indicate average concentrations measured in the end-members samples. *Error bars* show standard deviation of the average end-member salinity and nitrate concentration

high-nitrate seawater with low-nitrate groundwater nitrate concentrations rapidly decrease. The dependences between nitrate concentrations and salinity are not linear indicating nitrate's nonconservative behavior.

Thus, other processes beside 'dilution', brought about by mixing of seawater and groundwater, influence nitrate concentrations in pore water. Figure 4.17 presents the relationship between nitrite concentrations and salinity. Nitrite behaves in a similar way to nitrate. The rapid, non-linear nitrite decrease along with salinity decrease is clearly visible. Thus, nitrate can also be named as a nonconservative constituent of water.
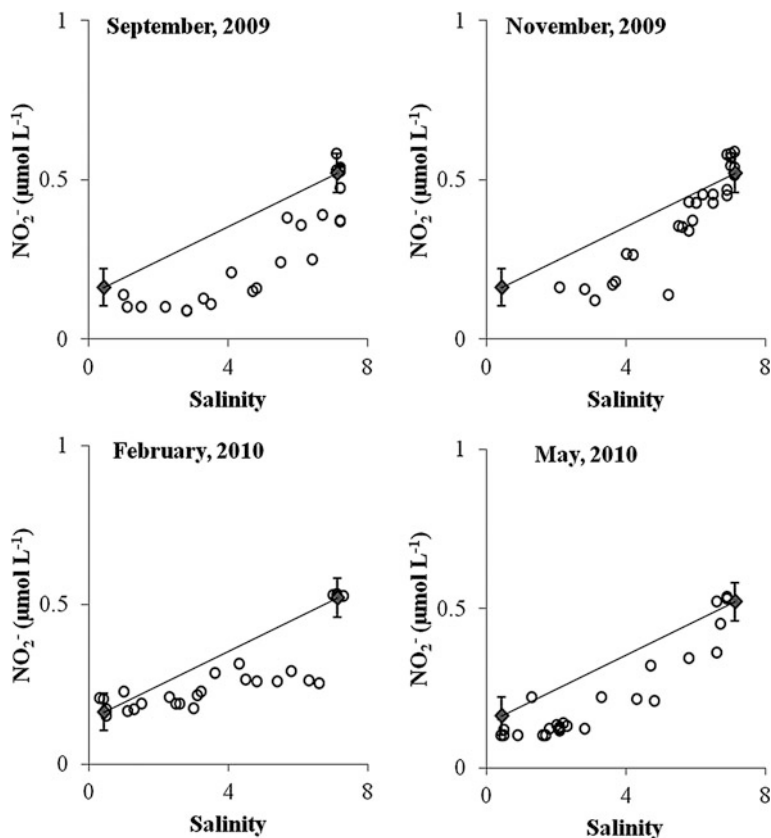
Fig. 4.17 The dependences between nitrite concentrations and salinity in the pore water profiles in the GI-area (September 2009; November 2009; February 2010, and May 2010). *Solid lines* represent nitrite concentrations changes under conservative mixing of groundwater with seawater, while *solid symbols* indicate average concentrations measured in the end-members samples. *Error bars* show standard deviation of the average end-member salinity and nitrite concentration

The nonconservative behavior of nitrate and nitrite can be explained by redox reactions (Jørgensen 2006). The decrease of nitrate and nitrite concentrations is closely related to oxygen availability. Generally, oxygen is introduced into the sediments through seawater intrusion (Jørgensen 2006; Pempkowiak and Obarska-Pempkowiak 2002).

Within the pore water of uppermost sediment layers nitrate concentrations and nitrite concentrations can be still at a high level. Within the mixing layer of oxic seawater and anoxic groundwater, nitrate concentrations and nitrite concentrations rapidly decrease due to nitrate and nitrite reduction (Jørgensen 2006). In groundwater nitrate and nitrite concentrations remain at trace levels. This is due to the reductive conditions there indicated by low ORP values. Ammonium concentrations versus salinity are presented in Fig. 4.18, as averages, in November 2009;
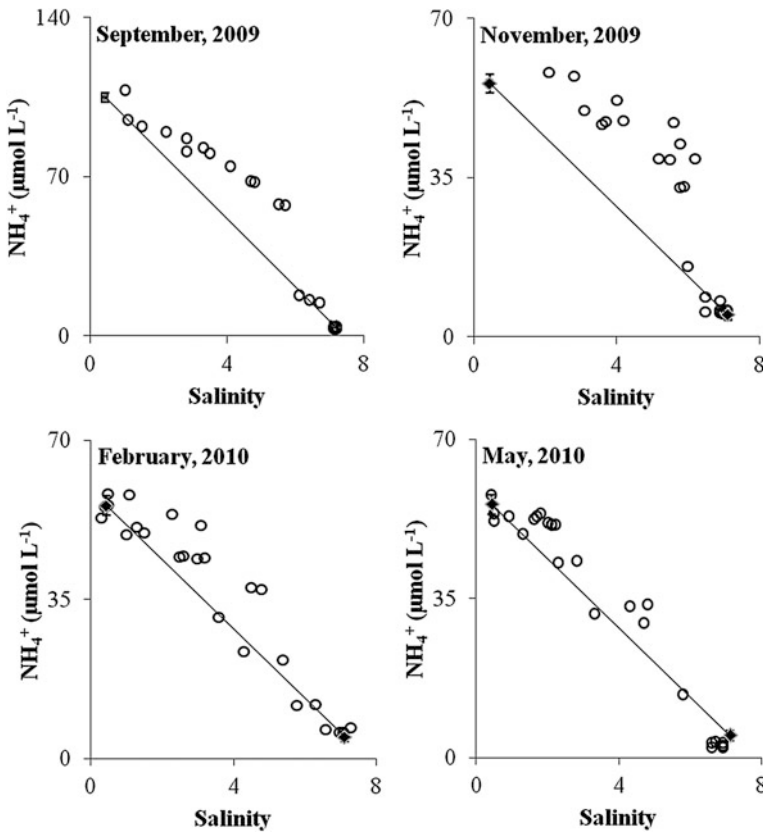
Fig. 4.18 The dependences between ammonium concentrations and salinity in the pore water profiles in the GI-area (September 2009; November 2009; February 2010 and May 2010). *Solid lines* represent ammonium concentrations changes under conservative mixing of groundwater with seawater, while *solid symbols* indicate average concentrations measured in the end-members samples. *Error bars* show standard deviation of the average end-member salinity and ammonium concentration

February 2010 and May 2010. The groundwater end-member was calculated excluding the ammonium concentration in groundwater measured in September 2009.

Average ammonium concentration in groundwater end-member was calculated based on November 2009; February 2010; May 2010. September 2009 data were omitted. In September 2009 ammonium concentrations in pore water profiles were extremely high and it was decided that for a clearer presentation of the ongoing processes these values should be treated separately. The observed trend was similar for each of the sampling campaigns. Ammonium concentrations decrease with the increase of salinity. The dependences are not linear confirming the nonconservative behavior of ammonium. It seems that, during the mixing ammonium was released

to pore water as a result of an active source of ammonium distribution in pore water, for example reduction of nitrites.

Ammonium is produced during the decomposition of organic matter in sediments (Burska et al. 2011). The accumulation of ammonium occurs in the anoxic layers of sediments, in this case in the seepage water and groundwater layer.

Figure 4.19 presents phosphate concentrations versus salinity in collected pore water samples. The decrease of phosphate concentrations with the increase of salinity is visible. Similarly to other nutrients the observed concentration changes
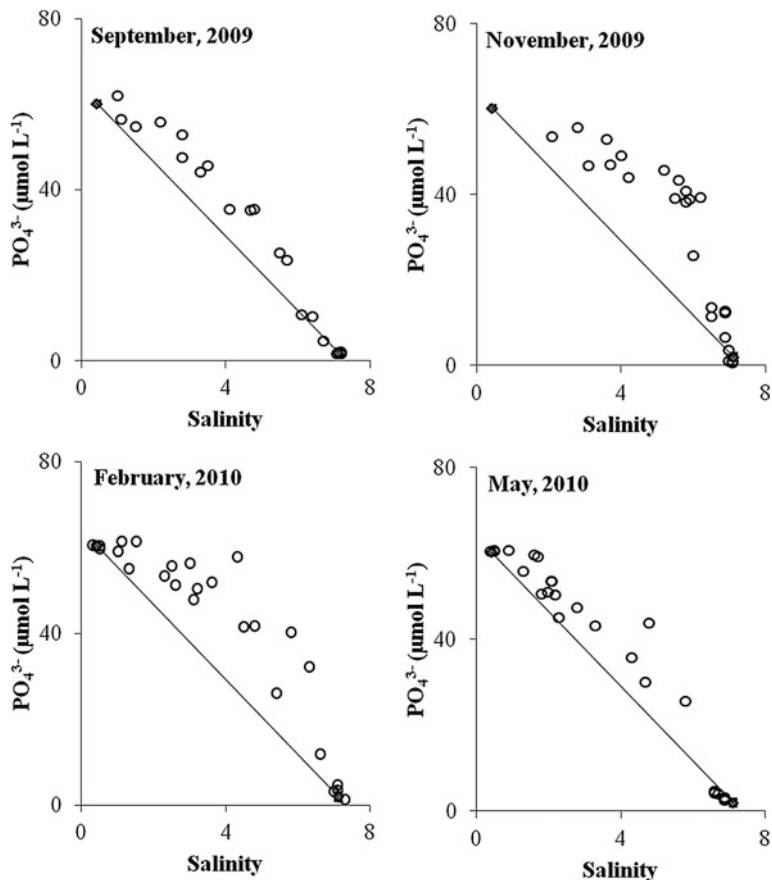
Fig. 4.19 The dependences between phosphates concentrations and salinity in the pore water profiles in the GI-area (September 2009; November 2009; February 2010 and May 2010). *Solid lines* represent phosphate concentrations changes under conservative mixing of groundwater with seawater, while *solid symbols* indicate average concentrations measured in the end-members samples. *Error bars* show standard deviation of the average end-member salinity and phosphate concentration

are nonconservative. Comparable dependences of phosphate concentrations versus salinity were observed in Hwasun Bay and Bangdu Bay, off volcanic island Jeju, Korea (Kim et al. 2011).

The patterns observed in NH_4 and PO_4 data resemble those reported by Ullman et al. (2003) wherein nutrient concentrations in sediment pore waters from Cape Henlopen, Delaware (a sandy beach face) showed signs of dispersive mixing between saline and groundwater end-members, as well as a diagenetic contribution (or removal). Thus, the main factors controlling nitrogen and phosphorous distribution in the groundwater-seawater mixing area are groundwater seeping rates and red-ox conditions in subsurface pore water, which influence the transformation processes and mobility of nitrogen and phosphorous (Slomp and Van Cappellen 2004). It was also suggested that when anoxic groundwater meets oxic seawater, the degree of anoxia of the discharging groundwater will determine the chemical characteristics of groundwater and thus also the distribution of nitrogen and phosphorous in the coastal zone. If organic matter decomposition is not carbon limited and proceeds beyond denitrification, nitrate will be absent in groundwater while ammonium can be released from organic matter and will be a major input of nitrogen (Slomp and Van Cappellen 2004). Phosphates, in turn, will be released from organic matter and through reduction of Fe-oxides and will be accumulated in groundwater. When groundwater enriched with phosphates and iron(II) meets oxic seawater, Fe-oxides may precipitate and bind the phosphates. Thus, a decrease in phosphate concentrations can be observed with increasing salinity. Such a situation occurs not only in the Bay of Puck, but in other areas as well, for example in the Waquoit Bay, Massachusetts (Charette and Sholkovitz 2002) (Figs. 4.20 and 4.21).

Figure 4.22 presents the relationship between metals and salinity. Dissolved metals concentrations and speciation are important for metal levels in biota (Pempkowiak et al. 2006). Within the concentrations of metals two types of mixing can be distinguished, namely conservative and not-conservative mixing.

Dissolved Co and Zn both exhibit conservative distribution relative to salinity and show depletion in seawater and enrichment in groundwater. Thus changes of the concentrations are caused only by dilution. Dissolved Cu, Ni and Cr concentrations differ substantially from those expected in the case of conservative mixing and show nonconservative behavior on the end-members mixing. Dissolved Ni and Cu both show depletion in groundwater and enrichment in seawater while the trend for Cr shows an opposite trend—enhancement in groundwater and depletion in seawater. Dissolved Cr and Cu show nonconservative removal from soluble phase while Ni exhibited nonconservative enrichment through the flow path. Dissolved Pb, Cd and Mn concentrations did not show clear trends to salinity. Thus, the elements with nonconservative (Cu, Ni, Cr) or not clear trends (Pb, Cd, Mn) relative to salinity are under influence of other processes not just dilution..

The dependences between mercury concentrations and salinity are presented in Fig. 4.23. They indicate nonconservative behaviour of mercury upon the mixing of high mercury seawater and low mercury groundwater. This is manifested by the
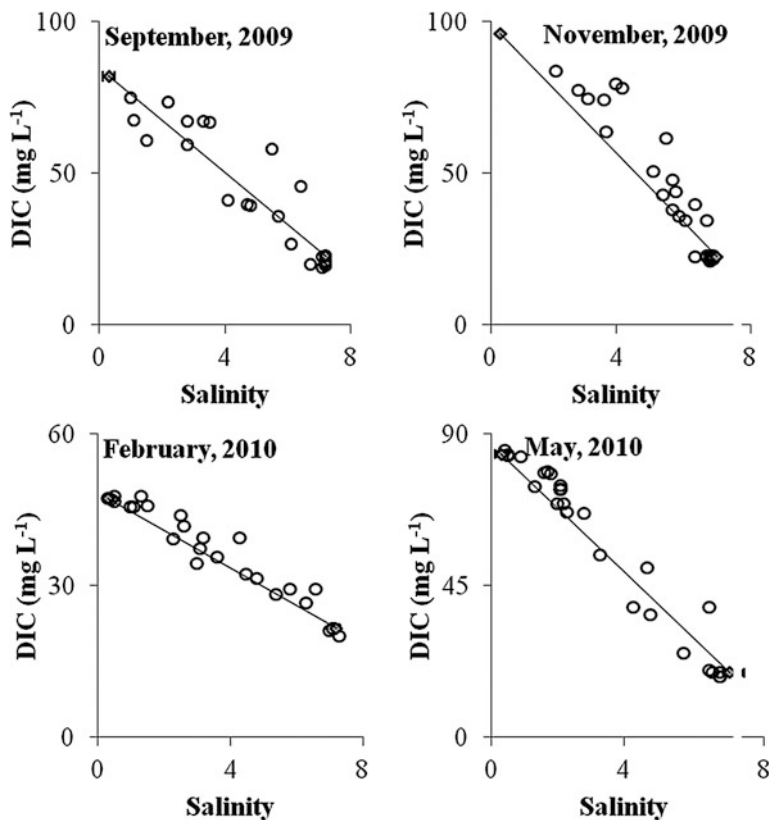
Fig. 4.20 The dependences between dissolved inorganic carbon (DIC) concentrations and salinity in the pore water profiles in the GI-area (September 2009; November 2009; February 2010 and May 2010). *Solid lines* represent DIC concentrations changes under conservative mixing of groundwater with seawater, while *solid symbols* indicate average concentrations measured in the end-members samples. *Error bars* show standard deviation of the average end-member salinity and DIC concentration

departure from a straight line joining concentrations of the two end-members of the system. This shows that, there are constituents of pore water that impact mercury distribution in natural waters (Lamborg et al. 2004; Ravichandran 2004; Bełdowski and Pempkowiak 2007). Mercury is removed from saline pore water; however, it is not clear what mechanism is responsible for the removal. The sorption of mercury on solid phase, complexation by organic substances, uptake by biota, and precipitation/co-precipitation; all may be responsible for the phenomenon (Szymczycha et al. 2013). The coprecipitation is likely to occur since the uppermost layer of sediments in the study area is characterized by a steep redox gradient (Bełdowski and Pempkowiak 2007).
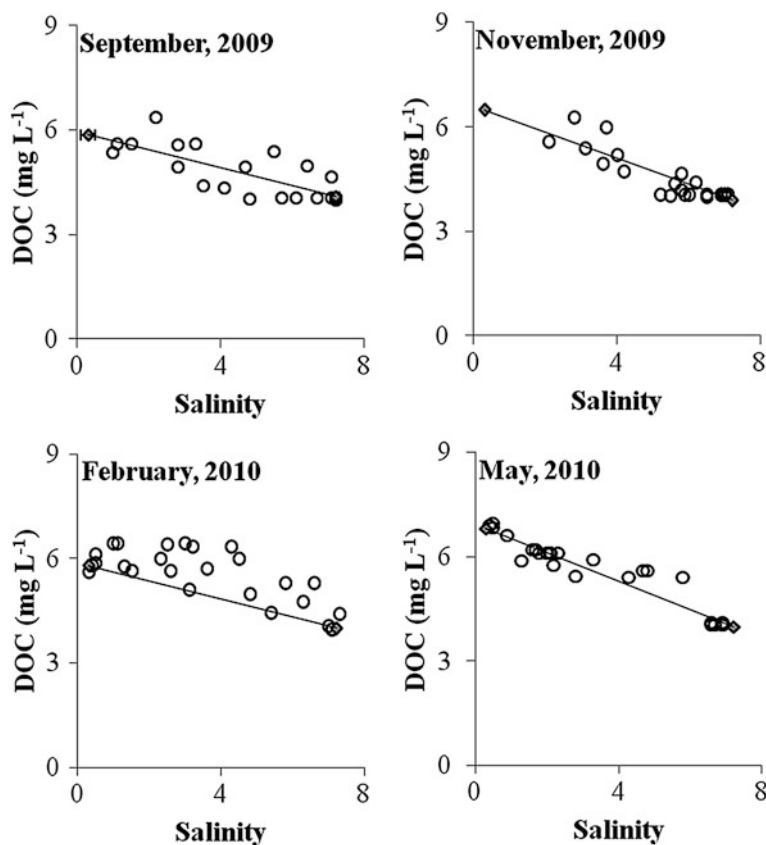
Fig. 4.21 The dependences between dissolved organic carbon (DOC) concentrations and salinity in the pore water profiles in the GI-area (September 2009; November 2009; February 2010 and May 2010). *Solid lines* represent DOC concentrations changes under conservative mixing of groundwater with seawater, while *solid symbols* indicate average concentrations measured in the end-members samples. *Error bars* show standard deviation of the average end-member salinity and DOC concentration

4.3.3   The Importance of Groundwater Redox Chemistry

The redox conditions in the groundwater strongly influence geochemical processes taking part in the groundwater-seawater mixing zone e.g. the transformation processes and speciation of several water constituents including nitrogen and phosphorous species (Slomp and Van Cappellen 2004). The dependences of both phosphates concentrations versus ORP and ammonium concentrations versus ORP are presented in Fig. 4.24.

When anoxic groundwater meets oxic seawater, the degree of anoxia of the discharging groundwater will determine the chemical characteristics of groundwater
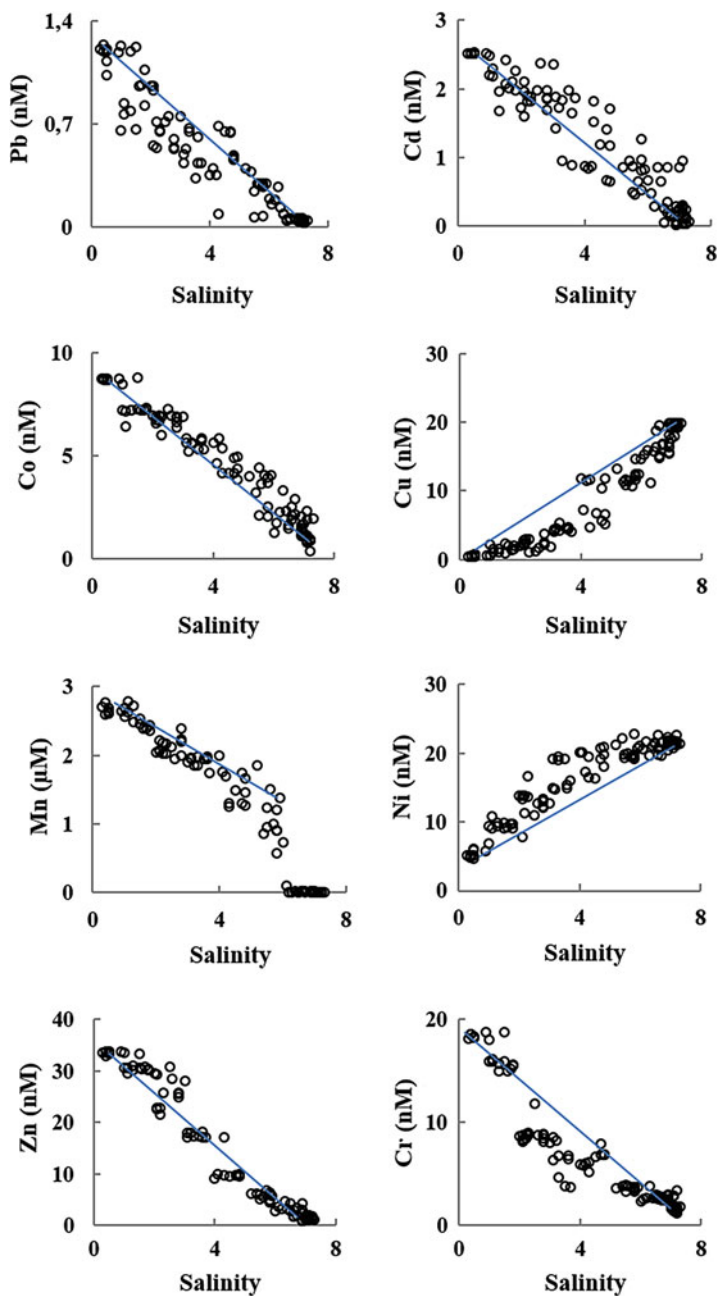
Fig. 4.22 The dependences between trace metals pore water concentrations and salinity obtained of groundwater impacted areas
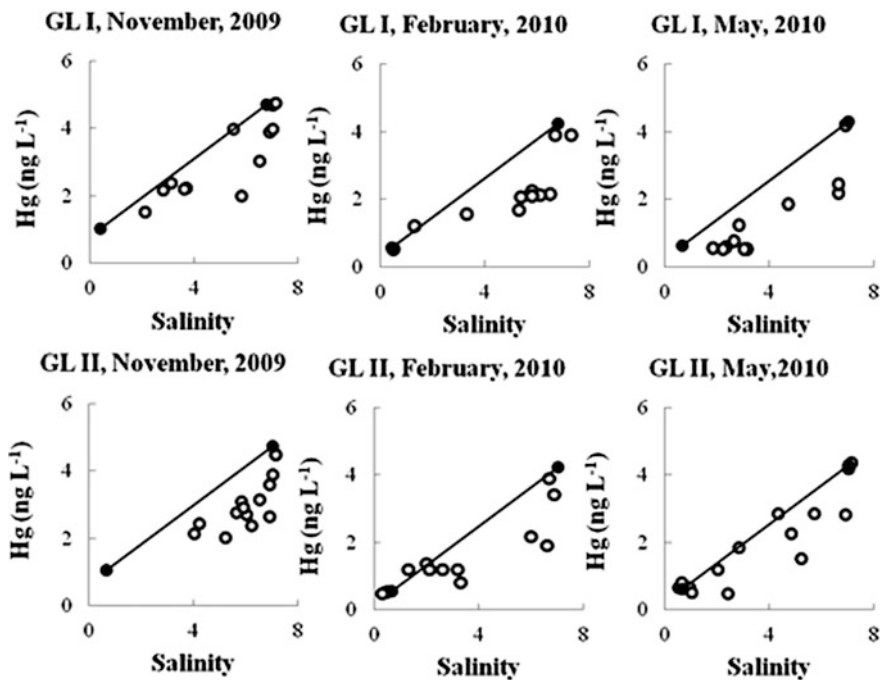
Fig. 4.23 The dependences of mercury concentrations versus salinity. *Solid lines* represent mercury concentrations changes under conservative mixing of groundwater with seawater, while *solid symbols* indicate average concentrations measured in the end-members samples
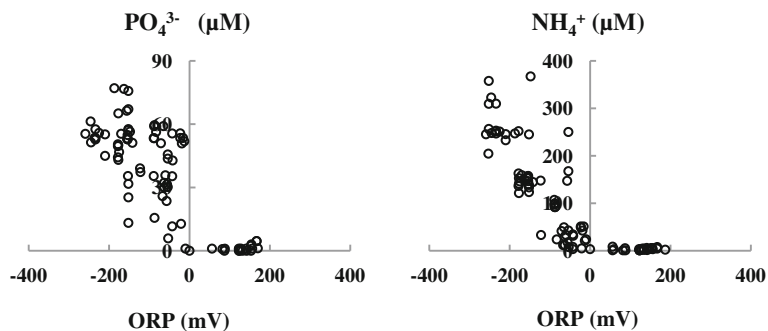
Fig. 4.24 The dependences of phosphates and ammonium concentrations versus ORP

and thus also the distribution of nitrogen and phosphorous in the coastal zone. If organic matter decomposition proceeds beyond denitrification, nitrate will be absent in groundwater while ammonium can be released from organic matter and will be a major form of nitrogen (Slomp and Van Cappellen 2004).

Fig. 4.25 The dependences of phosphates concentrations versus manganese concentrations
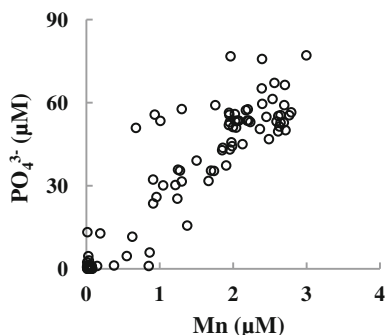
Phosphates, in turn, will be released on mineralization of organic matter and through reduction of Fe-oxido-phosphates and will be accumulated in groundwater. When groundwater enriched with phosphates and manganese(II) meets oxic seawater, Mn-oxides precipitate and bind the phosphates (Fig. 4.25). Thus, a decrease in phosphate concentrations can be observed with increasing salinity. Such a situation occurs not only in the Bay of Puck, but for example in the Waquoit Bay, Massachusetts (Charette and Sholkovitz 2002).

The dependences between Pb, Cd, Cu, Mn, Cr, Ni and ORP present clearly relationship: possible influence of red-ox equilibria on distribution of metals (Fig. 4.26). The red-ox equilibria are quantified as ORP here. Concentrations of several constituents are influenced by ORP directly (Mn) or indirectly (Pb). The changes of the oxidation reduction potential impacts the speciation of the metals
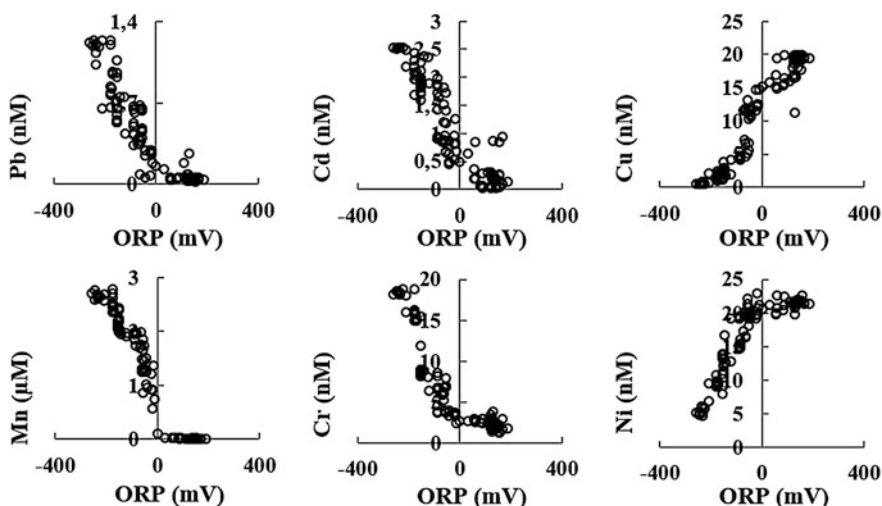
Fig. 4.26 The dependences between dissolved Pb, Cd, Cu, Mn, Cr, Ni and ORP in the SGD impacted area

(Schulz and Zabel 2006). Dissolved Pb, Cd, Mn, and Cr decrease most likely due to the change from dissolved to solid while the ORP increase. When ORP is higher than zero the concentrations of dissolved Pb, Mn and Cr are close to zero and constant. The opposite trend represents Ni and Cu concentrations- with higher ORP values the concentrations of the both metals dissolved species increase as well. As not only mixing between groundwater and seawater influences speciation of these metals it can be safely assumed that in case of dissolved Ni sediment can be an additional source of Ni while the concentrations of dissolved Cu can be influenced more by the behavior of dissolved ligands. Other processes controlling behavior of metals can be advection or diffusion upwards and coprecipitation with manganese oxides upon entering the truly oxic layer (Pempkowiak et al. 2000).

4.4   Upscaling Nutrients, Dissolved Carbon, and Metals Loads Delivered to the Southern Baltic Sea Via SGD

4.4.1   Nutrients, Dissolved Carbon, and Metls Fluxes Via SGD to the Study Area

Groundwater flux was measured by means of the seepage meter. Seepage water percolating through the sediment displace water trapped in the chamber forcing it up through the port into the PTE bag. The change in volume of water in the bag, over a measured time interval, provides the seepage water flux. The contribution of groundwater to the flux estimates was established using the end-member method. This method is commonly used for separation of seepage water fluxes into the groundwater and seawater components if one can identify composition of the end members with sufficient sensitivity and resolution (Sect. 4.1.2).

The groundwater fluxes (Table 4.1) and chemical substances concentrations measured in groundwater (Table 4.4) were used to calculate the loads of nutrients and dissolved carbon delivered into the study area via SGD. The results are presented in Table 4.9.

In September 2009 and November 2009 nutrients loads delivered via SGD to the study area were approximately one order of magnitude higher than in February 2010 and May 2010. The loads of ammonium and phosphate were significantly higher than the combined nitrate and nitrite loads. The high fluxes of ammonium and phosphate can be explained by high concentration of ammonium and phosphate in groundwater. Generally, groundwater is enriched with nitrate and phosphate (Moore 2010). In this study, due to the highly anoxic conditions in the sediments, nitrate and nitrite are reduced, and consequently low loads of nitrate and nitrite are delivered via SGD to the study area.

The highest DIC fluxes and DOC fluxes via SGD were calculated for September 2009 and November 2009. In September 2009 DIC fluxes were equal to 2115 ± 197 mg d^{-1} m^{-2}, while DOC fluxes were equal to 151 ± 14 mg d^{-1} m^{-2}. In November 2009 DIC fluxes were equal to 1765 ± 518 mg d^{-1} m^{-2}, while DOC

Table 4.9 The nutrients and dissolved carbon fluxes delivered *via* SGD to the study area

Sampling campaign	Flux (L d^{-1} m^{-2})	Nutrients loads to the study area (mg d^{-1} m^{-2})				Dissolved DIC and DOC loads to the study area (mg d^{-1} m^{-2})	
		NO_3^-	NO_2^-	NH_3^+	PO_4^{3-}	DIC	DOC
September 2009	25.8 ± 2.4	0.3 ± 0.03	0.2 ± 0.1	49.2 ± 4.6	148.3 ± 13.8	2115 ± 197	151 ± 14
November 2009	18.4 ± 5.4	0.2 ± 0.06	0.1 ± 0.02	18.5 ± 5.4	105.8 ± 31.0	1765 ± 518	119 ± 35
February 2010	3.0 ± 2.1	0.04 ± 0.03	0.03 ± 0.04	3.0 ± 2.1	17.1 ± 11.9	141 ± 99	17 ± 12
May 2010	3.6 ± 0.1	0.03 ± 0.001	0.02 ± 0.001	3.5 ± 0.1	20.7 ± 0.6	302 ± 8	24 ± 1

fluxes were equal to 119 ± 35 mg d^{-1} m^{-2}. Once released into surface water SGD-derived DIC might be consumed by biological production stimulated by nutrients supplied from groundwater (Liu et al. 2012), while DOC enters the organic matter pool of seawater. It can be assumed that during summer and autumn groundwater is a more significant source of DIC and DOC concentrations to the study area then in winter and spring. Similar seasonal variations were found on the west Ireland (Smith and Cave 2012).

Upon sediment resuspension, the precipitated heavy metals are returned to seawater, moved to the deeper regions of the sea where they are deposited to the seafloor again (Uścinowicz 2011). Thus groundwater seeping to the Bay of Puck delivers loads of metals to the bay, irrespective of their conservative/nonconservative behavior.

Metal fluxes via SGD were calculated using the average annual concentrations of each metal and the established groundwater flux. It was possible to use the annual average concentrations of each metal due to small seasonal concentration variations. The calculated standard deviation originate predominately the uncertanities in groundwater discharge rate. The calculated average annual concentrations of each metal and corresponding fluxes are presented in Table 4.10.

As expected of the SGD rates in the study area, the SGD-driven fluxes of trace elements were approximately one order of magnitude higher in September 2009 and November 2009 than in February 2010 and May 2010. Jeong et al. (2012) estimated Mn, Co, Ni and Cu fluxes via SGD into the Bangdu Bay, Jeju Island. The obtained fluxes were equal to 2.5×10^3 nmol Mn d^{-1} m^{-2}, 4×10^2 nmol Co d^{-1} m^{-2}, 2.4×10^3 nmol Ni d^{-1} m^{-2}, 0.7×10^2 nmol Cu d^{-1} m^{-2}. Generally, the Mn fluxes via SGD were lower than Mn fluxes measured during this study, Co fluxes were comparable to these determined in this study while Ni and Cu loads via SGD were significantly higher than those obtained here. Thus, in groundwater discharged to the Bangdu Bay Ni and Cu concentrations were higher than in seawater as compared to the Bay of Puck.

Mercury fluxes calculated as a product of the groundwater discharge rate and the measured concentrations of the dissolved mercury were equal to 9.7 ± 0.7 ng d^{-1} m^{-2} in November 2009; 1.6 ± 0.0 ng d^{-1} m^{-2} in February 2010 and 3.0 ± 1.1 ng d^{-1} m^{-2} in May 2010. Mercury fluxes were highest in November 2009, corresponding to the high SGD rates. The calculated fluxes of dissolved mercury via SGD were lower than mercury loads via SGD into the Sothern California Coastal Lagoon (Ganguli et al. 2012).

4.4.2   Nutrients, Dissolved Carbon and Metals Fluxes Via SGD to the Bay of Puck

Chemical substances loads from SGD are usually calculated as the products of seepage water flux and concentration of chemical species measured in inland groundwater sources (Oberdorfer et al. 1990). This method assumes that chemical

Table 4.10 The metals yearly average concentrations measured in the groundwater samples in the GI-area and corresponding specific metals fluxes to the study area via SGD

Metals	Concentration ± SD (nmol L^{-1})	Flux intensity ± SD (nmol d^{-1} m^{-2})			
		September 2009	November 2009	February 2010	May 2010
Pb	1.2 ± 0.1	30.2 ± 2.8	21.5 ± 6.3	3.5 ± 2.5	4.2 ± 0.1
Cd	2.5 ± 0.0	65.0 ± 6.0	46.4 ± 13.6	7.6 ± 5.3	9.1 ± 0.3
Co	8.7 ± 0.0	225.2 ± 21.0	160.6 ± 47.1	26.2 ± 18.3	31.4 ± 0.9
Mn	(2.7 ± 0.1) × 10^3	(68.6 ± 6.4) × 10^3	(48.9 ± 14.4) × 10^3	(8.0 ± 5.6) × 10^3	(9.6 ± 0.3) × 10^3
Cu	0.6 ± 0.1	15.7 ± 1.5	11.2 ± 3.3	1.8 ± 1.3	2.2 ± 0.1
Ni	5.3 ± 0.5	136.5 ± 12.7	97.3 ± 28.6	15.9 ± 11.1	19.0 ± 0.5
Cr	18.3 ± 0.2	472.7 ± 44.0	337.1 ± 98.9	55.0 ± 38.5	66.0 ± 1.8
Zn	33.6 ± 0.3	866.1 ± 80.6	617.7 ± 181.3	100.7 ± 70.5	120.9 ± 3.4

substances concentrations from coastal and inland groundwater sources do not differ from each other. Due to the questionable nature of this assumption Szymczycha et al. (2012) measured the actual chemical substances concentrations in groundwater samples collected throughout the study by means of groundwater lances and seepage meters. They assumed a continuous supply of chemicals transported by groundwater migration through the sediment driven by the hydraulic gradient. Nienchesky et al. (2007) measuring average nutrient concentrations in water samples collected from permanent land-based wells, beach groundwater, and samples from the surf zone, inner shelf and open ocean. However, there is limitation to the implemented method, since in the groundwater-seawater mixing layer biogeochemical transformations of the measured water components may substantially alter the actual concentration an consequently discharge of the measured species.

In this study the same approach was used to calculate nutrients, metals and dissolved carbon fluxes via SGD to the Bay of Puck.

Nutrients The sum of the measured NO_3, NO_2 and NH_4 concentrations formed the basis of the dissolved inorganic nitrogen (DIN) concentration. The PO_4 concentration served as a measure of dissolved phosphates. A groundwater flux estimate of 0.03 km³ year^{-1} was adopted from Piekarek-Jankowska (1994) and Piekarek-Jankowska (1996). The seepage discharged rates estimated by Piekarek-Jankowska (1994, 1996) have been made for the entire Puck Bay. The calculation was based on hydrogeological method and allowed to estimate the role of SGD in the water balance of the entire Puck Bay. The seepage discharged rates estimated during this study were characteristic of the active SGD at the study area and thus exceed those calculated by Piekarek-Jankowska (1994). Table 4.11 gives the loads calculated as products of fluxes and average yearly concentrations of nutrients. The NH_4 concentration was 47 times higher in groundwater than in seawater and the PO_4 concentration was almost 99 times higher. In their study along a coastal lagoon barrier in southern Brazil, Nienchesky et al. (2007) also showed that groundwater is enriched with NO_3 and NH_4, but comprised only slightly elevated levels of PO_4. The ranges of NH_4 and PO_4 levels

Table 4.11 Phosphate and DIN fluxes to the Bay of Puck via external sources

Source	Fluxes			
	P-PO$_4{}^{3-}$	N-DIN[c]	P-PO$_4{}^{3-}$	N-DIN
	t year^{-1}		kmol year^{-1}	
Atmosphere[a]	18	485	581	34,626
Rivers and point sources[a]	70	220	2260	15,706
Resuspension[a]	97	825	3132	58,899
SGD[b]	60	30	1911	2118

[a]Bolałek et al. (1993)
[b]This study
[c]DIN = $[NO_3^-]$ + $[NO_2^-]$ + $[NH_4^+]$

in groundwater samples from their study, however, were lower than those reported here (Table 4.11). In a study by Lee et al. (2009) of the Masan Bay, a site recognized as the most eutrophic embayment in Korea, reported similar DIN concentrations to those reported here. The PO_4 concentrations in groundwater samples measured by Lee et al. (2009), however, were approximately ten times lower than those reported here. The PO_4 concentrations reported here also exceed those measured at other seepage locations (Beck et al. 2007; Leote et al. 2008; Lee et al. 2009). Hosono et al. (2012) reported SGD amounting to 6000 m^3 day^{-1} over a 20,000 m^2 area as well as DIN and DP fluxes of 920 mol day^{-1} and 56 mol day^{-1} respectively. Street et al. (2008) described sites along the Hawaii coast with SGD fluxes ranging 0.02 to 0.65 m^3 m^{-2} d^{-1}, delivering nitrogen loads of 0.04 to 40 mmol m^{-2} d^{-1} and phosphate loads of 0.01 to 1.6 mmol m^{-2} d^{-1}. Given this scale in relation other locations, the SGD site investigated in this study is interpreted as a major source of nutrients input into the surrounding coastal ecosystem due to substantial concentrations on nitrogen and phosphorous in groundwater.

Carbon fluxes DIC flux via SGD to the Bay of Puck is 1.9 ± 0.2 kt C $year^{-1}$ and the corresponding DOC flux is 0.2 ± 0.002 kt C $year^{-1}$. The most significant riverine carbon source for the Bay of Puck is the River Reda with DIC and DOC loads of 5.4 kt C $year^{-1}$ and 0.5 kt C $year^{-1}$ respectively. The Rivers Gizdepka (0.25 kt C $year^{-1}$ DIC, 0.03 kt C $year^{-1}$ DOC) and Zagórska Struga (0.73 kt C $year^{-1}$ DIC, 0.08 kt C $year^{-1}$ DOC) are smaller carbon sources. DIC and DOC fluxes via SGD make up ca 30 % of the carbon river runoff discharged into the Bay of Puck. Liu et al. (2012) estimated the role of submarine groundwater discharge and its impact on the carbonate system in the northern South China Sea. The DIC flux via SGD was in the range of 1836–4164 kt C $year^{-1}$, which is equal to approximately 23–53 % of the riverine DIC export flux there. Comparatively high concentrations of DIC to, for example, river water that is discharged in the region were measured in the groundwater at the study site. The explanation of a higher DIC concentration in groundwater and, as a result, high loads of DIC via SGD can be found in the geological structure of the southern Baltic Sea. The content of carbonates within the geological structures of the Baltic Sea's continental drainage area is much higher than in the drainage area covering the Scandinavian Peninsula. Being a land-locked sea, the Baltic covers an area of geological structures similar to the land surrounding it (Uścinowicz 2011). The south-western part of the Baltic Sea, where the study area is located, lies on the Palaeozoic West European Platform separated from the East European Platform by the Teisseyre Tornquist Fault Zone. The northern part of the Baltic Sea lies over the Baltic Shield, while the southern part is situated on the East European Platform. The study area is located on a sediment layer consisting of dolomites, calcites, limestones, syrrulian clays and silts with carbonate-rich dolomites. The higher DIC concentration in groundwater and, as a result, the high loads of DIC via SGD, can thus be attributed to the geological structure of the southern Baltic. Other possibilities here are the

Table 4.12 Loads of trace metals to the Bay of Puck from rivers and groundwater discharge

Metal	Metals fluxes to the Bay of Puck									
	SGD		Gizdepka		Płutnica		Zagórska Struga		Reda	
	mol year^{-1}	kg year^{-1}	mol year^{-1}	kg year^{-1}	mol year^{-1}	kg year^{-1}	mol year^{-1}	kg year^{-1}	mol year^{-1}	kg year^{-1}
Pb	35 ± 2	7.3 ± 0.4	3.03	0.63	3.3	0.7	6.2	1.3	2.4	0.5
Cd	76.1 ± 0.1	8.50 ± 0.01	0.34	0.06	0.8	0.1	2.5	0.3	0.5	0.1
Co	262 ± 1	15.40 ± 0.04	17.66	1.01	18.7	1.1	17.0	1.0	12.8	0.8
Mn	79,750 ± 1725	4381.3 ± 94.8	17.91	1.01	30,143.2	1656.0	5990.7	329.1	3982.2	218.8
Cu	18 ± 4	1.2 ± 0.3	59.63	3.78	16.2	1.0	157.3	10.0	80.8	5.1
Ni	160 ± 15	9.4 ± 0.9	9.53	0.57	1497.9	87.9	1605.4	94.2	1273.2	74.6
Zn	1008 ± 8	65.9 ± 0.5	122.75	8.01	140.6	9.2	316.2	20.7	147.1	9.7
Cr	551 ± 7	28.7 ± 0.4	9.11	0.50	4.4	0.3	22.2	1.1	13.1	0.7

reduction-oxidation processes of the system. The groundwater is anoxic (Szymczycha et al. 2013), so the oxidation pathways of organic matter include both sulphate reduction and methane production. Both these processes lead to an increase in carbonates in the system (Schulz and Zabel 2006). This also explains the higher alkalinity and carbon concentrations in 'continental' rivers entering the sea along the southern coast compared with rivers draining the Scandinavian Peninsula.

Metals The loads of trace metals via groundwater discharge to the Bay of Puck were compared to river metals fluxes and presented in Table 4.12. The rates of metals via groundwater discharge were significantly higher than rivers metals fluxes. This is 92 % for Pb, 99 % for Cd, 98 % for Co, 97 % for Mn, 48 % for Cu, 38 % for Ni, 95 % for Zn and 99 % for Cr of the annual sum of river and groundwater fluxes to the Bay of Puck.

4.4.3 Nutrients, Metals and Dissolved Carbon Loads Via SGD to the Baltic Sea

SGD to the Baltic Sea or its parts, have been a subject of several studies (f.e. Zekster et al. 1973; Piekarek-Jankowska 1994, 1996; Falkowska and Piekarek-Jankowska 1999; Kaleris et al. 2002; Peltonen 2002; Viventsowa and Voronow 2003; Schlüter et al. 2004; Kryza and Kryza 2006; Piekarek-Jankowska 2007; Zekster et al. 2007; Pempkowiak et al. 2010; Lidzbarski 2011; Szymczycha et al. 2012, 2013, 2014). In this approach we will present a compilation of the published and our own studies results.

To calculate chemical substances fluxes via SGD to the Baltic Sea and its parts the extrapolation of the results was made. The reason for extrapolation of chemicals loads via SGD to the entire Baltic Sea has an intension of establishing the order of magnitude of chemicals substances loads entering the sea with SGD, rather, than indicating actual loads. This serves a purpose of establishing possible SGD related fluxes important to material budget of the sea. There are several factors that influence the compounds loads values established as a result of scaling up: representatives of concentrations for a given sampling campaign, representatives of concentrations for the entire year, representatives of the study area for the entire Baltic Sea and accuracy of the groundwater estimations (Szymczycha et al. 2012, 2013, 2014).

Pore water samples were collected and the seepage water fluxes were measured within several days long campaigns. It has been proven that both fluxes and chemical concentrations were relatively constant over these time spans (Tables 4.4; 4.5; 4.6; 4.7; 4.8). This is also confirmed by the land based studies by Pruszkowska and Przewłócka (2007). On the other hand fluxes varied in subsequent seasons that

Table 4.13 P-PO$_4$ and
N-DIN fluxes from external
sources to the Baltic Sea

Fluxes to the Baltic Sea	P-PO$_4$ (t year^{-1})	N-DIN[a] (t year^{-1})
Atmosphere	<1730[a]	196,000[b]
Rivers and point sources	30,200[b]	641,000[b]
SGD	8680[c]	4350[c]

[a]N-DIN = [N-NO$_3^-$] + [N-NO$_2^-$] + [N-NH$_4^+$]
[b]The fluxes obtained in 2000, HELCOM (2005a, b)
[c]This study

gives rise to increased uncertainty. Chemical substances concentrations in groundwater were rather stable throughout a year.

The conventionally considered sources of nutrient discharges to the Baltic Sea are: direct atmospheric deposition to the Baltic surface; river inputs of nutrients to the sea; point sources discharging directly to the sea (HELCOM 2005a, b, 2009). The reports do not provide nutrient loads from SGD, though. Loads of DIN and PO$_4$ to the Baltic Sea from the sources are presented in Table 4.13 (Syzmczycha et al. 2012). The calculated loads of N-DIN and P-PO$_4$ delivered via SGD to the Baltic Sea are equal to 4350 ± 1680 t year^{-1} and 8680 ± 760 t year^{-1}, respectively. Waterborne inputs constitute the main rout of nitrogen (77 %) and phosphorous (96 %) to the Baltic Sea. The SGD load of N-DIN constitutes a small fraction of total nitrogen delivered to the Baltic Sea. However, the P-PO$_4$ load discharged to the sea is significant in view of loads delivered from other sources. Comparing results from this study to total nutrient fluxes from other sources, the following picture emerges: P-PO$_4$ input via SGD constitutes approximately 21 %, while N-DIN input via SGD equals to approximately 0.5 % of the total respective dissolved nutrients fluxes to the Baltic Sea (this study; HELCOM 2005a, b). Keeping in mind that coastline areas with permeable sediment layers are the most common groundwater impacted areas, these values indicate significant role of SGD discharge in the coastal ecosystems. This can lead to eutrophication and harmful algal blooms in the coastal areas of the Baltic Sea (Andersen et al. 2007).

The obtained dissolved inorganic carbon (DIC) and dissolved organic carbon (DOC) concentrations in the coastal groundwater (S ≤ 0.5) and the earlier measured SGD fluxes (Piekarek-Jankowska 1994) were used to calculate carbon fluxes to the Baltic Sea Sub-Basins and the entire Baltic Sea (Szymczycha et al. 2014). The results are presented in Table 4.14. The DIC and DOC fluxes via SGD to the Baltic Sea were estimated at 283.6 ± 66.7 kt C year^{-1} and 25.5 ± 4.2 kt C year^{-1}, respectively. Thus the DIC fluxes were approximately 11 times higher than DOC fluxes. The total carbon flux to the Baltic Sea (sum of DIC and DOC) amounts to 0.31 Tg C year^{-1}. DIC and DOC fluxes via SGD are significant compared to other carbon sources for the Baltic Sea, presented by Kuliński and Pempkowiak (2011). They are slightly lower than atmospheric deposition (0.57 Tg C year^{-1}) and higher than point sources (0.04 Tg C year^{-1}).

Table 4.14 Submarine groundwater discharge and associated carbon fluxes to the Baltic Sea Basins and the Baltic Sea

Study area	SGD ± SD km³ year⁻¹	Carbon concentrations ± SD mg l⁻¹		Carbon fluxes ± SD kT year⁻¹		References
		DIC	DOC	DIC	DOC	
The Baltic Sea	4.40 ± ND[a]	64.5 ± 15.0	5.8 ± 0.5	283.8 ± 44.0	25.5 ± 2.2	This study [SGD rate based on Peltonen (2002)]
• The Polish and German coast	1.90 ± ND	64.5 ± 15.0	5.8 ± 0.5	122.6 ± 19.0	11.0 ± 1.0	This study [SGD rate based on Peltonen (2002)]
• The Gulf of Gdańsk	0.06 ± ND	64.5 ± 15.0	5.8 ± 0.5	3.9 ± 0.6	0.3 ± 0.03	This study [SGD based on Kozerski (2007)]
• The Puck Bay	0.03 ± ND	64.5 ± 15.0	5.8 ± 0.5	1.9 ± 0.2	0.2 ± 0.002	This study [SGD based on Piekarek-Jankowska (1994)]
• The Gulf of Finland	0.60 ± ND	64.5 ± 15.0	5.8 ± 0.5	38.7 ± 6.0	3.5 ± 0.3	This study [SGD based on Viventsowa and Voronow (2003)]

SGD derived carbon fluxes to other coastal areas are presented for comparison

[a]*ND* no data

There are few reports devoted to carbon loads delivered to the coastal seas via SGD. These showed that SGD fluxes of both dissolved inorganic carbon (DIC) and dissolved organic carbon (DOC) are important carbon pathways from land to coastal ocean. Cai et al. (2003) estimated DIC fluxes as—20 to 170×10^9 mol year^{-1} and concluded it to exceed river inputs in South Carolina. Moore et al. (2006) calculated that SGD fluxes of DIC and DOC from the marshes around the Okatee estuary, South Carolina, amounted to 1400×10^3 mol d^{-1} and 120×10^3 mol d^{-1}, respectively. These carbon fluxes were comparable with river inputs to the marsh. Liu et al. (2012) estimated that DIC load carried by SGD to the East China Sea equaled 153–347×10^9 mol year^{-1}, a value representing 23–53 % of DIC contributions from the Pearl River to the sea. The source of SGD was mostly recirculated seawater that brought an equivalent of 12–21 % of the Pearl River discharge.

In a recent paper Kuliński and Pempkowiak (2011) quantified major sinks and sources of carbon to the Baltic. In the constructed carbon budget, CO_2 exchange through the air-seawater interface was used as a closing term. The results obtained identify the entire Baltic Sea as a source of CO_2 to the atmosphere amounting to -1.05 ± 1.71 Tg C year^{-1}. The accuracy of CO_2 exchange between seawater and atmosphere depended on uncertainties of each component of the budget. Despite the uncertainties significance, the CO_2 exchange through the air-seawater interface, categorized the Baltic Sea as basin with a near neutral balance of annual CO_2 exchange, with slight skewness towards the emissions. However, the seepage carbon flow (FSGD) was not included in the budget. When the budget is supplemented with $\mathbf{F_{SGD}}$ (0.31 Tg C year^{-1}) the new mass balance of carbon in the Baltic Sea is obtained:

$$Fe + Fi + Fo + F_{CO_2} + Ff + Fp + Fr + Fm + Fs + \mathbf{F_{SGD}} = 0 \qquad (1)$$

$$F_{CO_2} = Fe + Fi + Fo + Ff + Fp + Fr + Fm + Fs + \mathbf{F_{SGD}} \qquad (2)$$

where Fe—export to North Sea, Fi—import from the North Sea, Fo—atmospheric deposition, F_{CO_2}—net CO_2 exchange between seawater and the atmosphere, Ff—fisheries, Fp—point sources, Fr—river input, Fm—return flux from sediments to the water column, Fs—accumulation in the sediments, FSGD—submarine groundwater discharge.

As the outcome of calculations, similarly to Kuliński and Pempkowiak (2011), net emissions of CO_2 to the atmosphere were calculated, amounting to 1.36 ± 1.71 Tg C year^{-1}. The average CO_2 emission reached -3.5 g C m^{-2} year^{-1} (-12.9 g CO_2 m^{-2} year^{-1}). Thus, the Baltic Sea's status as a source of CO_2 to the atmosphere was confirmed. Moreover, when the SGD carbon loads are supplemented to the Baltic carbon budget, the status of the sea defined to date as 'marginally heterotrophic' turns into firmly heterotrophic.

The projected estimations of dissolved carbon input into the Baltic Sea via SGD should draw attention to the significance of SGD in hydrologic carbon cycles. The

projections demonstrate that SGD sites may transport substantial loads of carbon to the coastal areas. One immediate consequence of this is the modification of biodiversity in the seepage affected areas.

The flux of trace metals to the southern Baltic Sea was calculated using two literature calculations based on hydrological balances. Peltonen (2002) estimated the groundwater discharge to the southern Baltic Sea to be 1.4 km^3 year^{-1}, while 40 % of it comes from Poland.

This estimation was based on regional studies located in Poland. Kryza and Kryza (2006) also made a model estimation of the direct groundwater inflow to the Baltic Sea from Polish territory. The result was one order of magnitude smaller than this calculated by Peltonen (2002) and equaled 0.2 km^3 year^{-1}. The possible explanation of smaller groundwater discharge rate calculated by Kryza and Kryza (2006) compared to the one made by Peltonen (2002) is that Kryza and Kryza (2006) assumed that groundwater had to escape at the shoreline.

The loads of metals via SGD to the southern Baltic Sea are presented in Table 4.15 Loads of dissolved Mn, Zn, Cr and Co are three (Mn) or two (Zn, Cr, Co) orders of magnitude higher than loads of dissolved Pb, Cd, Ni and Cu. Assuming that the average trace metals groundwater concentrations obtained during this study are representative of the Baltic Sea region and calculating the total dissolved metal fluxes via groundwater using groundwater discharge estimation made by Peltonen (2002) it is possible to compare it with total metals fluxes via different sources (Table 4.16). The SGD delivered load in relation to the total load delivered from other sources is equal to 0.3 % for Pb, 5 % Cd and less than 1 ‰ for Cu. On this basis, we can conclude that metals fluxes via SGD to the southern Baltic can be a significant source of metals only locally e.g. in the Bay of Puck.

Table 4.15 Trace metals fluxes via SGD to the southern Baltic Sea

Metal	Metals fluxes via groundwater discharge to the southern Baltic Sea			
	Based on groundwater discharge calculated by Kryza and Kryza (2006)		Based on groundwater discharge calculated by Peltonen (2002)	
	Average ± SD (mol year^{-1})	Average ± SD (kg year^{-1})	Average ± SD (mol year^{-1})	Average ± SD (kg year^{-1})
Pb	235 ± 13	50 ± 3	704 ± 40	146 ± 8
Cd	504 ± 1	56.7 ± 0.1	1512 ± 2	170 ± 0.2
Co	1746 ± 4	102.9 ± 0.3	5239 ± 13	309 ± 1
Mn	531,668 ± 11,501	29,209 ± 632	1,595,004 ± 34,504	87,626 ± 1896
Cu	121 ± 27	8 ± 2	363 ± 81	23 ± 5
Ni	1070 ± 100	63 ± 6	3210 ± 300	188 ± 18
Zn	6718 ± 52	440 ± 4	20,154 ± 155	1318 ± 10
Cr	3675 ± 45	190 ± 2	11,025 ± 135	573 ± 7

Table 4.16 Total heavy metal flux entering the Baltic Sea from rivers discharges, municipalities and industrial plants in 1995 (HELCOM 1998)

Metal	Metals fluxes via different sources to the Baltic Sea							
	Rivers		Municipalities		Industries		Total	
	kmol year^{-1}	t year^{-1}	kmol year^{-1}	t year^{-1}	kmol year^{-1}	t year^{-1}	kmol year^{-1}	t year^{-1}
Pb	1452	300.5	159	32.9	19.1	3.96	1628	337.4
Cd	146	16.4	58.6	6.6	5.4	0.61	210	23.61
Cu	23,122	1469	1194	75.9	781	49.63	25,098	1595
Hg	57.7	11.6	5.7	1.14	3.0	0.61	66.5	13.33

Modified after Pohl et al. (2002)

4.5   Assessment of the Global Chemical Substances Fluxes Via SGD

It is now well appreciated that SGDs occur in most of the coastal areas and that it is an important source of nutrients, metals, dissolved carbon and pollutants (Knee and Paytan 2011) to the coastal ocean. SGD can have different role in varied coastal settings. Many studies have been focused on: identification and estimation of SGD in local areas; developing methods used to measure SGD; quantification of nutrients, metals, dissolved carbon and other chemical constituents in groundwater impacted areas and their fluxes via SGD; finally efforts are also focused on estimating SGD fluxes of water, nutrients, metals, dissolved carbon at a global scale. It is important to understand what fraction of nitrogen, phosphorus, or other chemical species in the marine environment originates from SGD. Such knowledge is required not only to know and understand biogeochemical cycles today, but also to interpret the paleoceangraphic record, which is used, for example, to infer the characteristics of the Earth's climate in the geologic past. Ground-water has different stable isotopic composition than river-water, thus, assuming that all terrestrial inputs were derived from rivers can be problematic if SGD inputs were actually significant (Knee and Paytan 2011).

There have been several attempts to estimate the total subterranean flux of fresh water to the ocean (Moore 2010). These studies often were based on a water budget. The attempt reconcile precipitation, evapotranspiration and river runoff. The world river discharge is estimated to range from 35 to 40×10^{12} m^3 $year^{-1}$ (Berner and Berner 1996; Alley et al. 2002; Emerson and Hedges 2008); world precipitation is calculated to be in the range from 95 to 115×10^{12} m^3 $year^{-1}$; while evapotranspiration estimates range from 60 to 74×10^{12} m^3 $year^{-1}$ (Burnett et al. 2003). Considering only the differences of averages, the flux of SGD would be zero (Moore 2010). However, each of the terms has a range of ± 10 % which makes SGD flux range from 0 to 13×10^{12} m^3 $year^{-1}$.

Another method used to estimate global SGD is based on an integrated hydrologic-hydrogeologic approach (Zekster et al. 2007). The method assumes that groundwater input to rivers that drain specific hydrogeologic provinces is similar to SGD to the ocean from these provinces (m^3 km^{-1} $year^{-1}$). The assumption is limited to groundwater discharge only from the upper zones of the provinces (the same zones that drains into rivers) and may miss flux from deeper zones (e.g. confined aquifers) that drain into ocean. Zekster et al. (2007) estimated a fresh groundwater flux to the ocean to be in the range from 2.2 to 2.4×10^{12} m^3 $year^{-1}$ which amounts to 5–6 % of the world river flow (Moore 2010).

In this study we have made an attempt to calculate chemical substance loads via SGD to global ocean basing on literature fresh groundwater discharge to ocean (Burnett et al. 2003; Zekster et al. 2007; Moore 2010) and literature chemical concentrations measured in groundwater.

Table 4.17 presents a comparison of nutrients concentrations found in different groundwater seeps. The concentrations from different SGD impacted areas

Table 4.17 Nutrients concentrations found in different groundwater environments as either a range or an average ± standard deviation (NR–not reported)

Study area	Concentrations of nutrients in SGD µmol L^{-1}				References
	PO$_4$	NH$_4$	NO$_3$	NO$_2$	
West Neck Bay, Long Island, NY	0.26–0.67	ND[a]	254–457	ND	Beck et al. (2007)
Hwasun Bay, off Jeju, Korea	0.7–5.9	ND	40–780	ND	Kim et al. (2011)
Bangdu Bay, off Jeju, Korea	1.0–4.0	ND	40–210	ND	Kim et al. (2011)
Southwestern shelf of Taiwan	–	19.2[b] ± NR			Zavialov et al. (2012)
Bay of Puck, Baltic Sea	42.5–78.7	17.3–219.1	0.3–0.5	0.14–0.26	Szymczycha et al. (2012)
Laoye Lagoon, Hainan, China	0.1–28.4	0.1–20.1	12.8–489	0.0–3.2	Ji et al. (2013)
Messiniakos Gulf, SE Ionian Sea	0.05–0.10	Up to 50	Up to 50		Pavlidou et al. (2014)
Palma Beach, Balearic Islands)	0.3–2.5	7–810[b]			Rodellas et al. (2014)
Tolo Harbour, Hong Kong	0.11–2.68	24.54–62.28			Luo et al. (2014)
Sanggou Bay, China	0.535 ± NR	150[b] ± NR			Wang et al. (2014)
Godavari estuary, India	4.6–95.5	0.05–7.65	3.63–86.9	0–24.4	Rengarajan and Sarma (2015)
Port Jefferson Harbor, NY	b.d.l–36.2	b.d.l–15	14.4–165.6		Young et al. (2015)

[a]*ND* not detected
[b]DIN
b.d.l below detection limit

represent different orders of magnitude. Nitrate is the most common groundwater pollutant worldwide (Spalding and Exner 1993) however its form is most prevalent in freshwater oxic conditions. It can enter groundwater from both natural and anthropogenic sources. Nitrite and ammonium are typically much lower than nitrate in oxic conditions, however in some anaerobic or suboxic conditions, ammonium can be a dominant nitrogen form (Slomp and Van Cappellen 2004). Phosphates in groundwater, especially oxic groundwater, often form insoluble, inorganic compounds that sorb to rocks and particles (Wong et al. 1998). In anaerobic conditions phosphates concentrations of phosphates are, most often, substantial.

As nitrogen and phosphorous are considered the primary limiting nutrients in coastal and estuarine systems, although there is a need to calculate their fluxes via SGD to understand nutrient limitation of the system system.

Table 4.18   Nutrients fluxes via SGD to global ocean

SGD flux to Global Ocean	Nutrients fluxes to global ocean mol year^{-1} × 10^9				
	PO$_4$	NH$_4$	NO$_3$	NO$_2$	DIN
2.2 × 10^{12} (Zekster et al. 2007)	0.1–173	0.1–482	0.7–1716	0–54	15–1782
2.4 × 10^{12} (Zekster et al. 2007)	0.1–188	0.1–526	0.7–1872	0–59	17–1944
13 × 10^{12} (Moore 2010)	0.7–1023	0.7–2847	3.9–10,140	0–317	91–10,530

In this study it has been decided to calculate ranges of nutrients fluxes via SGD to the global ocean by multiplying literature smallest and highest concentrations. The SGD fluxes to global ocean according to Zekster et al. (2007) and Moore (2010) were taken. The uncertainties of this approach originate from general factors, thus, the projected nutrient load calculations constrain the first approximation of SGD inputs to the Global Ocean rather than approximating actual loads. Results are presented in Table 4.18.

DIN fluxes via SGD are in the range (15–1944) × 10^9 mol year^{-1} according to Zekster's et al. (2007) SGD global fluxes and from (0 to 10,530) × 10^9 mol year^{-1} according to Moore's (2010) SGD global fluxes. According to the literature rivers discharge about 300 × 10^9 mol year^{-1} of DIN to the global continental margins while rivers plus groundwater and ice discharge from 1000 × 10^9 mol year^{-1} (Chen et al. 2003) to 15,000 × 10^9 mol year^{-1}. As all of the presented fluxes have several uncertainties it is hard to compare them. However, it is clear that DIN fluxes via SGD are important component of the globalflux that is comparable to load via river runoff. Although more studies are essential in order to estimate global DIN fluxes via SGD more precisely.

Phosphates fluxes via SGD to global ocean are in the range 0.1–188 × 10^9 mol year^{-1} according to Zekster's (2007) SGD global fluxes and from (0 to 1023) × 10^9 mol year^{-1} according to Moore's (2010) SGD global fluxes, while literature phosphates fluxes via rivers are estimate to be 1000 × 10^9 mol year^{-1} (Chen et al. 2003).

The global carbon cycle involves processes among the major global reservoirs of this element: the atmosphere, ocean and land. The fundamental carrier in carbon cycling is CO$_2$. Ocean carbonate chemistry has a great impact on CO$_2$ partial pressure in the atmosphere. So far, no carbon fluxes via SGD to the World Ocean have been considered in the global carbon. As indicated, however, the SGD-derived carbon load constitutes a significant portion of the carbon budget in entire coastal basins. Moreover, it has been estimated that the total flux of SGD to the Atlantic Ocean is comparable in volume to the riverine flux (Moore 2010). Hence, in order to establish the order of magnitude of the SGD derived carbon load, carbon fluxes via SGD to the World Ocean have been calculated. Global SGD rates and dissolved carbon concentrations are required for this purpose.

There are few reports on carbon concentrations in groundwater impacted areas (Table 4.19) and equally few as regards global groundwater discharges (Zekster et al. 2007; Moore 2010). It has been decided to use literature DIC and DOC concentrations and literature derived SGDs to the World Ocean to establish the load of carbon that might enter the marine environment with SGD (Table 4.20).

Table 4.19 Comparison of dissolved carbon (DIC-dissolved inorganic carbon; DOC dissolved organic carbon) concentrations found in different groundwater environments as either a range or average ± standard deviation (NR—not reported)

Study area	Dissolved carbon concentrations in fresh SGD μmol L^{-1}		References
	DIC	DOC	
North Inlet, South Carolina	2500 ± NR	–	Cai et al. (2003)
Sapelo Island Hannock, GA	–	250–1080	Snyder et al. (2004)
Waquoit Bay, Ma	–	10–703	Charette and Sholkovitz (2006)
Okatee Estuary, South Carlina	16,000 ± NR	–	Moore et al. (2006)
West Neck Bay, Long Island, NY	–	21–118	Beck et al. (2007)
Indian River Lagoon, FL	–	1–700	Roy et al. (2010)
FL Gulf Coast	–	150–550	Santos et al. (2009)
South China Sea[a]	5100 ± 4300	–	Liu et al. (2012)
West Ireland	–	448 ± 40	Smith and Cave (2012)
Bay of Puck, Baltic Sea	5375 ± 1250	484 ± 42	Szymczycha et al. (2014)
Okatee Estuary, West Bank	–	613 ± 27	Porubsky et al. (2014)
Okatee Estuary, East Bank	–	1390 ± 53	Porubsky et al. (2014)
Gloucester Point STE	–	300–3000	O'Connor et al. (2015)
Godavari estuary, India	2200–29,600	–	Rengarajan and Sarma (2015)

[a]Saline SGD

Table 4.20 Comparison of dissolved carbon fluxes (DIC-dissolved inorganic carbon; DOC dissolved organic carbon) via SGD and rivers

Surface discharge to the World Ocean	Flow rate m^3 year^{-1}	Dissolved carbon fluxes kT year^{-1}		References
		DIC	DOC	
SGD	2.2 × 10^{12} (Zekster et al. 2007)	(58–781) × 10^3	(0.03–79) × 10^3	This study
	2.4 × 10^{12} (Zekster et al. 2007)	(63–852) × 10^3	(0.03–87) × 10^3	This study
	13 × 10^{12} (Moore 2010)	(343–462) × 10^3	(0.2–47) × 10^3	This study
Rivers	35 × 10^{12}	402 × 10^3	–	Emerson and Hedges (2008)
	–	384 × 10^3	324 × 10^3	Chen et al. (2003)
	–	320 × 10^3	205 × 10^3	Ludwig et al. (1996)

The calculated carbon fluxes are in the following ranges: $(58–852) \times 10^3$ kt C year^{-1} (DIC) and $(0.03–87) \times 10^3$ kt C year^{-1} (DOC) according to Zekster et al. (2007) global SGD estimates and $(0–4617) \times 10^3$ kt C year^{-1} (DIC) and $(0–468) \times 10^3$ kt C year^{-1} (DOC) according to Zekster et al. (2007) global SGD estimates. Reports define the carbon load delivered to the sea with river run-off with much better precision (Ludwig et al. 1996; Chen et al. 2003; Emerson and Hedges 2008). It follows from the data in Table 4.20 that the SGD-derived carbon load and the carbon load delivered with riverine discharge are comparable. Hence, the carbon flux associated with groundwater discharge may well prove to be an important component of the carbon cycle and have the potential to significantly change the projected sequestration of CO_2 by the ocean.

References

Andersen S, Baron L, Gudbjerg J, Gregersen J, Chapellier D, Jakobsen R, Postma D (2007) Discharge of nitrate-containing groundwater into a coastal marine environment. J Hydrol 336:98–114

Alley WM, Healy RW, LaBaugh JW, Reilly TE (2002) Flow and storage in groundwater systems. Science 296:1985–1990

Almroth-Rosell E, Eilola K, Hordoir R, Meier HEM, Hall POJ (2011) Transport of fresh and resuspended particulate organic material in the Baltic Sea—a model study. J Mar Syst 87:1–12

Bates RG (1982) pH measurements in the marine environment. Pure Appl Chem 54:229–232

Beck AJ, Rapaglia JP, Cochran JK, Bokuniewicz HJ (2007) Radium mass-balance in Jamaica Bay, NY: evidence for substantial flux of submarine groundwater. Mar Chem 106:419–441

Beck AJ, Cochran JK, Sañudo-Wilhelmy SA (2010) The distribution and speciation of dissolved trace metals in a shallow subterranean estuary. Mar Chem 121:145–156

Bełdowski J, Pempkowiak J (2003) Horizontal and vertical variabilities of mercury concentration and speciation in sediments of the Gdansk Basin, Southern Baltic Sea. Chemosphere 52:645–654

Bełdowski J, Pempkowiak J (2007) Mercury transformations in marine coastal sediments as derived from mercury concentration and speciation changes along source/sink transport pathway (Southern Baltic). Estuar Coast Shelf Sci 72:370–378

Bełdowski J, Miotk M, Pempkowiak J (2009) Mercury fluxes through the sediment water interface and bioavibility of mercury in southern Baltic Sea sediments. Oceanologia 52:263–285

Berner EK, Berner RA (1996) Global environment: water, air and geochemical cycles. Prentice Hall, Englewood Cliffs

Bolałek J (1992) Ionic macrocomponents of interstitial water of Puck Bay. Oceanologia 33: 131–158

Bolałek J, Falkowska L, Korzeniewski K (1993) In: Korzeniewski K (ed) Hydrochemia Zatoki: Zatoka Pucka. Fundacja Rozwoju Uniwersytetu Gdańskiego, Gdańsk, Poland, pp 222–281

Bolałek J, Graca B, Burska D (2011) In: Uścinowicz Sz (ed) Composition of interstitial waters: geochemistry of Baltic Sea surface and sediments. Polish Geological Institute-National Research Institute, Warsaw, Poland, pp 292–306

Borges AV (2005) Do we have enough pieces of the jigsaw to integrate CO_2 fluxes in the coastal ocean? Estuaries 28:3–27

Boszke L (2005) Fluxes and balance of mercury in the inner Bay of Puck, southern Baltic, Poland: an overview. Oceanology 47:325–350

Burnett WC, Bokuniewicz H, Huettel M, Moore WS, Taniguchi M (2003) Groundwater and pore water inputs to the coastal zone. Biogeochem 66:3–33

Burnett WC, Aggarwal PK, Aureli A, Bokuniewicz HJ, Cable JE, Charette MA, Kontar E, Krupa S, Kulkarni KM, Loveless A, Moore WS, Oberdorfer JA, Oliveira J, Ozyurt N, Povinec P, Privitera AMG, Rajar R, Ramessur RT, Scholten J, Stieglitz T, Taniguchi M, Turner JV (2006) Quantifying submarine groundwater discharge in the coastal zone via multiple methods. Sci Total Environ 367:498–543

Burska D, Graca B, Bolałek J (2011) In: Uścinowicz Sz (ed) Nitrogen: geochemistry of Baltic Sea surface and sediments. Polish Geological Institute-National Research Institute, Warsaw, Poland, pp 197–199

Burska D, Pryputniewicz D, Falkowska L (2005) Stratification of particulate organic carbon and nitrogen in the Gdańsk Deep (southern Baltic Sea). Oceanologia 47:21–217

Burt RA (1993) Ground-water chemical evolution and diagenetic processes in the Upper Floridan aquifer, southern South Carolina and northeastern Georgia. US Geol Surv Water-Supply Pap 2392:76 pp

Cable JE, Burnett WC, Chanton JP (1997) Magnitude and variations of groundwater along a Florida marine shoreline. Biogeochemistry 38:189–205

Cai WJ, Wang YC, Krest J, Moore WS (2003) The geochemistry of dissolved inorganic carbon in a surficial groundwater aquifer in North Inlet, South Carolina, and the carbon fluxes to the coastal ocean. Geochim Cosmochim Acta 67:631–639

Capone DG, Slater JM (1990) Interannual patterns of water table height and groundwater derived nitrate in nearshore sediments. Biogeochemistry 10:277–288

Charette MA, Sholkovitz ER (2002) Oxidative precipitation of groundwater-derived ferrous iron in the subterranean estuary of a coastal bay. Geophys Res Lett 29:1444–1452

Charette MA, Sholkovitz ER (2006) Trace element cycling in a subterranean estuary: Part 2. Geochemistry of the pore water. Geochemica et Cosmochimica Acta 70:811–826

Charette MA, Sholkovitz ER, Hansel CM (2005) Trace element cycling in a subterranean estuary Part 1. Geochemistry of the permeable sediments. Geochemica et Cosmochimica Acta 66:2095–2109

Chen C-TA, Borges AV (2009) Reconciling opposing views on carbon cycling in the coastal ocean: continental shelves as sinks and near-shore ecosystems as sources of atmospheric CO_2. Deep-Sea Res II 56:578–590

Chen C-TA, Liu K-K, Macdonald R (2003) Continental margin exchanges, ocean biogeochemistry: the role of the ocean carbon cycle in global change, IGBP Book Series, Springer, Berlin, pp 53–97

Chester R (2003) Marine geochemistry (2nd edn). Blackwell Science, London, 506 pp

Cyberski J, Szefler K (1993) In: Korzeniewski K (ed) Klimat Zatoki i jej zlewiska: Zatoka Pucka. Fundacja Rozwoju Uniwersytetu Gdańskiego, Gdańsk, Poland, pp 14–39

Dera J (1992) Marine physics. Elsevier, Amsterdam 515 pp

Dickson AG (1984) pH scales and proton-transfer reactions in saline media such as seawater. Geochim Cosmochim Acta 48:2299–2308

Dzierzbicka-Glowacka L, Kuliński K, Maciejewska A, Pempkowiak J (2010) Particulate organic carbon in the southern Baltic Sea: numerical simulations and experimental data. Oceanologia 52:621–648

Dzierzbicka-Glowacka L, Kulinski K, Maciejewska A, Jakacki J, Pempkowiak J (2011) Numerical modelling of POC dynamics in the southern Baltic under possible future conditions determined by nutrients, light and temperature. Oceanologia 53(4):971–992

Emerson SR, Hedges JI (2008) Chemical oceanography and the marine carbon cycle. Cambridge University Press, Cambridge, 453 pp

Falkowska L, Piekarek-Jankowska H (1999) Submarine seepage of fresh groundwater: disturbance in hydrological and chemical structure of the water column in the Gdańsk Basin. J Mar Sci 56:153–160

Ganguli PM, Conway CH, Swarzenski Izbicki JA, Flegal AR (2012) Mercury speciation and transport via submarine groundwater discharge at a Southern California Coastal Lagoon System. Environ Sci Technol 46:1480–1488

Graca B, Bolałek J (2011) In: Uścinowicz Sz (ed) Phosphorous: geochemistry of Baltic Sea surface and sediments. Polish Geological Institute-National Research Institute, Warsaw, Poland, pp 187–197

Grasshoff K (1976) Methods of seawater analysis. Verlag Chemie, Weinheim

Grzybowski, Pempkowiak (2003) Preliminary results on low molecular weight organic substances dissolved in the waters of the Gulf of Gdańsk. Oceanologia 45(4):693–704

Hedges JI (2002) Why dissolved organic matter. In: Hansell DA, Carlson CA (eds) Biogeochemistry of marine dissolved organic matter. Elsevier Science, San Diego, pp 1–33

HELCOM (1998) HELCOM scientific workshop: the effects of 1997 flood of the Odra and Vistula rivers. 13, Berlin. ISSN 0946-6010

HELCOM (2005a) Nutrient pollution to the Baltic Sea in 2000. Baltic Sea Environment Proceedings 100, 24 pp

HELCOM (2005b). Atmospheric supply of nitrogen, lead, cadmium, mercury and lindane to the Baltic Sea over the period 1996–2000. Baltic Sea Environment Proceedings 101, 79 pp

HELCOM (2009). Eutrophication in the Baltic Sea—an integrated thematic assessment of the effects of nutrient enrichment in the Baltic Sea region. Baltic Sea Environment Proceedings 115B, 152 pp

Herczeg AL, Broecker WS, Anderson RF, Schiff SL, Schindler DW (1985) A new method for monitoring temporal trends in the acidity of fresh waters. Nature 315:133–135

Hosono T, Ono M, Burnett WC, Tokunaga T, Taniguchi M, Akimichi T (2012) Spatial distribution of submarine groundwater discharge and associated nutrients within a local coastal area. Environ Sci Technol 46:5319–5326

Huettel M, Cook P, Drazek JM, COSA participants (2004). COSA: coastal sands as biocatalytical filters translating scientific results to the general audience and policy makers. Coastline Rep 2:149–154

Huzarska K (2013) Spatial distribution of biological and physical sediment parameters in the western Gulf of Gdańsk. Oceanologia 55:53–470

IPCC (2007) Climate change 2007. Synthesis Report. A contribution of working groups I, II and III to the Fourth Assessment Report of the Intergovernmental Panel on Climate Change. Cambridge University Press, Cambridge, The United States, p 104

Jeong J, Kim G, Han S (2012) Influence of trace elements fluxes from submarine groundwater discharge (SGD) on their inventories in coastal waters off volcanic island, Jeju, Korea. Appl Geochem 27:37–43

Ji T, Du J, Moore WS, Zhang G (2013) Nutrient inputs to a Lagoon through submarine groundwater discharge: the case of Laoye Lagoon, Hainan, China. J Marine Syst 111–112:253–262

Jørgensen BB (2006) In: Schulz HD, Zabel M (ed) Bacteria and marine biogeochemistry: marine geochemistry. Springer, Berlin, pp 182–184

Kaleris V, Lagas G, Marczinek S, Piotrowski JA (2002) Modelling submarine groundwater discharge: an example from the western Baltic Sea. J Hydrol 265:76–99

Kim G, Kim JS, Hwang DW (2011) Submarine groundwater discharge from oceanic islands standing in oligotrophic oceans: implications for global biological production and organic carbon fluxes. Limnol Oceanogr 56:673–682

Kirkwood D (1994) Nutrients: practical notes on their determination in seawater. In: Topping G, Harms U (eds) ICES/HELCOM workshop on quality assurance of chemical analytical procedures for the Baltic monitoring programme. Baltic Sea Environment Proceedings, vol 58, pp 23–47

Knee Kl, Paytan A (2011) Submarine groundwater discharge: a source of nutrients, metal and pollutants to the coastal ocean. In: Wolanski E, McLucky DS (eds) Treatiseon estuarine and coastal science, vol 4. Academic Press, Waltham, pp 205–233

Korzeniowski K (1993) Zatoka Pucka. Instytut Oceanografii Uniwersytetu Gdańskiego, Gdynia

Kotwicki L, Grzelak K, Czub M, Dellwig O, Gentz T, Szymczycha B, Brottcher M (2014) Submarine groundwater discharge to the Baltic coastal zone—impact on the meiofaunal community, J Marine Sys 129:118–126

Kozerski B (2007) Gdański system wodonœeny. Wyd. Politechniki Gdanskiej

Kroeger KD, Swarzenski PW, Greenwood JW, Reich C (2007) Submarine groundwater discharge to Tampa Bay: nutrient fluxes and biogeochemistry of the aquifer. Mar Chem 104:85–97

Kryza J, Kryza H (2006) The analytic and model estimation of the direct groundwater flow to Baltic Sea on the territory of Poland. Geologos 10:154–165

Kuliński K, Pempkowiak J (2008) Dissolved organic carbon in the southern Baltic Sea: quantification of factors affecting its distribution. Estuar Coast Shelf Sci 78:38–44

Kuliński K, Pempkowiak J (2011) The carbon budget of the Baltic Sea. Biogeosciences 8:3219–3230

Kuliński K, Pempkowiak J (2012) Carbon cycling in the Baltic Sea, Springer, Berlin, 129 pp

Lamborg CH, Fitzgerald WF, Skoog A, Visscher PT (2004) The abundance and source of mercury-binding organic ligands in Long Island Sound. Mar Chem 90:151–163

Lee YW, Rahman MDM, Kim G, Han S (2011) Mass balance of total mercury and monomethylmercury in coastal embayments of a volcanic islands: Significance of submarine groundwater discharge. Environ Sci Technol 45:9891–9900

Lee YW, Hwang DW, Kim G, Lee WC, Oh HT (2009) Nutrient inputs from submarine groundwater discharge (SGD) in Masan Bay, an embayment surrounded by heavily industrialized cities, Korea. Sci Total Environ 407:3181–3188

Leote C, Ibánhez JPS, Rocha C (2008) Submarine groundwater discharge as a nitrogen source to the Ria Formosa studied with seepage meters. Biogeochemistry 88:185–194

Lidzbarski M (2011) In: Uścinowicz Sz (ed) Groundwater discharge in the Baltic Sea basin: geochemistry of Baltic Sea surface and sediments. Polish Geological Institute-National Research Institute, Warsaw, Poland, pp 138–145

Liu Q, Dai M, Chen W, Huh CA, Wang G, Li Q, Charette MA (2012) How significant is submarine groundwater discharge and its associated dissolved inorganic carbon in a river-dominated shelf system. Biogeosciences 9:1777–1795

Ludwig W, Amiotte-Suchet P, Probs JL (1996) River discharges of carbon to the world's oceans: determining local inputs of alkalinity- and of dissolved and particulate organic carbon, Centre de geochimie de la surface. CNRS 323:1007–1014

Luo X, Jiao JJ, Moore WS, Lee CM (2014) Submarine groundwater discharge estimation in an urbanized embayment in Hong Kong via short-lived radium isotopes and its implication of nutrient loadings and primary production. Mar Pollut Bull 82:144–154

Marion GM, Millero FJ, Feistel R (2009) Precipitation of solid phase calcium carbonates and their effect on application of seawater SA-T-P models. Ocean Sci 5:285–291

Marion GM, Millero FJ, Camões MF, Spitzer P, Feistel R, Chen C-TA (2011) Mar Chem 126:89–96

Massel S (2001) Circulation of groundwater due to wave set-up on a permeable beach. Oceanologia 43:279–290

Massel S, Przyborska A, Przyborski M (2005) Attenuation of wave-induced groundwater pressure in shallow water. Part 2 Theory. Oceanologia 47:232–291

Millero FJ (1993) What is PSU? Oceanography 6:67

Millero FJ, DiTrolio B, Suarez AF, Lando G (2009a) Spectroscopic measurements of the pH in NaCl brines. Geochim Cosmochim Acta 73:3109–3114

Millero FJ, Woosley R, DiTrolio B, Waters J (2009b) The effect of ocean acidification on the speciation of metals in natural waters. Oceanography 22:72–85

Millham NP, Howes BL (1994) Freshwater flow into a coastal embayment: groundwater and surface water inputs. Limnol Oceanogr 39:1928–1944

Moore WS (2010) The effect of submarine groundwater discharge on the ocean. Ann Rev Mar Sci 2:59–88

Moore WS, Blanton JO, Joye SB (2006) Estimates of flushing times, submarine ground water discharge, and nutrient fluxes to Okatee Estuary, South Carolina. J Geophy Res 111:C09006. doi:10.1029/2005JC003041

Nienchesky LFH, Windom HL, Moore WS, Jahnke RA (2007) Submarine groundwater discharge of nutrients to the ocean along a coastal lagoon barrier, Southern Brazil. Mar Chem 106:546–561

Oberdorfer JA, Valentino MA, Smith SV (1990) Groundwater contribution to the nutrient budget of Tomas Bay, California. Biogeochemistry 10:199–216

O'Connor AE, Luek J, McIntosch HA, Beck A (2015) Geochemistry of redox-sensitive trace elements in a shallow subterranean estuary. Mar Chem 172. doi:10.1016/j.marchem.2015.03.001. http://www.researchgate.net/journal/0304-4203_Marine_Chemistry

Pazdro Z, Kozerski B (1990) Hydrogeologia Ogólna. Wydawnictwo Geologiczne, Warsaw, Poland, 624 pp

Pempkowiak J (1983) C18 reversed-phase trace enrichment of short- and long-chain (C2-C8-C20) fatty acids from dilute aqueous solutions and sea water. J Chromatogr 258:93–102

Pempkowiak J, Obarska-Pempkowiak H (2002) Long-term changes in sewage sludge stored in a reed bed. Sci Total Environ 297:59–65

Pempkowiak J, Widrowski M, Kuliński W (1984) Dissolved organic carbon and particulate carbon in the Southern Baltic in September, 1982. In: Proceedings XIV conference of Baltic oceanographers, IMGW, Gdynia, pp 699–713

Pempkowiak J, Cossa D, Sikora A, Sanjuan J (1998) Mercury in water and sediments of the southern Baltic Sea. Sci Total Environ 213:185–192

Pempkowiak J, Chiffoleau J-F, Staniszewski A (2000) The vertical and horizontal distribution of selected trace metals in the Baltic Sea off Poland. Estuar Coast Shelf Sci 51:115–125

Pempkowiak J, Walkusz-Miotk J, Bełdowski J, Walkusz W (2006) Heavy metals in zooplankton from the Southern Baltic. Chemosphere 62:1697–1708

Pempkowiak J, Szymczycha B, Kotwicki L (2010) Submarine groundwater discharge (SGD) to the Baltic Sea. Rocznik Ochrony Środowiska 12:17–32

Peltonen K (2002) Direct groundwater inflow to the Baltic Sea. TemaNord, Nordic Councils of Ministers, Copenhagen, Holand, 79 pp

Piekarek-Jankowska H (1994) Zatoka Pucka jako obszar drenażu wód podziemnych. Wydawnictwo Uniwersytetu Gdańskiego, Gdańsk, Poland

Piekarek-Jankowska H (1996) Hydrochemical effects of submarine groundwater discharge to the Puck Bay (Southern Baltic Sea, Poland). Geographia Polonica 67:103–119

Piekarek-Jankowska H (2007) In: Kozerski B (ed) (2010) Podmorski drenaż wód podziemnych gdańskiego system wodonośnego: Gdański system wodonośny. Wydawnictwo Politechniki Gdańskiej, Gdańsk, Poland, pp 34–49

Pohl C, Hennings U, Siegel H, Bachor A (2002) Trace metal impact into the Baltic Sea during the exceptional Oder flood in summer 1997. Mar Chem 79:101–111

Porubsky WP, Weston NB, Moore WS, Ruppel C, Joye SB (2014) Dynamics of submarine groundwater discharge and associated fluxes of dissolved nutrients, carbon, and trace gases to the coastal zone (Okatee River estuary, South Carolina). Geochim Cosmochim Acta 131:81–97

Pruszkowska M, Przewłócka M (2007) In: Kozerski B (ed) Jakość wód podziemnych: Gdański system wodonośny. Wydawnictwo Politechniki Gdańskiej, Gdańsk, Poland, pp 51–64

Pytkowicz RM (1979) pH of seawater. Environ Int 2:417–418

Rapaglia JP (2007) Using direct measurements of submarine groundwater discharge to investigate the coupling between surface and pore waters. PhD Dissertation, Stony Brook: Marine and Atmospheric Science

Ravichandran M (2004) Interactions between mercury and dissolved organic matters: a review. Chemosphere 55:319–331

Rengarajan R, Sarma VVSS (2015) Submarine groundwater discharge and nutrient addition to the coastal zone of the Godavari estuary. Mar Chem 172:57–69

Rodellas V, Garcia-Orellana J, Tovar-Sánchez A, Basterretxea G, Jm López-Garcia, Sánchez-Quiles D, Garcia-Solsona E, Masqué P (2014) Submarine groundwater discharge as a source of nutrients and trace metals in a Mediterranean bay (Palma Beach, Balearic Islands). Mar Chem 160:56–66

Rosenberry DO (2008) A seepage meter designed for use in flowing water. J Hydrol 359:118–130

Roy M, Martin JB, Cherrier J, Cable JE, Smith CG (2010) Influence of sea level rise on iron diagenesis in an east Florida subterranean estuary. Geochim Cosmochim Acta 74:5560–5573

Santos IR, Burnett WC, Dittmar T, Suryaputra IGNA, Chanton J (2009) Tidal pumping drives nutrient and dissolved organic matter dynamics in a Gulf of Mexico subterranean estuary. Geochemica at Cosmochimica Acta 73:1325–1339

Schulz HD, Zabel M (2006) Marine geochemistry. Springer, Berlin, 534 pp

Schlüter M, Sauter EJ, Andersen CA, Dahlgaard H, Dando PR (2004) Spatial distribution and budget for submarine groundwater discharge in Eckernförde Bay (Western Baltic Sea). Limnol Oceanogr 49:157–167

Slomp CP, Van Cappellen P (2004) Nutrient inputs to the coastal ocean through submarine groundwater discharge: controls and potential impact. J Hydrol 295:64–86

Smith AM, Cave RR (2012) Influence of fresh water, nutrients and DOC in two submarine-groundwater-fed estuaries on west of Ireland. Sci Total Environ 438:260–270

Snyder M, Taillefert M, Ruppel C (2004) Redox zonation at the saline-influenced boundaries of a permeable surficial aquifer: effects of physical forcing on the biogeochemical cycling of iron and manganese. J Hydrol 296:164–178

Spalding RF, Exner ME (1993) Occurrence of nitrate in groundwater—a review. J Environ Qual 22:392–402

Sprynskyy M, Buszewski B, Terzyk AP, Namieśnik J (2006) Study of the selection mechanism of heavy metal (Pb^{2+}, Cu^{2+}, Ni^{2+}, and Cd^{2+}) adsorption on clinoptilolite. J Colloid Interface Sci 304:21–28

Street JH, Knee KL, Grossman EE, Paytan A (2008) Submarine groundwater discharge and nutrient addition to the coastal zone and coral reefs of leeward Hawai'i. Mar Chem 109:355–376

Stumm W, Morgan JJ (1981) Aquatic chemistry, 2nd edn. Wiley, New York

Suslow TV (2004) Oxidation-reduction potential for water disinfection monitoring, control, and documentation, University of California Davis

Szymczycha B (2015) Submarine groundwater discharge to the Bay of Puck. In: Zieliński T, Węsławski M, Kuliński K (eds) Southern Baltic Sea and its possible changes with regard to the predicted climate changes, in impact of climate changes on marne environments. Springer, London, pp 61–75

Szymczycha B, Vogler S, Pempkowiak J (2012) Nutrient fluxes via submarine groundwater discharge to the Bay of Puck, southern Baltic Sea. J Total Environ 438:86–93

Szymczycha B, Miotk M, Pempkowiak J (2013) Submarine groundwater discharge as a source of mercury in the Bay of Puck, the Southern Baltic Sea. Water Air Soil Pollut 224. doi:10.1007/s11270–013-1542-0

Szymczycha B, Maciejewska A, Winogradow A, Pempkowiak J (2014) Could submarine groundwater discharge be a significant carbon source to the southern Baltic Sea? Oceanologia 56:327–347

Takahashi T, Sutherland SC, Sweeney C, Poisson A, Metzl N, Tilbrook B, Bates N, Wanninkof R, Feely RA, Sabine C, Olafsson J, Nojiri Y (2009) Global sea–air CO_2 flux based on climatological surface ocean pCO_2, and seasonal biological and temperature effects. Deep-Sea Res II 49:1601–1622

Thomas H, Pempkowiak J, Wulff F, Nagel K (2003) Autotrophy, nitrogen accumulation and nitrogen limitation in the Baltic Sea: a paradox or a buffer for eutrophication? Geophy Res Lett 30(21):2130 pp

Thomas H, Schiettecatte LS, Suykens K, Kone YJM, Schadwick EH, Prowe AEF, Bozec Y, de Baar HJW, Borges AV (2009) Enhanced ocean carbon storage from anaerobic alkalinity generation in coastal sediments. Biogeosciences 6:267–274. doi:10.5194/bg-6-267-2009

Ullman WJ, Chang B, Miller DC, Madse JA (2003) Groundwater mixing, nutrient diagenesis, and discharges across a sandy beachface, Cape Henlopen, Delaware (USA). Estuarin Coastal Shelf Sci 57:539–552

UNESCO (1981) The practical salinity scale 1978 and the international equation of state seawater, 1980. Tech Pap Mar Sci 36

Uścinowicz S (2011) Geochemistry of the Baltic Sea surface sediments, Polish Geological Institute-National Research Institute, Warsaw

Van Loon G, Duffy S (2011) Environmental chemistry—a global perspective (3rd edn). Oxford University Press, Oxford, pp 235–248. ISBN 978-0-19-922886-7

Viventsowa EA, Voronow AN (2003) Groundwater discharge to the Gulf of Finland (Baltic Sea): ecological aspects. Environ Ecol 45:221–225

Wang X, Du J, Ji T, Wen T, Liu S, Zhang J (2014) An estimation of nutrient fluxes via submarine groundwater discharge into the Sanggou Bay—a typical multi-species culture ecosystem in China. Mar Chem 167:113–122

Witek, Ochocki S, Maciejowska M, Pastuszak M, Nakonieczny J, Podgórska B, Kownacka JM, Wrzesińska-Kwiecień TM (1997) Phytoplankton primary production and its utilization by the pelagic community in the coastal zone of the Gulf of Gdańsk (southern Baltic). Mar Ecol Prog Ser 148:169–186. http://dx.doi.org/10.3354/meps148169

Wong JWC, Chan CWY, Cheung KC (1998) Nitrogen and phosphorus leaching from fertilizer applied on golf course. Water Air Soil Pollut 107:335–345

Young C, Tamborski J, Bokuniewicz H (2015) Embayment scale assessment of submarine groundwater discharge nutrient loading and associated land use. Estuar Coast Shelf Sci 158:20–30

Zavialov PO, Kao RC, Kremenetskiy VV, Peresypkin VI, Ding CF, Hsu JT, Kopelevich OV, Korotenko KA, Wu YS, Chen P (2012) Evidence for submarine groundwater discharge on the Southwestern shelf of Taiwan. Cont Shelf Res 34:18–25

Zekster IS, Ivanov VA, Meskheteli AV (1973) The problem of direct groundwater discharge to the seas. J Hydrol 20:1–36

Zekster IS, Everett LG, Dzhamalov RG (2007) Submarine groundwater. CRC Press, Boca Raton, 512 pp

Chapter 5
Conclusions

Submarine Groundwater Discharge (SGD) is a worldwide phenomenon. SGD, defined as fresh groundwater flux to the coastal zone, is part of a wider understanding assuming any flux of water from sediments to the overlying seawater to be a submarine groundwater discharge. The advantage of the approach taken in this study is that load of chemical substances (also heat, freshwater etc.) via SGD can be established in order to compare to loads originated from other sources and budgets studies. In this book SGD defined as fresh groundwater flux to the Bay of Puck, Baltic Sea has been described.

Although numerous studies have been devoted to SGD, and a number of effective methods have been developed to measure and characterize SGD, the study of this phenomenon is only beginning to mature. Many questions remain unanswered. Partly, this is caused by problems as regards collecting representative samples of SGD. In the study carried out in the Bay of Puck and the southern Baltic Sea off Poland that is the topic of this book, the problem was solved by several days long periods of a day to day, sampling campagnes carried out within subsequent seasons. This proved large variability of groundwater hydraulic flows and led to large standart errors of SGD fluxes, while fluctuations as regards concentrations of the measured chemical constituents were much smaller, and therefore were deemed to characterize well, SGD in the study area. Thus, uncertainties as regards material transport via SGD are, primary, associated with quantification of the the groundwater discharge.

The Bay of Puck was selected as a study area since both its hydrology and hydrogeology had been well documented in the literature. Also studies of groundwater composition on land in the vicinity of the study area are extensive (Pruszkowska and Przewłócka 2007). The studies had indicated constant concentrations of major ions in groundwater, collected by means of land based piezometers within two–three month long periods, as typical of the Puck Bay coastline. Thus the sampling frequency used in the study may be close to the limit necessary to provide reliable averaging.

The Bay of Puck drenage area- the Pomerania is a typical area of the southern Baltic coast, i.e. an area dominated by agriculture (Peltonen 2002). Little is known on groundwater discharges along the northern Baltic coast, both in terms of fluxes intensity, composition and fluxes location. However, geological structure of the

Baltic Sea indicates that seeps occur, mainly along the southern and eastern coasts of the sea, which are densely populated and agriculture dominated. Uścinowicz (2011) indicates that the Bay of Gdansk might be the most important discharge area in the Baltic Sea. Thus the study area might well prove to be typical of the regional SGD.

The estimations on some chemical substances fluxes via SGD to the the study area were upscalled to the entire Baltic Sea and were compared with loads delivered with river runoff and atmospheric deposition. The conclusion was that loads of some substances, namely phosphates, carbonates and some metals were large enough to alter material budgets of the sea. Upscaling the phenomenon world-wide, although based on few studies, indicated possible importance of the SGD derived loads of selected chemical substances to material budget of the world ocean.

References

Peltonen K (2002) Direct groundwater inflow to the Baltic Sea. TemaNord, Nordic Councils of Ministers, Copenhagen, Holand, 79 pp

Pruszkowska M, Przewłócka M (2007) Jakość wód podziemnych: Gdański system wodonośny. In: Kozerski B (ed) Wydawnictwo Politechniki Gdańskiej, Gdańsk, Poland, pp 51–64

Uścinowicz Sz (2011) Geochemistry of Baltic Sea surface and sediments. Polish Geological Institute-National Research Institute, Warsaw, Poland

Index